Theoretical studies of water clusters containing OH{e}HO structure and electron-hydrogen bond

Takeshi Tsurusawa

Doctor of Philosophy

Department of Structural Molecular Science
School of Mathematical and Physical Science
Graduate University for Advanced Studies

1999

Contents

Chapter 1

General introduction

1.1 Solvated electron in condensed phase

Historically speaking, the concept of solvated electron arose over a century ago in an attempt to interpret the unique phenomena, which occur when alkali metals are dissolved in liquid ammonia. In 1864 W. Weyl noted that when sodium or potassium metal is dissolved in the liquid [1], the solution turns blue. In early 1960s, short-living solvated (hydrated) electrons in liquid water and in aqueous electrolyte solutions are really observed by injection of an excess electron into liquid water and aqueous electrolyte solutions [2, 3], and this discovery catalizes the interest in solvated electron. These early optical spectroscopic data showed that solvated electrons are characterized by a exceptionally broad ($\sim$ 85 eV), structureless and asymmetric band. In these bands, the low-energy side shows a steep rise, while they gradually decrease at the high-energy side [4, 5]. The physical nature of solvated electron is generally accepted to be analogous to that of solvated atomic anions. The electron occupies a cavity in the solvent and is surrounded by favorably oriented water molecules. Excess electrons trapped in glasslike matrices at low temperatures have also been found to exhibit properties similar to those of solvated electron [6]. From the ESR study in a glass, Kevan inferred that an electron is hydrated by six water molecules in an octahedral configuration with the O-H bond in each water molecule oriented toward the electron [7]. Many experimental and theoretical studies have been devoted to understanding

the size of cavity and the geometry of the solvation shell, and the origin of the characteristic broad and structureless electronic optical absorption band. Theoretical studies of the solvated electron have emphasized quantum chemical calculation of negatively charged clusters. However, quantum chemical approaches remain limited to rather small clusters, and further, it is difficult to account for the appropriate thermal averaging or the relevant solvent configurations characteristic of the liquid. To treat the larger system, quantum path integral simulation techniques with model potential between electron and water molecule have been applied [8, 9, 10, 11], but in these model potential calculations, the effect of electron on the geometry of the water molecule is not fully considered.

1.2 Experimental studies for solvated electron in clusters

As mentioned above, the ESR study in a glass reveals six water molecules surrounding the electron, while solvated electron in liquid water is thought to occupy a roughly spherical cavity. Such microscopic pictures of electron solvation phenomena have invoked interest in negatively charged gas phase water clusters as possible models of the trapping site. Although a water molecule does not have stable negative ion state, electrons can be readily trapped in localized states in liquid or solid water, which imply that the association of electrons with water is multibodied interaction requiring a collection of molecules. This suggest that water clusters of some size should bind excess electrons.

Gas-phase water cluster anions, $(H_2O)_n^-$, were observed mass spectrometrically by Haberland and co-workers for the first time [12, 13, 14, 15]. Following this development, several experimental and theoretical studies on water cluster anions were undertaken [16, 17, 18, 19, 20, 21, 22, 23, 24, 25, 26, 27, 28, 29, 30, 31, 32, 33, 34, 35, 36, 37, 38, 39, 40, 41]. The photoelectron spectra of $(H_2O)_{n\leq 11}^-$ [16, 17, 23, 24, 25] exhibit structure, with vibrational features observed on the high electron binding energy side of the main peaks for $n = 2$, 3, 6 and 7. Isotopic and source condition studies suggest that the two lowest electron binding energy (EBE) features in the spectra of $n = 6$, 7, 8, 10 and 11 may represent different isomers of each of these species. Also in these spectra for $n = 2$, 3, 6 and 7,

there are the vibrational features which suggested that some of free OH bonds in the cluster hydrogen bond to the excess electron and geometry change in electron detachment process is not small [17, 23]. These spectra of $(H_2O)^-_{n>11}$ [16] consist of single, broad, asymmetric peaks. The EBEs of the peak maxima in these spectra were interpreted as vertical detachment energies (VDEs), and these shift to successively higher EBEs with increasing n. When VDEs are plotted against $n^{-1/3}$, the VDEs plot linearly with $n^{-1/3}$ and extrapolate to an intercept of 3.3 eV. The intercept, VDE at $n = \infty$, is close to an estimated value of the bulk phtoelectric threshold of hydrated electron ($\sim$ 3.2 eV [16]). For $n \geq 11$, $(H_2O)^-_n$ seems to be counterparts to bulk hydrated electrons, which will mature with size toward condensed-phase hydrated electrons. Electronic absorption spectra for $n = 6 - 50$ [21] and photodetachment cross section for $n = 2$, 6, 7 and 11 [22, 24] are also observed. Recently, OH stretch vibrational spectra are observed for $n = 2$, 3, 5–9 and 11 and showed that the spectrum for hexamer anion exhibits characteristic two intense and largely downward shifted peaks for OH stretching modes [26, 27].

Water cluster complex containing a group 1 metal atom is another model system to studying the microscopic structure of hydrated electron. Advances in molecular beam technique permit to prepare the clusters consisting of a group 1 metal atom and water molecules, $M(H_2O)_n$ (M=Li, Na and Cs) [42, 43, 44]. In these clusters, the valence electron of a metal atom is expected to be transferred to the solvent molecules at a certain cluster size, and the ground states of clusters may have an ion-pair character as in the case of bulk fluids. The ionization energies (IEs) of all these clusters have been found to become constant for $n \geq 4$ independent of metal element and its limiting values ($n \rightarrow \infty$) are close to an estimated photoelectric threshold of ice (3.2 eV). Since the experimental data are limited to IE, understanding of these experimental results requires supports from theoretical studies inevitably.

Bibliography

[1] W. Weyl, Pogg. Ann., 123 (1864) 350.

[2] G. W. Boag and E. Hart, Nature, 197 (1963) 45.

[3] E. Hart and G. W. Boag, J. Am. Chem. Soc., 84 (1963) 4090.

[4] A.M. Brodsky and A.V. Tsareevsky, Adv. Chem. Phys., 44 (1980) 483.

[5] D.-F. Feng and L. Kevan, Chem. Rev., 80 (1980) 1.

[6] L. Kevan, in M. Burton and J. Magee, Eds., *Advances in Radiation Chemistry*, Vol. 4, Wiley, New York, 1974.

[7] L. Kevan, Acc. Chem. Res., 14 (1981) 138.

[8] F.A. Webster, P.J. Rosskey, and R.A. Friesner, Comput. Phys. Commun., 63 (1991) 494

[9] F.A. Webster, J. Schnitker, M.S. Friedrichs, R.A. Friesner, and P.J. Rossky, Phys. Rev. Lett., 66 (1991) 3172

[10] T.H. Murhprey and P.J. Rossky, J. Chem. Phys., 99 (1993) 515

[11] B. J. Schwartz and P.J. Rossky, J. Chem. Phys., 101 (1994) 6902

[12] M. Armbruster, H. Haberl and, H.-G. Schindler, Phys. Rev. Lett., 47 (1981) 323.

[13] H. Haberland, H. Langosch, H.-G. Schindler, D.R. Worsnop, J. Phys. Chem., 88 (1984) 3903.

[14] H. Haberland, C. Ludewigt, H.-G. Schindler, D.R. Worsnop, J. Chem. Phys., 81 (1984) 3742.

[15] J.H. Hendricks, H.L. de Clercq, S.A. Lyapustina, C.A. Fancher, T.P. Lippa, J.M. Collins, S.T. Arnold, G.H. Lee, K.H. Bowen, in: T. Kondow (Ed.), Sturctures and Dynamic of Clusters, Procdeedings of the Yamada Conference XLIII, Universal Academy, Tokyo, 1995, p. 321.

[16] J.V. Coe, G.H. Lee, J.G. Eaton, S.T. Arnold, H.W. Sarkas, K.H. Bowen, C. Ludewigt, H. Haberland, D.R. Worsnop, J. Chem. Phys., 92 (1990) 3980.

[17] S.T. Arnold, Ph.D. Thesis, The Johns Hopkins University, 1993.

[18] L.A. Posey, M.A. Johnson, J. Chem. Phys., 89 (1988) 4807.

[19] L.A. Posey, P.J. Campagnola, M.A. Johnson, G.H. Lee, J.G. Eaton, K.H. Bowen, J. Chem. Phys., 91 (1989) 6536.

[20] P.J. Campagnola, L.A. Posey, M.A. Johnson, J. Chem. Phys., 92 (1990) 3243.

[21] P. Ayotte, M. A. Johnson, J. Chem. Phys., 106 (1997) 811.

[22] T. Maeyama, T. Tsumura, A. Fujii, N. Mikami, Chem. Phys. Lett., 264 (1997) 292.

[23] C.G. Bailey, J. Kim, M.A. Johnson, J. Phys. Chem., 100 (1996) 16782.

[24] C.G. Bailey, M.A. Johnson, Chem. Phys. Lett., 265 (1997) 185.

[25] J. Kim, I. Becker, O. Cheshnovsky, M.A. Johnson, Chem. Phys. Lett., 297 (1998) 90.

[26] P. Ayotte, C.G. Bailey, J. Kim, M.A. Johnson, J. Chem. Phys., 108 (1998) 444.

[27] P. Ayotte, G.H. Weddle, C.G. Bailey, M.A. Johnson, F. Vila, K.D. Jordan, J. Chem. Phys., 110 (1999) 6268.

[28] R.N. Barnett, U. Landman, C.L. Cleveland, J. Jortner, J. Chem. Phys., 88 (1988) 4429.

[29] D.M. Chipman, J. Phys. Chem., 83 (1979) 1657.

[30] R.N. Barnett, U. Landman, S. Dhar, N.R. Kestner, J. Jortner, A. Nitzan, J. Chem. Phys., 91 (1989) 7797.

[31] K.S. Kim, I. Park, S. Lee, K. Cho, J.Y. Lee, J. Kim, J.D. Joannopoulos, Phys. Rev. Lett., 76 (1996) 956.

[32] S. Lee, S.J. Lee, J.Y. Lee, J. Kim, K.S. Kim, I. Park, K. Cho, J.D. Joannopoulos, Chem. Phys. Lett., 254 (1996) 128.

[33] K.S. Kim, S. Lee, J. Kim, J.Y. Lee, J. Am. Chem. Soc., 119 (1997) 9329.

[34] S. Lee, J. Kim, S.J. Lee, K.S. Kim, Phys. Rev. Lett., 79 (1997) 2038.

[35] J. Kim, J.M. Park, K.S. Oh, J.Y. Lee, S. Lee, K.S. Kim, J. Chem. Phys., 106 (1997) 10207.

[36] D.M.A. Smith, J. Smets, Y. Elkadi, L. Adamowicz, J. Chem. Phys., 107 (1997) 5788.

[37] D.M.A. Smith, J. Smets, Y. Elkadi, L. Adamowicz, J. Chem. Phys., 109 (1998) 1238.

[38] D.M.A. Smith, J. Smets, L. Adamowicz, J. Chem. Phys., 110 (1999) 3804.

[39] Y. Bouteiller, C. Desfrançois, J.P. Schermann, Z. Latajka, B. Silvi, J. Chem. Phys., 108 (1998) 7967.

[40] T. Tsurusawa, S. Iwata, Chem. Phys. Lett., 287 (1998) 553.

[41] T. Tsurusawa, S. Iwata, Chem. Phys. Lett., 315 (2000) 433.

[42] R. Takasu, F. Misaizu, K. Hashimoto, and K. Fuke, J. Phys. Chem., A101 (1997) 3078.

[43] I.V. Hertel, C.P. Hüglin, C. Nitsch, and C.P. Schulz, Phys. Rev. Lett., 67 (1991) 1767.

[44] F. Misaizu, K. Tsukamoto, M. Sanekata, and K. Fuke, Chem. Phys. Lett., 188 (1992) 241.

Chapter 2

Dipole-bound and interior electrons in water dimer and trimer anions: ab initio MO studies

Chemical Physics Letter 287 (1998) 553–562

2.1 Introduction

Since the first observation of the water cluster anions in the gas phase, many experimental and theoretical works have been reported [1–4]. In the experimental studies, it is known that the water molecule itself cannot be able to bind the excess electron. On the other hand, water cluster anions, $(H_2O)_n^-$, $n \geq 2$, can be found in mass spectra. Interestingly, the observed signals for n = 3, 4, 5, 8, 9 and 10 are very weak [1–6]. Following these earilier experiments, further spectroscopic studies were carried out by several groups [7–11]. In the theoretical point of view, the quantum path-integral simulations with model potentials showed that there are two distinct states for the excess electron in the water cluster anions [12]. One is the internal state, in which the exess electron is localized inside

the cluster. Another is the surface state, in which the excess electron is bound to the surface of the cluster. It was shown that the surface state is favored for small size clusters. Ab initio MO calculations for the water cluster anions were also reported by several authors [13–17]. For dimer anion, ab initio calculation illustrated that the excess electron can be weakly bound to the surface of the dimer. It is believed that the excess electron is bound by electric dipole field made by a neutral dimer, and it is often called a dipole-bound electron. It should be noted that a dipole-bound electron is not localized near the cluster but of very diffuse nature. Recently, it was also shown that the excess electron can be bound by a chain form of a water trimer and it is another example of dipole-bound electrons distributing on the surface of the neutral cluster [18]. For the larger cluster anions, with $n = 6$ and 12, Kim et al. showed that there are several isomers in both internal and surface states [15–17].

In this chapter, with extensive ab initio MO calculations, I will show that the excess electron can be bound to the dimer and trimer anions in the internal state as well as in the surface state. In the former, the structure indicates that mutual interaction of the excess electron cloud and the bond dipoles of water molecules form the stable anionic system.

2.2 Method

First, to find the possible isomers of the water cluster anions, I performed geometry optimization with 6-311++G** basis set at UHF, MP2 and B3LYP levels of calculations. Once the optimized geometries of the isomers are obtained, the diffuse functions are added to the basis 6-311++G** to take into account the diffuseness of the excess electron, and then the geometry is re-optimized. Two sets of the diffuse functions are examined. The first set consists of two s-type functions on each atom. The gaussian exponents are 0.02815 and 0.00938 for oxygen atoms, and 0.0120 and 0.0040 for hydrogen atoms; I call this basis set 2sOH. The second set contains seven s-type functions and seven p-type functions, and the center of these basis sets are optimized. This diffuse function set 7sp is the same as Chipman used for the water dimer anion [13], although Chipman fixed the center of

these diffuse functions at midpoint of two oxygen atoms. In my calculations with the basis set 7sp, two-step procedure is adopted. At the first step, the geometry of cluster anion is fixed at the structure optimized with 6-311++G**. Only the center of seven s and p functions are optimized. After the center of 7sp is determined, the geometry of cluster anion as well as the center of 7sp functions are both optimized. In the present work, the harmonic frequencies are evaluated after optimization with 6-311++G** and 2sOH, and all real frequencies are confirmed. Because the geometries obtained from 2sOH and 7sp calculations are nearly identical, the frequency calculations are not performed with 7sp basis set. In this chapter, I will show the results of the calculation with the basis sets 6-311++G** and 7sp.

For larger clusters, I found out that 7sp functions sometimes introduces an artificial attractive force between two water molecules near the center of 7sp functions. Therefore, for one of the trimer anions I will show in this chapter, I used four s and p type functions on all oxygen atoms in the cluster instead of using 7sp functions. The exponents of the four sp functions are α = 0.02815, 0.00938, 0.00312 and 0.00104.

All calculations are performed with Gaussian 94 [19] and GAMESS [20] program packages. The computaion was carried out on our workstations and on the supercomputers in the computer center of Institute for Molecular Science.

2.3 Results and discussion

Figures 1 and 2 show the optimized structures as well as the electron distribution in the singly occupied molecular orbital (SOMO) of each isomer, where 50 percent of the electron is contained within the depicted boundary. The energies and some of geometrical parameters are listed in Tables 1 and 2 for the dimer and trimer anions, respectively.

For each anion, I first show the results with 6-311++G**. It is known that a set of very diffuse basis functions is required to describe the excess electron of the dipole-bound state [13, 14]. For the

dipole-bound anion systems, the absolute value of the dipole moment determines the diffuseness of the wave function of the excess electron. If the dipole moment of the system is large enough, even the 6-311++G** basis set might be able to describe the wave function of the excess electron. This may be the case of the larger water cluster anions having large dipole moment [21]. However, as I will show below, the basis set 6-311++G** is not flexible enough for dimer and trimer anions. Thus, I have to proceed to use much more diffuse basis set 2sOH or 7sp. In the present chapter I discuss the results of the basis set 7sp.

2.3.1 Dimer

I have located two stable dimer anions, 2-S and 2-I, shown in Fig.1. The former is a well-known dipole-bound anion, and the latter is previously not reported in my knowledge. These two structures of water dimers can be found as the electron capturing units in larger water cluster anions such as hexamer and dodecamer anions [15–17, 21].

Dipole-bound dimer anion

The isomer 2-S, shown in Fig.1(a), is a typical dipole-bound anion. The excess electron is bound to the outside, or the surface of the dimer and is supported by hydrogen atoms. More correctly speaking, three bond dipoles of O-H bonds create the electrostatic field to capture an excess electron. When the excess electron is removed, the neutral cluster has a large dipole moment (4.6, 4.7 and 4.6 Debye by UHF, MP2 and B3LYP, respectively) enough to bind the excess electron. This structure looks similar to that of the neutral hydrogen-bonded water dimer. There is, however, an important difference. In the anion 2-S, three hydrogens are directed to the same side with respect to the O-O axis to maximize the total dipole moment of the dimer, and the excess electron is caught by the three O-H bonds. On the other hand, in the neutral dimer structure, a hydrogen of the proton-donor water is directed to the opposite side; this structure is favored by the dipole-dipole interaction of two waters. Even in this neutral optimized structure, the dipole moment (3.5, 3.3 and 3.2 Debye by UHF, MP2 and B3LYP,

respectively) is large enough to bind the excess electron. The electron correlation with the MP2 and DFT/B3LYP levels does change the geometry, but its change is small.

By freezing the structural frame of the dimer 2-S optimized with 6-311++G**, the center of diffuse functions 7sp is optimized. As just mentioned above, in this structure three O-H bond dipoles interact with the excess electrons. But this structure sacrifices the dipole-dipole interaction between two water molecules, because the proton-donor water is unfavorably directed. So in the next step, when I fully optimize the structure of the water dimer as well as the center of diffuse functions, the structure of water dimer returns to the one which is known to be the structure of the most stable neutral dimer. It should also be noted that the neutral dimer itself has a dipole moment (3.3D/MP2) large enough to bind the dipole-bound electron, but it is smaller than that of the structure of dimer anion determined with 6-311++G**. Because the dipole moment in the structure optimized with the 7sp basis set is smaller than that with 6-311++G**, the excess electron distribution becomes as large as shown in Fig.1(b). The scale, which is given at the side of each figure, demonstrates how the electron distribution becomes large. The dipole-dipole interaction of neutral waters wins against the interaction between the excess electron and the O-H bond dipoles. With the 6-311++G** basis set, the size of the excess electron cloud is not large, therefore, the interaction of the excess electron with the bond dipoles is strong. Thus, the latter interaction wins.

With the 6-311++G** basis set in three levels of approximations the vertical detachment energies (VDE) are all negative (see Table 1). With very diffuse basis set 7sp, the VDE becomes slightly positive, and it agrees with the calculated VDE in the previous work [13].

Internal dimer anion

In another dimer 2-I, shown in Fig.1(c), the excess electron is internally trapped between two water molecules. The electron is apparently bound by all four hydrogen atoms. The structure optimized with UHF, MP2 and B3LYP/6-311++G** has D_{2h} symmetry and all atoms are on a plane. Because the directions of the dipole moments of water molecules are opposite, the total dipole moment of

the neutral dimer of this structure is zero. Obviously the excess electron is not dipole-bound in an ordinary sense. Without the excess electron, two water molecules are interacted repulsively with each other. In that sense, the excess electron distribution binds two water molecules, or more properly, the electrostatic interaction between the excess electron and four hydrogen atoms (, or four O-H bond dipoles) stabilizes the system. As is seen in Table 1, the electron correlation plays an important role in lowering the anion energies. The O-O distance with MP2 and DFT calculations is much shorter than that with UHF level of calculation. When B3LYP is used, the vertical detachment energy (VDE) becomes positive for the dimer 2-I even with 6-311++G**.

Since the isomer 2-I has D_{2h} symmetry, the center of the 7sp diffuse functions is placed at the center of the dimer. Then, the geometry of the dimer is optimized. As the excess electron is allowed to be diffuse, two waters start apart, and the O-O distance is as large as 15.9 Å. Surprisingly, even with the UHF level, the VDE becomes positive. When the geometry is further optimized with the MP2 level, the O-O distance is 9.9 Å, and the VDE becomes 0.018eV as shown in Table 1.

The experimental VDE for dimer anion is 0.04 eV. My 7sp basis set is large enough to describe the dipole-bound electron. The smallest exponent is 0.000001, and its spacial extension is as large as 500 Å. The calculated VDE for the dipole-bound 2-S is only 0.006 eV. The electron correlation of the MP2 level does not increase it for 2-S. On the other hand, the calculated VDE of 2-I is 0.018 eV. The more extensive electron correlation treatment might increase it further. In the present status of the theoretical works, I cannot identify the stucture of the dimer anion experimentally observed. It is, however, certain that I cannot exclude the possibility of the previously-unknown dimer anion which traps an electron internally.

2.3.2 Trimer

With the 6-311++G** basis set, I have found three trimer anions as shown in Fig.2. The geometric parameters (the definitions are shown in Fig.3) and VDEs are given in Table 2.

Chain trimer anion, 3-C

One of these three isomers is almost equivalent to that recently reported by Smith *et al.* [18]. Three water molecules form a chain, and the electron is dipole-bound at its end. I call this isomer 3-C. Figure 2(a) is the structure determined with 6-311++G**. The structure of the end dimer is similar to that of Fig.1(a). Besides two hydrogens of proton-acceptor water, one of the hydrogens of the proton-donor water (in the hydrogen bonding dimer) seems working together to capture the excess electron. The geometry optimization with the electron correlation induces only the conformational change of the O_3-water (see Fig. 3 for the numbering of the atoms). In the resulting structure the free hydrogen atom of the proton donor water seems somewhat to take part in capturing the electron and the VDE becomes positive with B3LYP.

When 7sp diffuse functions are augumented, similarly to the case of 2-S, the electron cloud becomes huge as shown in Fig.2(b). Also the structure of the trimer core is subject to be changed. The torsional angle $\beta_{O_1O_2O_3H_f}$ becomes nearly 90 degree and the configuration of the middle water relative to O_3-water is similar to the neutral dimer, which implies that the structure of the hydrogen bonding dimer of O_2- and O_3-water molecules becomes close to that of the normal neutral dimer, as I have already seen in 2-S. My MP2 optimized geometrical parameters are very similar to those reported by Smith *et al.* [18], as far as they are presented in their paper. My calculated VDE is 0.06 eV with MP2, and Smith *et al.* gave it 0.12 eV with MP2 and 0.14 with CCSD(T) level of calculation.

Surface trapping trimer anion, 3-S

A more typical dipole-bound trimer anion is shown in Fig.2(c). The excess electron is distributed on the surface of the water trimer, or on the top of three hydrogens. The other three hydrogens form a hydrogen bonded ring network, which is similar to the case of the most stable neutral trimer. I have confirmed the true stability of the structure with UHF, MP2 and B3LYP methods, and all harmonic frequencies are real with these three methods. There is an important difference between the structures of the anion and neutral trimers; in the latter, one hydrogen is directed to the opposite side of the

plane of three oxygen atoms (*uud* form in Shütz *et al.*'s notation [22]), while in the anion cluster, all three hydrogen atoms are in the same side (*uuu*) to maximize the total dipole moment. In the neutral trimer, to maximize the dipole-dipole interaction among three waters, one of waters has to be directed oppositely. The dipole moment (0.8, 1.0 and 1.1 Debye by UHF, MP2 and B3LYP, respectively) of the most stable neutral trimer is not large enough to bind the excess electron.

Thus, in the trimer 3-S, I find the similar basis set dependence on the structure as in the dimer 2-S in a more drastic way. In short, the trimer 3-S turns out to be unstable, if the basis set is flexible enough. If the geometry is fixed at the one optimized with 6-311++G**, the excess electron is trapped by three O-H bond dipoles, very similarly to Fig.2(c) except for the size of the electron cloud, which becomes much larger than that of Fig.2(c). Then, when the geometries of three waters are also relaxed from the *uuu* ring trimer, one of the waters starts to rotate. Because the distribution of the excess electron is very diffuse, the interaction of the excess electron with hydrogens (, or with O-H bond dipoles) is weak, so that the trimer structure changes to maximize the water-water interaction. Eventually it reaches the most stable ring isomer of the neutral trimer. Meanwhile, the electron cloud becomes larger and larger, and the contribution from the gaussian function with the smallest exponent to SOMO becomes large. In other words, the electron becomes free. This is very reasonable since the total dipole of the neutral ring trimer is only 1.0 Debye at MP2 level of calculation, which is too small to support the dipole-bound electron.

I should emphasize that my 7sp basis set is flexible enough to describe unbound free electron.

As a conclusion, the isomer 3-S is an artifact of the limited size of the basis set. This structure is also found in larger water anion clusters as a trapping site of the excess electron [15-17, 21]. In these larger clusters, the rotation of the water molecules to destroy the *uuu* structure is constrained by the other hydrogen bonding network.

Internally trapping trimer anion, 3-I

The isomer 3-I, shown in Fig.2(d), has the internally bound excess electron; five hydrogen atoms trap the electron. The other hydrogen forms a hydrogen bond in a water dimer. The structure, optimized with 6-311++G**, has both units of dimers 2-I (Fig.1(c)) and 2-S (Fig.1(a)). The electron is clearly trapped between two water molecules as in the dimer 2-I, and therefore, the excess electron is not dipole-bound. A hydrogen of the third water might contribute to the stablization, but it is only of secondary importance. The electron correlation shortens the distance between two waters which trap the electron, and lowers the energy of the anion cluster. The internally bound type trimer 3-I has a positive VDE at MP2 and B3LYP levels of approximation even with the 6-311++G** basis set (see Table 2).

When the basis set is augumented with 7sp diffuse functions, the size of the electron cloud increases, and the distance between two waters becomes long, but not as much as in the case of the dimer 2-I. In particular, the distance between two waters is substantially shorten as is seen in Fig.2(e) and in Table 2. Besides, the two other changes from the structure of Fig.2(d) are found in Fig.2(e); the orientation of the non-hydrogen bonded water(O_1) and the position of the third water(O_3). Two hydrogens in the non-hydrogen bonded water are in the O_1-O_2-O_3 plane when the 6-311++G** basis is used, but the line connecting two hydrogens of the water(O_1) are perpendicular to the O_1-O_2-O_3 plane if the 7sp functions are added. As is given in Fig.3, the angle α_2 is the angle between O_2-O_3 axis in the dimer and the local dipole of electron trapping water(O_2), which is about 240° if 6-311++G** is used, independent of many-electron wave functions used. But, it becomes nearly 170° when 7sp basis set is used. As Fig.2(e) shows, the hydrogen of the water outside the electron cloud seems to have no interaction with the excess electron. The excess electron is trapped by two water molecules in 3-I as in 2-I.

With this basis set, the VDE is positive even with the UHF approximation. The MP2 VDE is as large as 0.126, which is close to the experimental VDE 0.142. The trimer 3-I is also a building block

of the water hexamer and dodecamer anions [15–17, 21].

Thus, as for the dimer anion, there are two candidates for trimer anions, 3-C and 3-I. Both dipole-bound and internally trapping anions are possible in terms of their stability. More experimental and theoretical studies are required to identify the structure.

2.3.3 Internally trapping trimer anion, 3W-a

In the previous sections, I showed two isomers of trimer anions. One of them is the chain-like structure having the dipole-bound electron, and in another isomer the excess electron is internally surrounded by a water molecule and a water dimer. Fig. 4 shows a new isomer 3W-a of D_{3h} symmetry. The electron cloud of the excess electron is depicted together with the optimized geometry. The surface of the sphere is defined such a way that the inside of the sphere contains a half of the excess electron. The isomer has a remarkable structure; there is no hydrogen bond in the cluster. The interaction between the excess electron distribution, which I will denote as $\{e\}$, and the surrounding OH bonds holds the structure. When the excess electron is removed, three water molecules are separated. The distance between the oxygen atoms in the cluster is 5.799 Å and the OH bond lengths are 0.963 Å. The SOMO extent measure (SEM), which is defined as a volume of a sphere containing a half of SOMO electron [23], of 3W-a is 257 $Å^3$ while the SEM for the chain-like trimer is as large as 804 $Å^3$. The OH frequency shifts in 3W-a are -113 cm^{-1} and -22 cm^{-1}. The former is doubly degenerated and corresponds to the combination of the symmetric stretching modes of three water molecules. The latter corresponds to the sum of the antisymmetric stretching modes. The VDE of this isomer is 0.227 eV. The experimental VDE is 0.142 ± 0.007 eV, and the isomer 3W-a is not likely to be the detected isomer. But, it is worth noting the stability of this remarkable structure.

2.4 Conclusion

I have illustrated that in addition to the well-known dipole-bound anion state, there is another type of anion state, in which the electron is internally trapped between water molecules even for the smallest sizes of water cluster anions. From another point of view, two different forms of the excess electron in water clusters are possible; dipole-bound and interior electrons. From theoretical point of view, the latter structure is interesting because of its sensitivity to the electron correlation and of its uniqueness of the interaction between the diffuse electron and hydrogen atoms (or O-H bond dipoles). As far as the VDE is concerned, both types are plausible for dimer and trimer anions. More extensive studies are definitely required to clarify the interaction of water molecules and the excess electron.

2.5 Acknowledgment

The present work was partially supported by the Grant-in-Aids for Scientific Research (A) (no.09304057) by the Ministry of Education, Science, Sports, and Culture, Japan. A part of calculations was carried out at the Computer Center of the Institute for Molecular Science. I acknowledge Mr. Mizutani of the Computer Center for providing me his molecular drawing program, PGV.

Bibliography

[1] M. Armbruster, H. Haberland, H.-G. Schindler, Phys. Rev. Lett., 47 (1981) 323.

[2] H. Haberland, H.-G. Schindler, D.R. Worsnop, Ber. Bunsenges. Phys. Chem., 88 (1984) 270.

[3] H. Haberland, H. Langosch, H.-G. Schindler, D.R. Worsnop, J. Phys. Chem., 88 (1984) 3903.

[4] H. Haberland, C. Ludewigt, H.-G. Schindler, D.R. Worsnop, J. Chem. Phys., 81 (1984) 3742.

[5] J.H. Hendricks, H.L. de Clercq, S.A. Lyapustina, C.A. Fancher, T.P. Lippa, J.M. Collins, S.T. Arnold, G.H. Lee, K.H. Bowen, in: T. Kondow (Ed.), Structures and Dynamics of Clusters, Proceedings of the Yamada Conference XLIII, Universal Academy, Tokyo, 1995, p. 321.

[6] S.T. Arnold, Ph.D. dissertation, Bowen Group, Johns Hopkins University, 1993.

[7] L.A. Posey, M.A. Johnson, J. Chem. Phys., 89 (1988) 4807.

[8] L.A. Posey, P.J. Campagnola, M.A. Johnson, G.H. Lee, J.G. Eaton, K.H. Bowen, J. Chem. Phys., 91 (1989) 6536.

[9] P.J. Campagnola, L.A. Posey, M.A. Johnson, J. Chem. Phys., 92 (1990) 3243.

[10] P. Ayotte, M.A. Johnson, J. Chem. Phys., 106 (1997) 811.

[11] Toshihiko Maeyama, Tohru Tsumura, Asuka Fujii, and Naohiko Mikami. *Chem.Phys.Lett.*, 264:292, 1997.

[12] R.N. Barnett, U. Landman, C.L. Cleveland, J. Jortner, J. Chem.Phys., 88 (1988) 4429.

[13] D.M. Chipman, J. Phys. Chem., 83 (1979) 1657.

[14] R.N. Barnett, U. Landman, S. Dhar, N.R. Kestner, J. Jortner, A. Nitzan, J. Chem. Phys., 91 (1989) 7797.

[15] J. Kim, J.M. Park, K.S. Oh, J.Y. Lee, S. Lee, K.S. Kim, J. Chem. Phys., 106 (1997) 10207.

[16] K.S. Kim, I. Park, S. Lee, K. Cho, J.Y. Lee, J. Kim, J.D. Joannopoulos, Phys. Rev. Lett., 76 (1996) 956.

[17] S. Lee, S.J Lee, J.Y. Lee, J. Kim, K.S. Kim, I. Park, K. Cho, J.D. Joannopoulos, Chem. Phys. Lett., 254 (1996) 128.

[18] D.M. Smith, J. Smets, Y. Elkadi, L. Adamowicz, J. Chem. Phys., 107 (1997) 5788.

[19] Gaussian 94 (Revision D.3), M.J. Frisch, G.W. Trucks, H.B. Schlegel, P.M.W. Gill, B.G. Johnson, M.A. Robb, J.R. Cheeseman, T.A. Keith, G.A. Petersson, J.A. Montgomery, K. Raghavachari, M.A. Al-Laham, V.G. Zakrzewski, J.V. Ortiz, J.B. Foresman, C.Y. Peng, P.Y. Ayala, M.W. Wong, J.L. Andres, E.S. Replogle, R. Gomperts, R.L. Martin, D.J. Fox, J.S. Binkley, D.J. Defrees, J. Baker, J.P. Stewart, M. Head-Gordon, C. Gonzalez and J.A. Pople, Gaussian, Inc., Pittsburgh PA, 1995.

[20] M.W. Schmidt, K.K. Baldridge, J.A. Boatz, S.T. Elbert, M.S. Gordon, J.H. Jensen, S. Koseki, N. Matsunaga, K.A. Nguyen, S. Su, T.L. Windus, M. Dupuis, J.A. Montgomery, J. Comput. Chem., 14 (1993) 1347.

[21] T. Tsurusawa, S. Iwata, Chem. Phys. Lett., 315 (2000) 433.

[22] M. Schütz, T. Bürgi, S. Leutwyler, H.B. Bürgi, J. Chem. Phys., 99 (1993) 5228.

[23] T. Tsurusawa, S. Iwata, J. Phys. Chem. A, 103 (1999) 6134.

Figure captions

Figure 1 (a) The structure 2-S optimized with the 6-311++G**/UHF level of approximation. Inside of the boundary, 50% of the electron density of the singly occupied molecular orbital (SOMO) is contained. The scale for 1Å is shown near the structure. The arrangement of the water molecules is illustrated at the lower left for clarity.

(b) The structure 2-S optimized with the 7sp/UHF level of approximation.

(c) The structure 2-I optimized with the 6-311++G**/MP2 level of approximation.

(d) The structure 2-I optimized with the 7sp/MP2 level of approximation.

Figure 2 (a) The structure 3-C optimized with the 6-311++G**/UHF level of approximation. (See also the figure caption of Fig.1)

(b) The structure 3-C optimized with the 7sp/UHF level of approximation.

(c) The structure 3-S optimized with the 6-311++G**/UHF level of approximation.

(d) The structure 3-I optimized with the 6-311++G**/MP2 level of approximation.

(e) The structure 3-I optimized with the 7sp/MP2 level of approximation.

Figure 3 (a) The geometric parameters for dimer anion 2-S.

(b) The geometric parameters for trimer anion 3-C.

(c) The geometric parameters for trimer anion 3-S.

(d) The geometric parameters for trimer anion 3-I.

Figure 4 The optimized structure and the singly occupied molecular orbital (SOMO) of 3W-a. This structure have D_{3h} symmetry. Inside of the sphere, 50% of the electron density of the SOMO is contained. The SEM (SOMO extent measure) is defined as the volume of the sphere. For clarity, the core structure of the water molecules is illustrated bellow.

Table 1
Geometric parameters and vertical detachment energy (VDE) of dimer anions

		R_{OO}(Å)	α_1 [a] (deg.)	α_2 [a] (deg.)	VDE(eV)	E.A.(adiabatic)(eV)
2-S	6-311++G**					
	HF	2.950	54.9	234.9	-0.789	-0.855
	MP2	2.855	43.5	235.1	-0.529	-0.606
	B3LYP	2.888	45.3	240.3	-0.210	-0.288
	7sp					
	HF	3.007	54.5	149.1	0.006	
	MP2	2.923	50.7	222.4	0.005	
	Ref.13	2.892	54.2	123.0	0.0002	
2-I	6-311++G**					
	HF	5.761			-0.525	-0.781
	MP2	5.288			-0.296	-0.619
	B3LYP	5.206			0.024	-0.293
	7sp					
	HF	15.941			0.005	
	MP2	9.907			0.018	
Exp. Ref.6					0.042 ± 0.006	

[a] The angles α_1 and α_2 are defined in Fig. 3.

Table 2
Geometric parameters and vertical detachment energy (VDE) of trimer anions

		R_{OO} [c]	R'_{OO} [c]	α_1 [a,d]	α_2 [a,d]	α_3 [a,d]	$\alpha_{O_1O_2O_3}$ [b,d]	$\beta_{O_1O_2O_3H_f}$ [b,d]	VDE[e]	E.A.(adiabatic)[e]
3-C	6-311++G**									
	HF	2.874	2.932		230.7		114.0	17.6	-0.561	-0.804
	MP2	2.778	2.828		235.0		112.2	19.9	-0.243	-0.570
	B3LYP	2.821	2.859		239.4		105.7	19.8	-0.124	-0.221
	7sp									
	HF	2.935	2.961		184.7		131.8	93.2	0.026	
	MP2	2.824	2.867		214.4		128.5	87.9	0.062	
	Ref.18	2.803	2.862				125.4		0.120	-0.146
3-S	6-311++G**									
	HF	3.092		8.0					-0.603	-0.883
	MP2	2.950		8.4					-0.382	-0.669
	B3LYP	2.939		12.9					-0.048	-0.292
3-I	6-311++G**									
	HF	2.983	5.694	41.1	242.5				-0.233	-0.745
	MP2	2.870	5.094	43.4	236.8				0.034	-0.613
	B3LYP	2.888	4.856	44.2	240.9				0.384	-0.267
	7sp									
	HF	2.989	9.138	44.8	175.5				0.042	
	MP2	2.878	6.332	40.8	165.6				0.126	
Exp. Ref.6									0.142 ± 0.007	

[a] The angles α_1,α_2 and α_3 are defined in Fig. 3.
[b] The angles $\alpha_{O_1O_2O_3}$ and $\beta_{O_1O_2O_3H_f}$ are a bond angle and a dihedral angle defined by O_1, O_2, O_3 and O_1, O_2, O_3, H_f, respectively
[c] In Å. [d] In degree. [e] In eV.

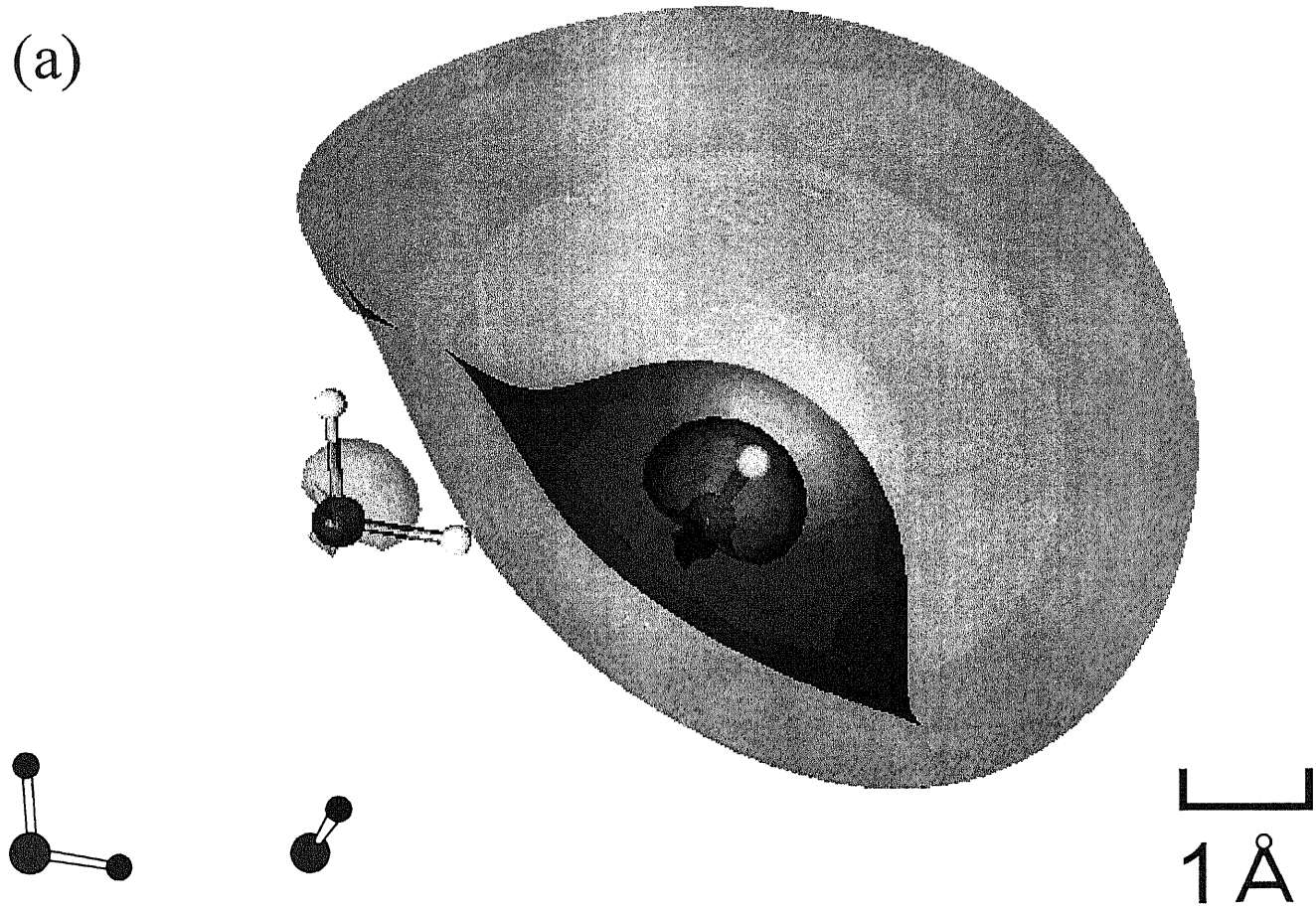

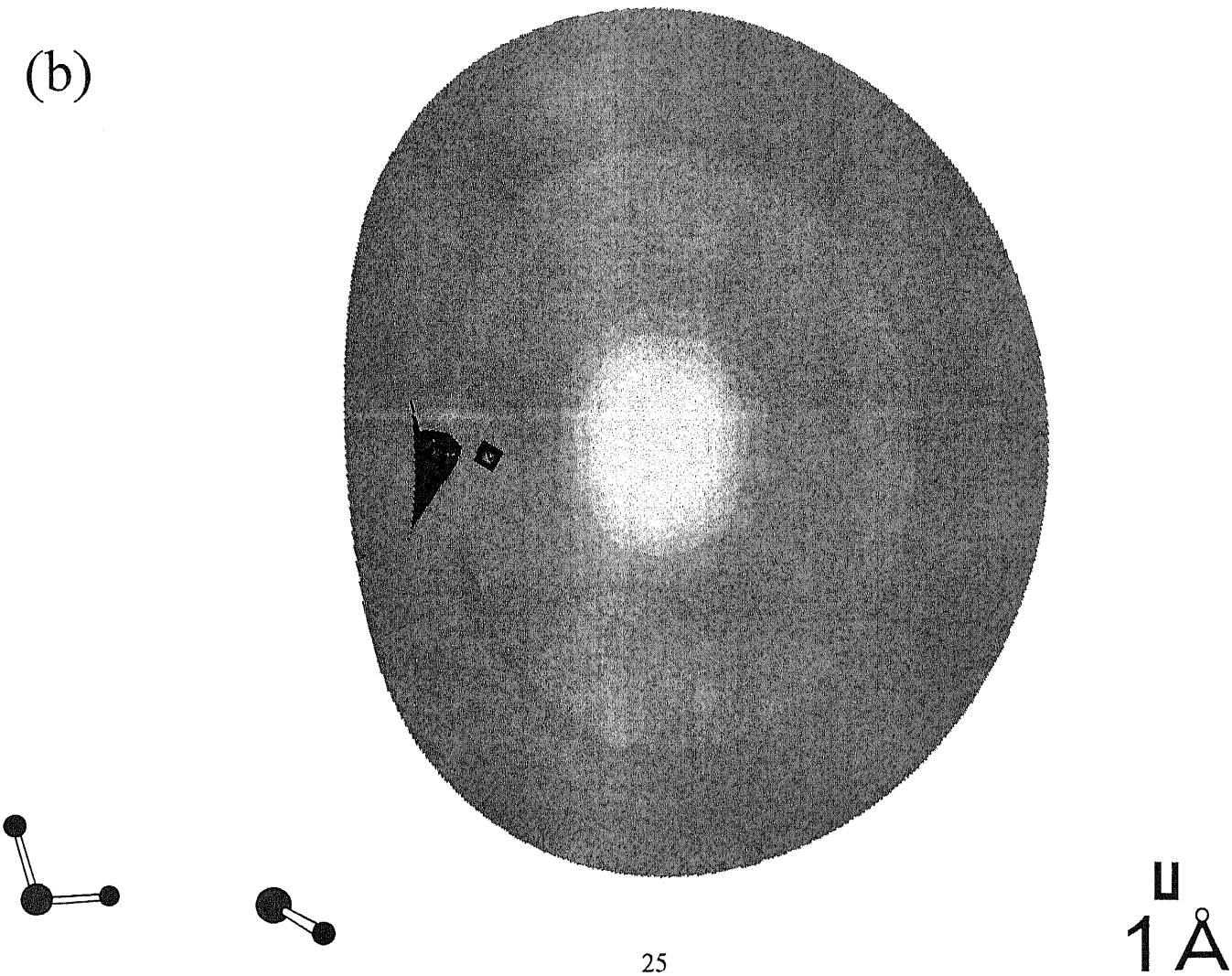

Fig. 1 (1/2)

(c)

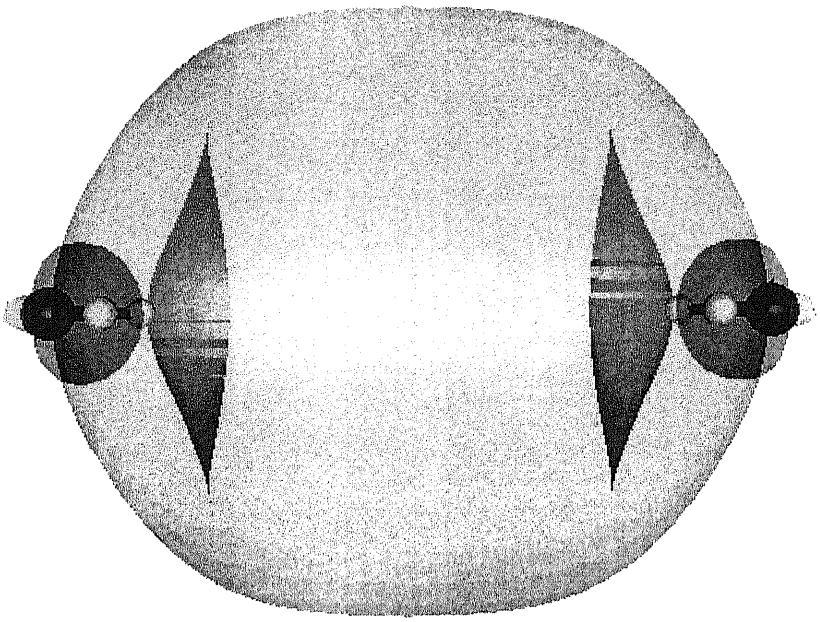

1 Å

(d)

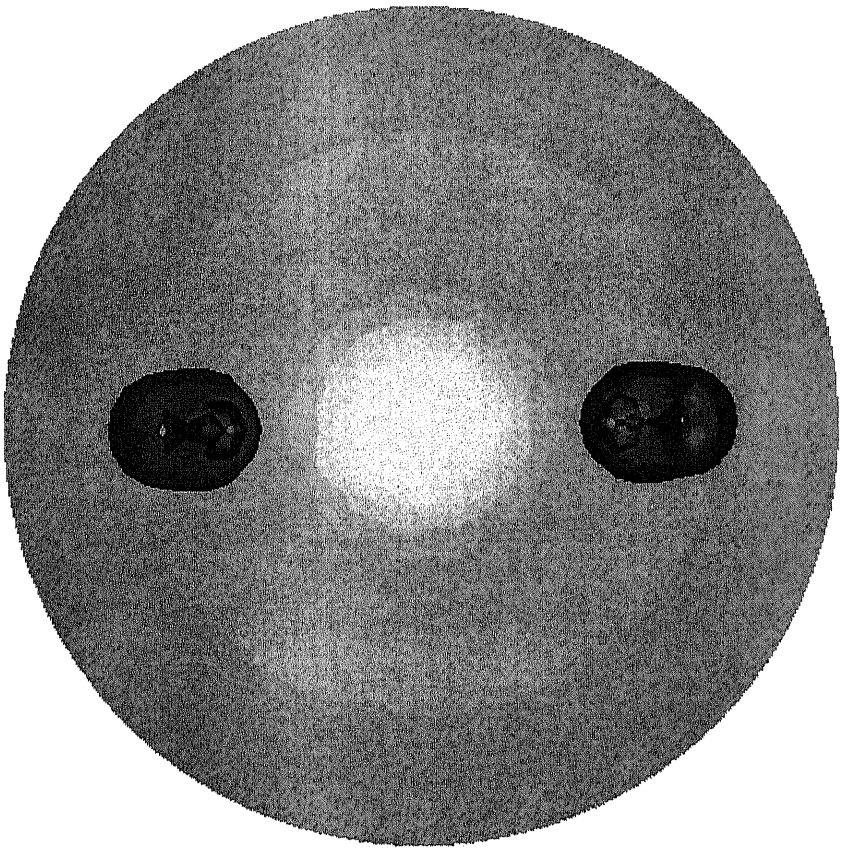

1 Å

Fig. 1 (2/2)

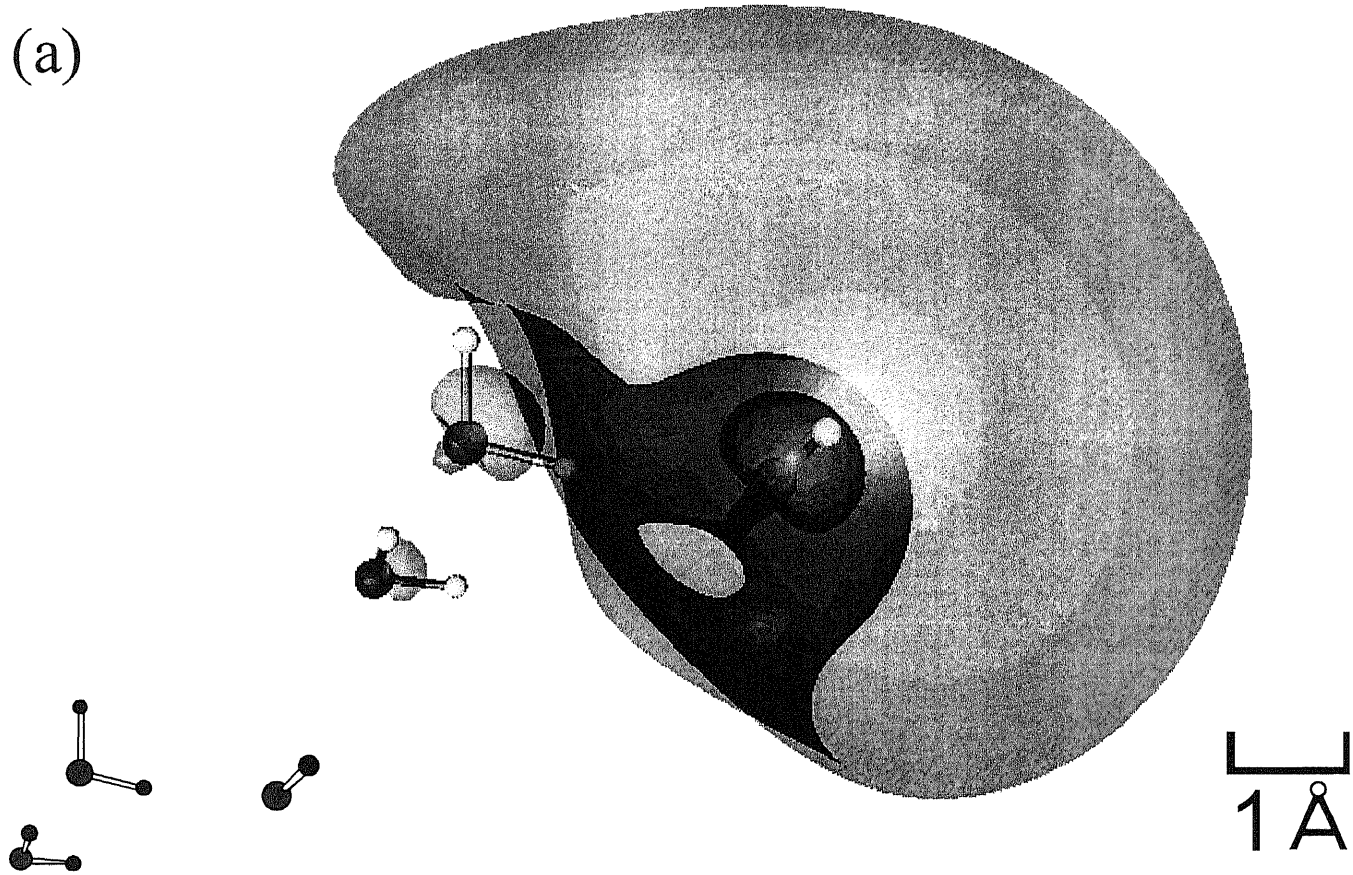

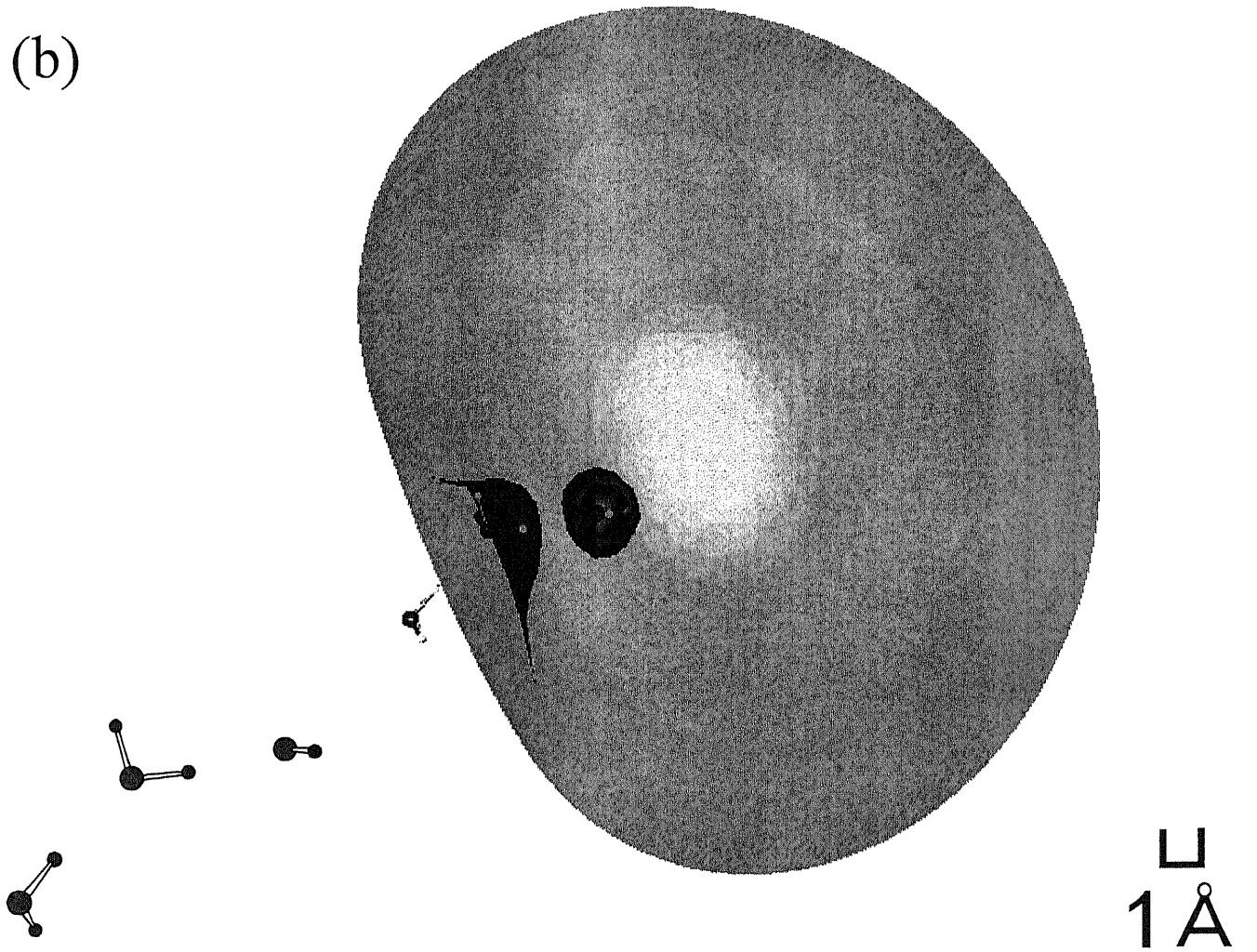

Fig. 2 (1/3)

(c)

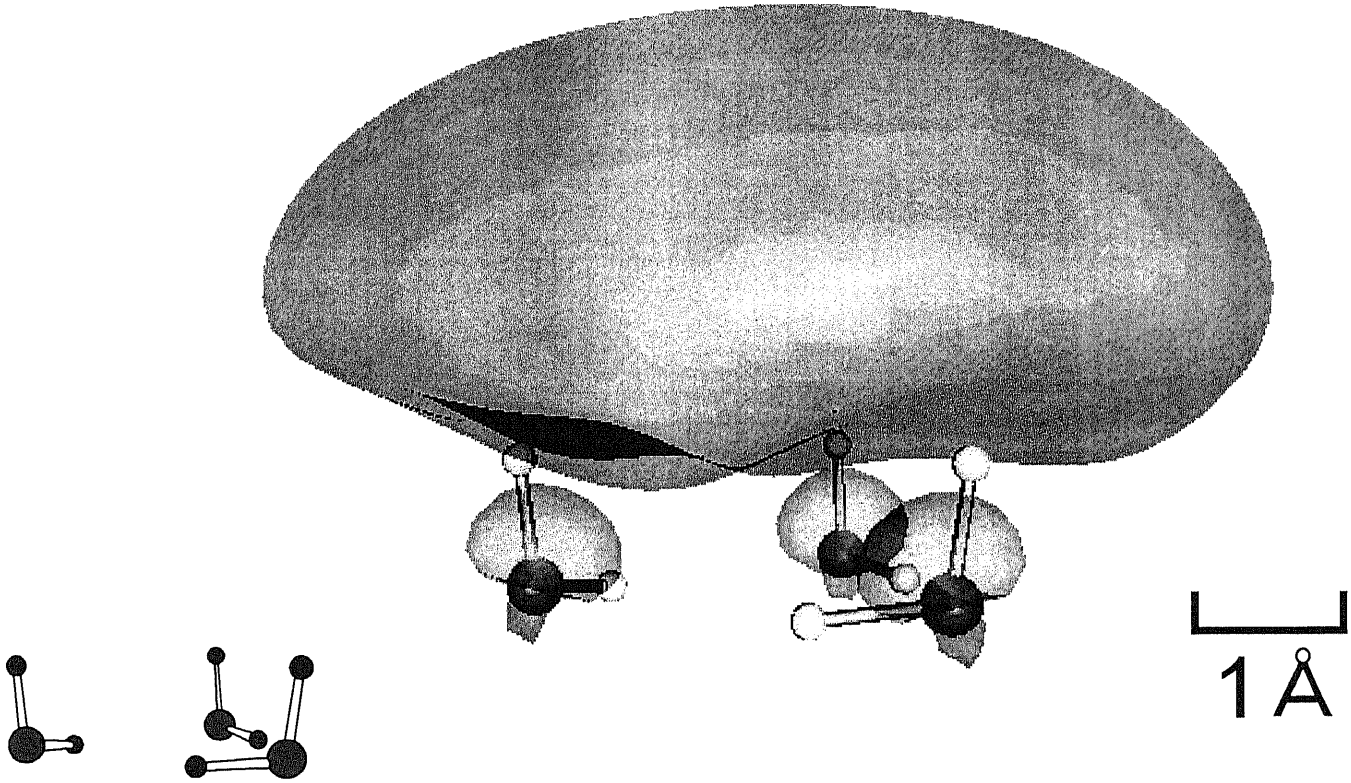

Fig. 2 (2/3)

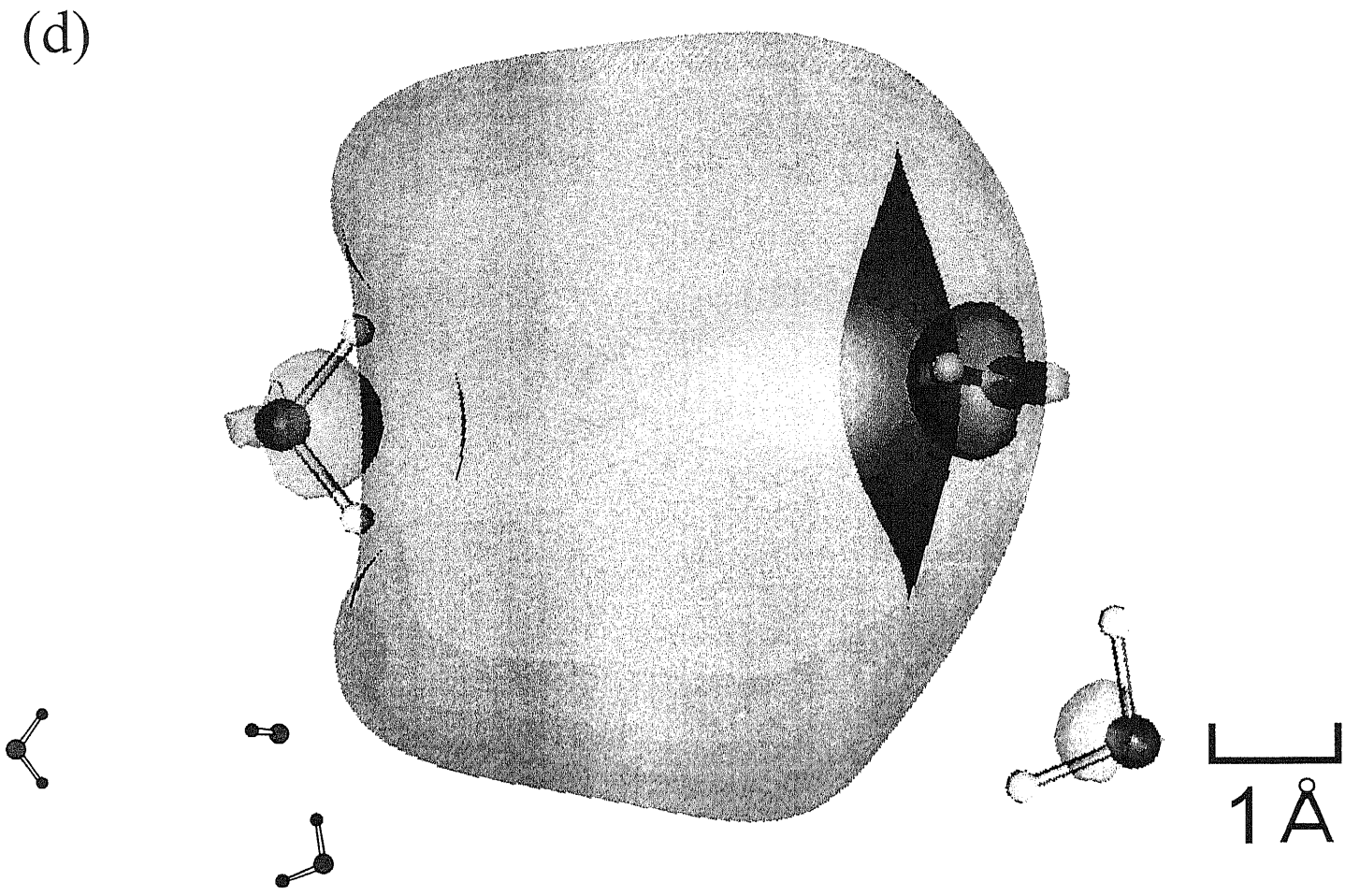

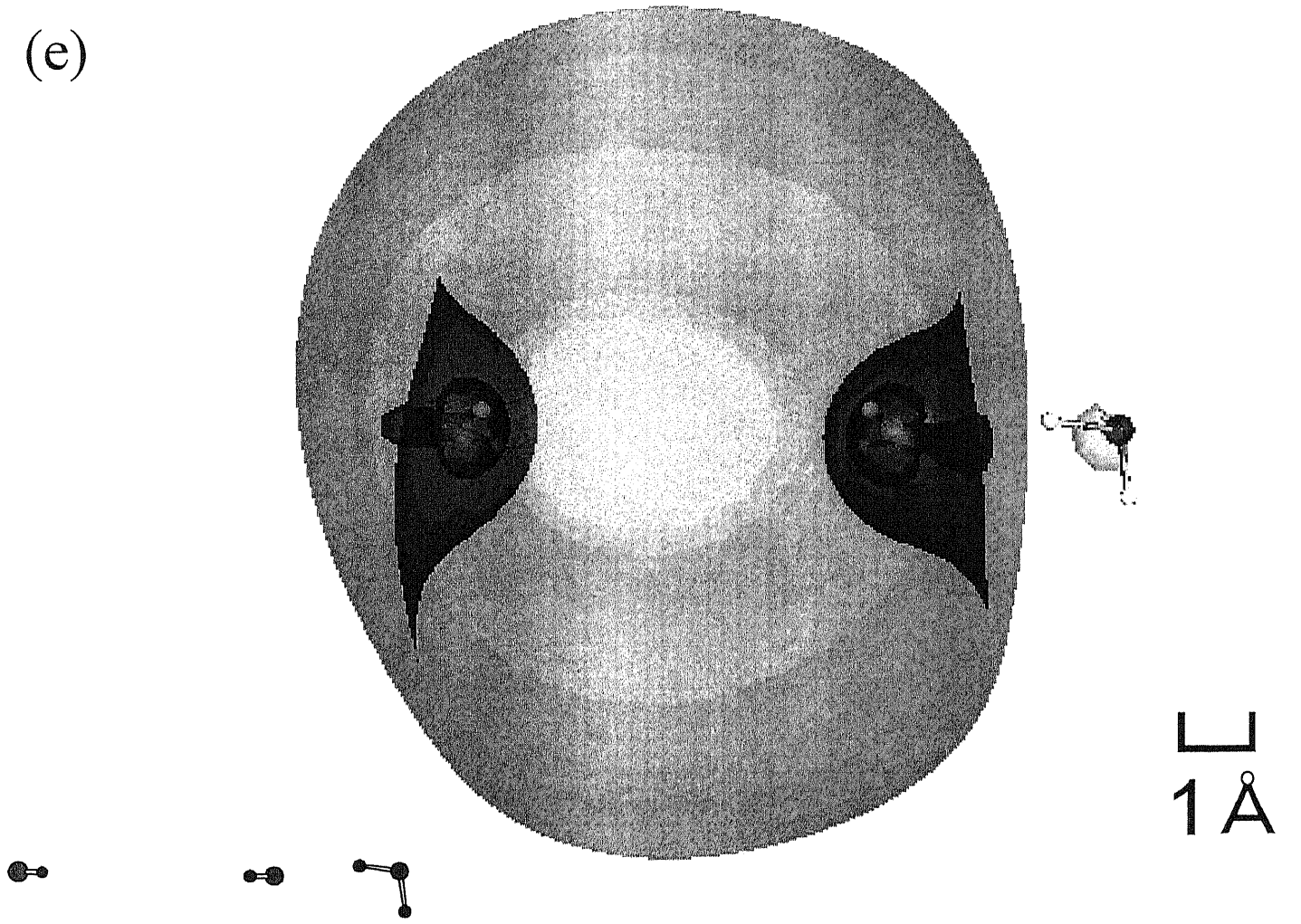

Fig. 2 (3/3)

2-S

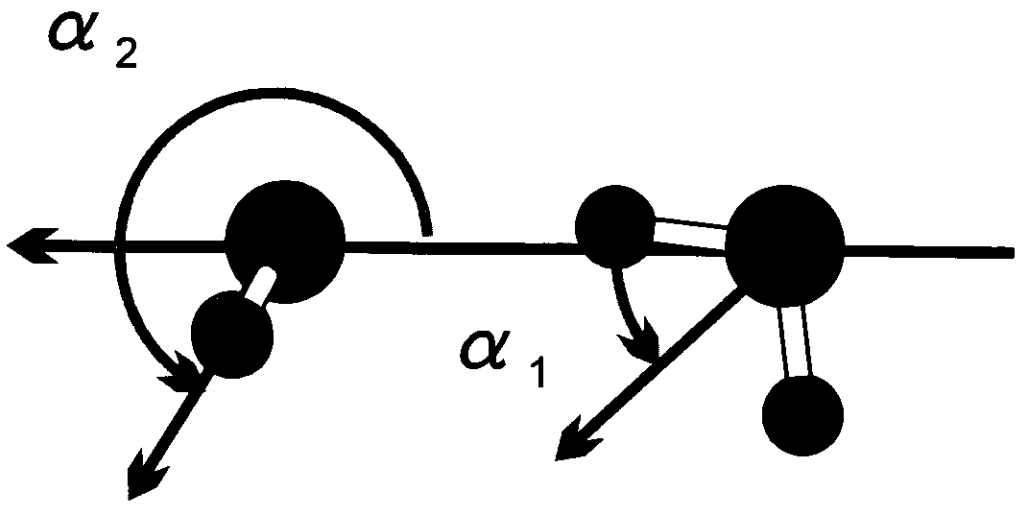

3-S

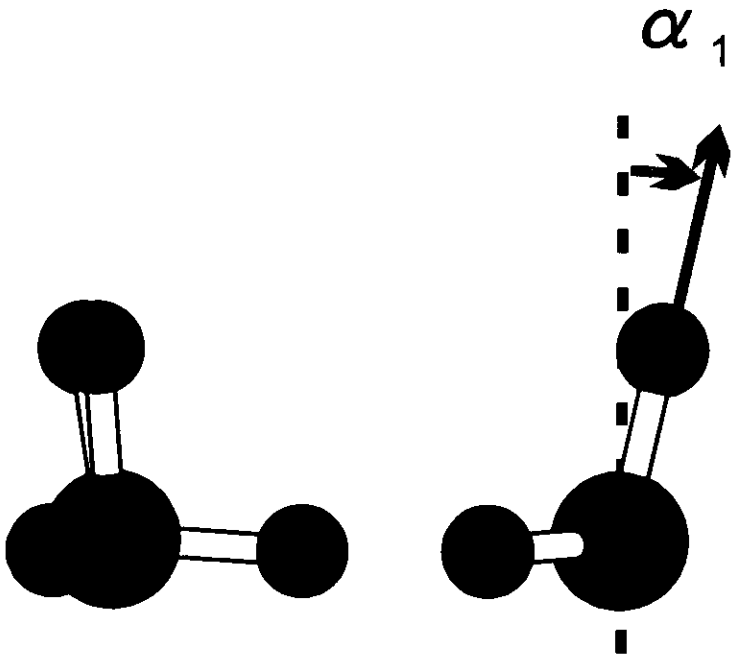

Fig. 3 (1/2)

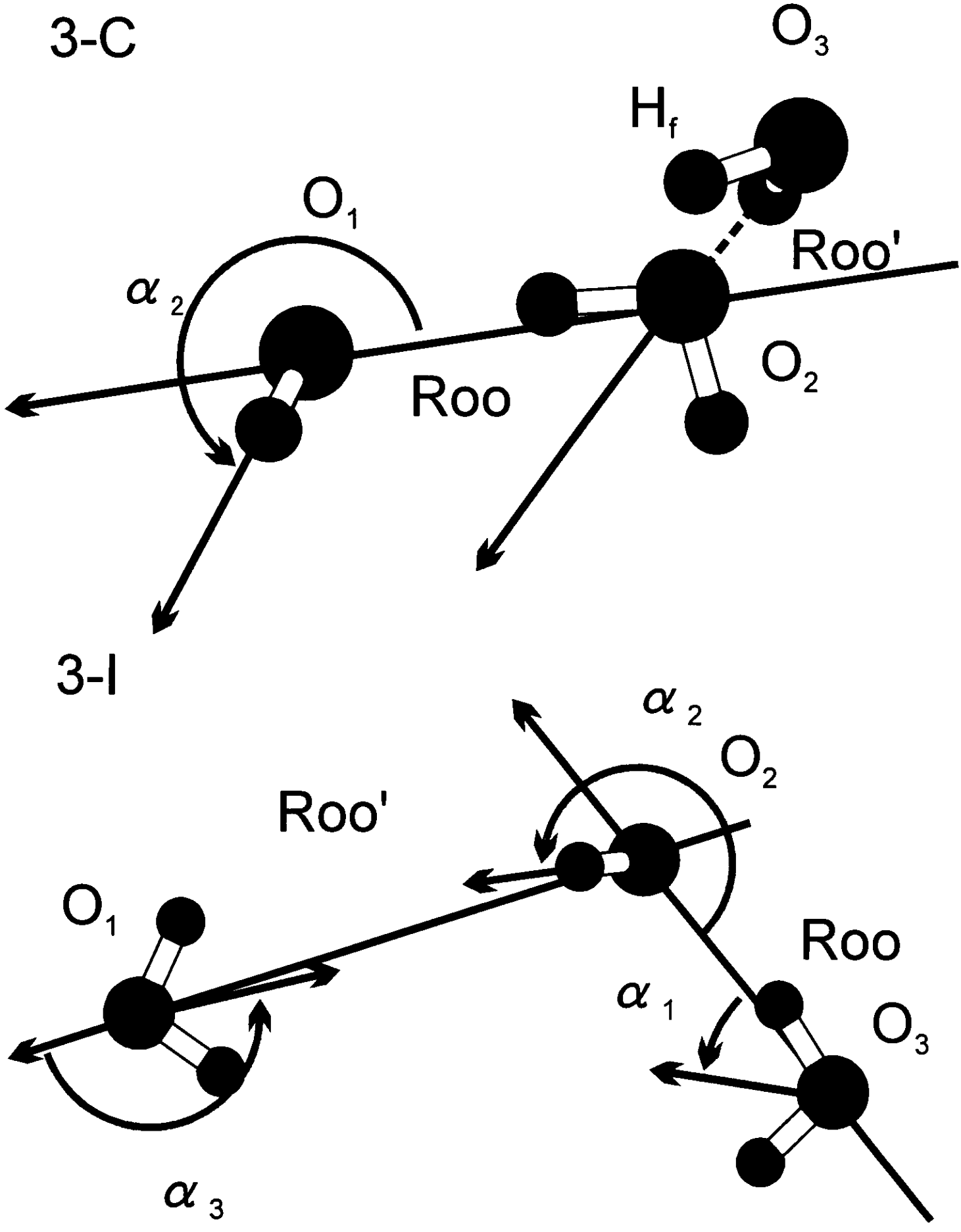

Fig. 3 (2/2)

3W-a (D_{3h})

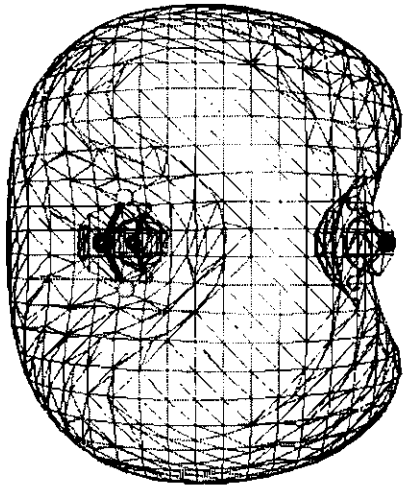

SEM = 257 Å^3
VDE = 0.227 eV

Figure 4

Chapter 3

Theoretical studies of the water cluster anions containing the OH{e}HO structure: energies and harmonic frequencies

Chemical Physics Letter, 315 (2000) 433–440

3.1 Introduction

Since the first observation of the water cluster anions in the gas phase [1, 2, 3], many experimental and theoretical works have been reported. In the experimental studies, water cluster anions, $(H_2O)_n^-$ for $n \geq 2$ are detected in mass spectra. It is known that a single water molecule itself cannot be able to bind the excess electron. Interestingly, the observed signals for n=3, 4, 5, 8, 9 and 10 are very weak [1, 2, 3, 4, 5, 6]. Following these earlier experiments, further spectroscopic studies were carried out by several groups [7, 8, 9, 10, 11, 12, 13, 14]. Recently, the vibrational spectra of $(H_2O)_n^-$ for

n = 2, 3, 5–9 and 11 are also reported [15, 16]. Although experimental information is still increasing, it is not enough to identify the structures of the observed anions without theoretical support. In the theoretical point of view, the quantum path-integral simulations with model potentials showed that there are two distinct states for the excess electron in the water cluster anions [17]. One is the internal state, in which the excess electron is localized inside the cluster. Another is the surface state, in which the excess electron is bound on the surface of the cluster. It was shown that the surface state is favored for small size clusters. Ab initio MO calculations for the water cluster anions were also reported by several authors [18, 19, 20, 21, 22, 23, 24, 25, 26, 27, 28, 29]. For the surface state anions, ab initio MO calculations illustrated that the excess electron is weakly bound on the surface of the cluster. It is believed that the excess electron is bound by the electric dipole field made by a neutral cluster, and it is often called a dipole-bound electron. It should be noted that a dipole-bound electron is not localized near the cluster, but it is very diffuse in nature. On the other hand, for the internal state, I have shown that even for dimer and trimer anions, there are stable internal states, and the interaction between the excess electron and the surrounding OH bonds plays an important role in holding the stable structure [29]. I call such a basic structure found in the internal state anions OH{e}HO structure. Recently, I also have found the isomers of the water clusters containing a group 1 atom $M(H_2O)_n$ (M = Li and Na), which have the similar OH{e}HO structure, and it turns out that the calculated vertical ionization energy (VIE) of these isomers can explain the abnormal observed trends [30]. To characterize the OH{e}HO structure in $M(H_2O)_n$ I calculated the vibrational frequency shifts $\Delta\nu_{OH}$ of the OH bonds. The shifts are as large as those in the OH bonds in the hydrogen bondings, and the OH bond lengths in the OH{e}HO structure are lengthened as in the ordinal hydrogen bonds [30, 31]. Because of this similarity between OH bonds in the OH{e}HO structure and those in the ordinal hydrogen bondings, the interaction between {e} and OH bonds in the OH{e}HO structure may be called electron-hydrogen bond. For the larger water cluster anions, with n = 6 and 12, Kim et al. showed that there are several isomers in both internal and surface states [20, 21, 22, 23, 24].

In this chapter, with extensive ab initio MO calculations, I will show the structures, the energies

and the harmonic vibrational frequencies of the OH bonds for tetramer and hexamer anions and explore the OH{e}HO structure in the anions.

3.2 Method

For the geometry optimization of the water cluster anions, the MP2 level of approximation is used. In my previous study for water dimer and trimer anions [29], I have found that it is necessary to work at least at the MP2 level of approximation to obtain the reliable results. The expectation value of S^2 in the MP2 wave function always satisfies $< S^2 >= 0.750$. Also I have examined how the optimized geometries of the water cluster anions which have the OH{e}HO structure are sensitive to the diffuse functions added to describe the excess electron. In the previous calculations for the dimer and the trimer of the water cluster anions, I employed a set of the floating gaussian functions to describe the excess electron. Instead, in the present studies, I use a set of diffuse s and p type functions on all oxygen atoms in the cluster. It is because I found out that for larger clusters, a set of floating gaussian functions sometimes introduces an artificial attractive force between two water molecules near the center of floating gaussian functions. To determine the number of diffuse functions for augmenting the 6-311++G(d,p) basis set, I performed the preliminary geometry optimization calculations, and decided to use three sp functions of α = 0.02815, 0.00938 and 0.00312 for tetramer anions. The first two functions are used for hexamers. The harmonic vibrational frequencies are also calculated and the stable structures are confirmed. All calculations are carried out with Gaussian98 [32] registered at the computer center of Institute for Molecular Science. To express the diffuseness of the excess electron, the SOMO extend measure (SEM), which is defined in the previous paper [30] as the volume of the sphere containing a half of SOMO electron, is evaluated.

3.3 Results and discussion

The optimized geometries and their infrared (IR) spectra are shown in Figures 1 and 2 for tetramer and hexamer, respectively. The SOMO extent measures (SEMs) and the vertical detachment energies (VDEs) are also listed in the figures. The frequency shifts corresponding to the OH stretching mode $\Delta\nu_{OH}$ are measured from the average of two calculated OH stretching frequencies of the monomer water molecule.

3.3.1 Tetramer

Three isomers of tetramer are shown in Fig. 1. Isomer 4W-a in Fig. 1(a) is an internally bound electron type isomer, in which the excess electron is surrounded by two linear dimers. In this isomer, there is no hydrogen bond between a pair of water dimers, and the interaction between the excess electron and the surrounding OH bonds holds this structure. This structure is similar to the structure of the trimer 3-I that I previously reported. In the trimer 3-I, a monomer water molecule replaces one of the dimer in 4W-a [29]. The VDE is 0.414 eV and SEM is 165 Å^3. The distance between two oxygen atoms in the water molecules W_1 and W_1' in Fig. 1(a) is 5.449 Å, which is shorter by 0.883 Å than in the isomer 3-I [29]. Because the terminal hydrogen atoms of the proton acceptor water molecule in the water dimer are more positive than that of the monomer, the interaction between the excess electron and the OH bonds is stronger than in 3-I. Therefore, the distance between two dimers becomes shorter. The $\Delta\nu_{OH}$ of the OH bonds interacting with the electron {e}, which I denote as {e}HO, are -158 cm^{-1} and -81 cm^{-1} for symmetric and antisymmetric stretching modes, respectively. In the figures, the IR bands of the OH stretching modes in the {e}HO bonds are indicated by the arrows. The $|\Delta\nu_{OH}|$ for the hydrogen bonded OH in the water dimers is 219 cm^{-1} and larger than those of the {e}HO bonds.

Isomer 4W-b has also an internally bound electron structure which consists of a water trimer and a water molecule. This isomer is reached when I start at a D_{4h} structure similar to the D_{3h} trimer

(3W-a). The isomer of D_{4h} structure has more than one imaginary frequencies and the potential energy surface is connected to 4W-a and 4W-b isomers. The VDE and SEM of isomer 4W-b are 0.447 eV and 145 Å^3. The distance between two oxygen atoms in the water molecules W_1 and W_2 is 5.945 Å and slightly longer than that of D_{3h} trimer. Although the largest shift $|\Delta\nu_{OH}|$ is of the stretching mode of the hydrogen bonded OH between W_1 (W_1') and W_3, as seen in Fig. 1(b), three modes of the {e}HO bonds appear in the range from -146 to -120 cm^{-1}. The mode at -49 cm^{-1} with the largest intensity is an antisymmetric stretching one of the {e}HO bonds.

Isomer 4W-c is the one that Smith et al. reported as the most stable isomer of the dipole-bound tetramer anions [26]. This structure has a ring structure and one of the water molecule (W_1) is a double proton acceptor water molecule. The structure is derived from the most stable neutral tetramer by flipping two molecules W_1 and W_4. The distribution of the excess electron of this isomer is very diffuse and its SEM is 521 Å^3. The electron in SOMO interacts mostly with the double proton acceptor water molecule W_1. Although the SEM is much larger than those of 4W-a and 4W-b, the shifts $|\Delta\nu_{OH}|$ of the {e}OH modes are -164 cm^{-1} and -68 cm^{-1}; comparable to those of 4W-a and 4W-b. As I have mentioned in the previous paper [30, 31], the double proton acceptor water molecule in $M(H_2O)_n$ interacts strongly with the SOMO electron and shows the large $|\Delta\nu_{OH}|$. It is also true in $(H_2O)_n^-$. The IR intensities of this isomer is larger than those of 4W-a and 4W-b. It is because SEM is large, and the OH stretching motions induce a large distortion in the electron distribution. The VDE is 0.163 eV. The largest two shifts $|\Delta\nu_{OH}|$ are for the breathing modes of the hydrogen bonded ring.

In my works on $M(H_2O)_n$ (M = Li and Na) [30], the nature of the SOMO electron in $M(H_2O)_n$ is determined by local bond dipoles of OH bonds, and by the long-range electrostatic potential of the hydrated metal cation. Similarly in $(H_2O)_n^-$, the characteristics of the excess electron is determined by the local interaction with the OH bonds, and by the total dipole moment of the neutral isomer or that of the neutral fragments surrounding {e}. The SEM is mostly determined by the latter. Therefore, SEM of $(H_2O)_n^-$ is larger than that of $M(H_2O)_n$. On the other hand, the shifts $|\Delta\nu_{OH}|$ of the {e}HO

bonds are obviously determined by the local interaction.

3.3.2 Hexamers

The optimized geometries and their calculated IR spectra for three isomers of hexamer anions are shown in Fig. 2. Kim and his co-workers reported many isomers for hexamer anions [23]. I have also located more isomers, and only representatives are discussed in this letter. Experimentally two isomers of hexamer anions (I and II) are distinguished in the photoelectron spectra [12, 13], but their structures are still controversial.

Isomer 6W-a is the one of the similar isomers of trimer 3-I and tetramer 4W-a. The excess electron {e} is surrounded by a pair of linear water trimer. In other words, two water trimers are fixed by the electron {e} as in trimer 3-I and in tetramer 4W-a. The distance between the oxygens of water molecules W_1 and W_1' is further shortened to 4.938Å. Its SEM is as small as $109Å^3$, which is the smallest among the anions in this work. A linear water trimer has a large dipole moment and the terminal hydrogen atoms are more positively charged. Thus, the excess electron distribution between the pair of trimers becomes smaller than in 4W-a. The VDE is 0.773 eV, which is the largest among the anions studied here. In the calculated IR spectrum, a pair of {e}HO modes are found at -199 and -129 cm^{-1}, which are further downward shifted from the corresponding ones (-158 and -81 cm^{-1}) in 4W-a. This is reasonable because of stronger interaction between {e} and HO bonds in 6W-a than in 4W-a. The modes of the hydrogen bonded OHs are more downward shifted; the shift of the stretching mode in W_2 (W_2') is larger than that of W_3 (W_3'), because W_2 and W_2' are the proton-accepting water molecules. As is seen in Fig. 2(a), these four peaks have appreciable intensities.

Isomer 6W-b consists of a four membered ring and two double proton acceptor water molecules. This structure is similar to one of the most stable hexamer anions reported by Kim and his co-workers; the one called Y42 [23]. But there is an important difference between 6W-b and Y42. In isomer Y42, two water molecules, standing on the top of the tetramer ring, are single proton acceptor water molecules. This difference influences on the strength of the interaction between {e} and OHs. In

6W-b, one of the OH bonds of the double proton acceptor water molecules (OH_1 and OH_1') directs to each other, and the excess electron {e} somewhat exist between these bonds. The similar conformation was found in the anion part of the ion pair $M^+(H_2O)_n^-$ (M=Li and Na), and it was shown that the interaction between {e} and OH bonds is strong in this type of conformation [30, 31]. For instance, in one of the isomers of $Li(H_2O)_6$, which has a double proton acceptor water molecule, the shift of the {e}HO mode is as large as -565 cm^{-1} and SEM is 53Å^3. In 6W-b, the SEM is 162Å^3 and the shifts of the {e}HO modes are -252 and -220 cm^{-1}, both of which have large IR intensities. The two {e}HO modes are the stretching vibrations of the OH_1 and OH_1'. Although the excess electron {e} in 6W-b interacts mainly with OH_1 and OH_1', it also interacts somewhat with OH_2 and OH_2'. In that sense, the electron {e} in this isomer is not a typical internally bound electron in the present level of approximate calculation. Weak bands at -313 and -274 cm^{-1} in the calculated spectrum are the breathing modes of the tetramer ring. The bands bellow $|\Delta\nu_{OH}| = 100$ cm^{-1} are the other OH stretching modes of the ring water molecules and those of OH_2 and OH_2'. I have examined the harmonic frequencies of Y42 and the shifts of {e}HO modes are -160, -155 and -86 cm^{-1}, which are smaller than those in 6W-b because Y42 has no double proton acceptor water molecules. In my calculations, the total energies of Y42 and 6W-b are very close; the latter is less stable by 2.81 kJ/mol than Y42.

Experimentally, Ayotte et al. observed the IR spectrum of $(H_2O)_6^-$ and the characteristics of the spectrum are a pair of strong bands at $\Delta\nu_{OH} = -440$ and -330 cm^{-1} [15]. The pair of strong IR bands both in the calculated spectrum for 6W-b and the observed spectrum by Ayotte et al. are similar to each other except for the absolute values of the shifts and the splitting. I found that the shifts $|\Delta\nu_{OH}|$ of the {e}HO bonds reflect the strength of the interaction between {e} and OH bonds [31]. Similarly in $(H_2O)_n^-$, the shifts are determined by the strength of the interaction between {e} and OH bonds. The splitting of two strong bands in Fig. 2(b) is the result of the coupling of OH_1 and OH_1' stretching modes through the interaction between {e} and OH bonds, and therefore the magnitude of the splitting is also related to the strength of the interaction between {e} and OH bonds. In the present

level of calculation, the strength of the interaction between {e} and OH bonds is underestimated, and the calculated frequency shifts and the splitting are smaller than the experimental values. For the geometry optimization and frequency calculations, more thorough studies with higher level of electron correlation are required to obtain more quantitative results for this type of isomers. As are seen in Figs. 1 and 2, the IR bands of {e}HO modes carry characteristical strong intensities. Fortuitously or not, the calculated VDE for 6W-b is 0.489eV, which is close to the experimental VDE (0.5 eV) [13] of isomer II of $(H_2O)_6^-$.

Isomer 6W-c is the most stable hexamer anion among the isomers examined, which include some of the isomers reported by Lee et al. [23]. The structure of 6W-c is derived from a prism isomer, which is one of the most stable neutral hexamers [33], by breaking two hydrogen bonds and flipping a water molecule to make the cluster have a larger dipole moment. Isomer 6W-c has two double proton acceptor water molecules, and the HOs of one of them (W_1) strongly interact with the excess electron {e}. While the local structure around W_1, W_2 and {e} is similar to that of 4W-c, the SEM of 6W-c is 209Å^3 which is much smaller than that of 4W-c (521Å^3), and the shifts (-231 and -154 cm^{-1}) of the {e}HO modes are larger than those in 4W-c (-199 and -129 cm^{-1}). The mode of the largest shift (340cm^{-1}) is the stretching mode of the OH in W_2, which hydrogen-bonds with W_1. The calculated VDE is 0.382 eV, and is smaller than that of 6W-b by 0.107 eV. The experimental VDE difference of two isomers is 0.3 eV, which is much larger than the VDE difference of 6W-b and 6W-c. I have also obtained the chain-like hexamer with MP2 calculation, and its SEM is as large as 268 Å^3, which is larger than that of 6W-c, as in typical dipole bound isomers.

Ayotte et al. claimed that the observed isomer II in their spectrum was a chain-like isomer [16]; at the end of the chain the electron is trapped as in the dipole bound electron of water dimer anion. They have assigned the two strong peaks in the IR spectrum to stretching modes of hydrogen bonded OH bonds. Bailey et al. estimated a 1.1 % change in the OH bond length in the photodetachment process [12]. When the electron is detached from the anions, the changes of the hydrogen bonded OH bonds are rather small, and therefore the progression in the photoelectron spectrum mainly reflects

the changes of the {e}HO bond lengths. In my calculation, the {e}HO bond lengths in double proton acceptor water molecules in 6W-b are as long as 0.9700 Å which is about 1.1 % longer than the OH bond length of a monomer water molecule (0.9595 Å), while the {e}HO bond lengths of the end water molecule in the chain-like hexamer are 0.9664 and 0.9672 Å.

3.3.3 Correlation of the calculated VDE with the SEM

In Fig. 3, VDE is plotted against SEM. Besides the all isomers shown in Figs. 1 and 2, the data for Y51 and Y42 hexamer anions in Ref. 23, a linear trimer anion, 3W-a trimer in chapter 2 and a hexamer anion with a five membered ring and a double proton acceptor water molecule, are included in the plot. A strong correlation of SEM with VDE is evident in the figure; as SEM decreases, VDE increases. The similar trend found by Bailey and Johnson in their hexamer anions [13]. If the isomer have a large SEM, the excess electron have, if any, little effect on the water cluster skeleton; the structure is similar to that of the stable neutral cluster [29]. In this situation, the excess electron is bound mainly by the dipole moment of the neutral cluster. On the other hand, when SEM is small, the excess electron deform the structure of the cluster in order to stabilize itself, and the shrinking of SEM interplays with the restructuring of the water cluster. The structural change from that of the stable neutral cluster leads to increase the energy of the neutral cluster. Consequently, VDE increases rapidly while SEM decreases. Fig. 3 suggests that the isomer I of the hexamer, whose VDE is about 0.2 eV [13], should have larger SEM than 6W-c, and that it is most likely to be a dipole bound electron isomer which has similar structure to the stable neutral cluster. For $M(H_2O)_n$, I also found a similar correlation between the vertical ionization energy (VIE) and the SEM. The VIE increases when the SEM decreases for the isomers with the same n [30].

3.4 Conclusion

I studied the structures and the IR spectra for tetramer and hexamer anions by ab initio MO method. I found the internally bound electron structure 4W-a, 4W-b and 6W-a. These structures consist of two separated water clusters, between which no hydrogen bonds are formed. Two clusters are held by the interaction between the excess electron {e} and the surrounding OH bonds. I call the core structure of the internally bound electron as OH{e}HO structure, and the interaction between {e} and OHs in OH{e}HO structure as an electron-hydrogen bond. In all calculated IR spectra shown here, the largest $|\Delta\nu_{OH}|$ corresponds to the stretching mode of the hydrogen bonded OHs. While the shifts $|\Delta\nu_{OH}|$ of the {e}HO bonds in $(H_2O)_n^-$ are smaller than that I found in $M(H_2O)_n$ clusters, the $|\Delta\nu_{OH}|$ of the {e}HO bond in the double proton acceptor water molecule is larger than those of the other {e}HO bonds. For hexamer anions, 6W-b isomer, which have two double proton acceptor water molecules, shows a qualitatively similar spectrum with the observed vibrational spectrum for the isomer II of $(H_2O)_6^-$, although Ayotte et al. claimed that the observed isomer II is a chain-like isomer. To draw the quantitative conclusion, more thorough studies with higher level of electron correlation are required. I also found the strong correlation between VDE and SEM. The VDE increases with decreasing SEM. From this correlation, the isomer I observed in the experiment for $(H_2O)_6^-$ is likely to be a dipole bound anion and to have a structure close to the stable neutral cluster.

Acknowledgement

The present work was partially supported by the Grant-in-Aids for Scientific Research (No.11640518) by the Ministry of Education, Science, Sports, and Culture, Japan, and by Research and Development Applying Advanced Computational Science and Technology, Japan Science and Technology Corporation (ACT-JST). A part of calculations was carried out at the Computer Center of the Institute for Molecular Science. I acknowledge Mr. Mizutani of the Computer Center for providing me his drawing program, PGV.

Bibliography

[1] M. Armbruster, H. Haberland, H.-G. Schindler, Phys. Rev. Lett., 47 (1981) 323.

[2] H. Haberland, H. Langosch, H.-G. Schindler, D.R. Worsnop, J. Phys. Chem., 88 (1984) 3903.

[3] H. Haberland, C. Ludewigt, H.-G. Schindler, D.R. Worsnop, J. Chem. Phys., 81 (1984) 3742.

[4] J.H. Hendricks, H.L. de Clercq, S.A. Lyapustina, C.A. Fancher, T.P. Lippa, J.M. Collins, S.T. Arnold, G.H. Lee, K.H. Bowen, in: T. Kondow (Ed.), Sturctures and Dynamic of Clusters, Procdeedings of the Yamada Conference XLIII, Universal Academy, Tokyo, 1995, p. 321.

[5] J.V. Coe, G.H. Lee, J.G. Eaton, S.T. Arnold, H.W. Sarkas, K.H. Bowen, C. Ludewigt, H. Haberland, D.R. Worsnop, J. Chem. Phys., 92 (1990) 3980.

[6] S.T. Arnold, Ph.D. Thesis, The Johns Hopkins University, 1993.

[7] L.A. Posey, M.A. Johnson, J. Chem. Phys., 89 (1988) 4807.

[8] L.A. Posey, P.J. Campagnola, M.A. Johnson, G.H. Lee, J.G. Eaton, K.H. Bowen, J. Chem. Phys., 91 (1989) 6536.

[9] P.J. Campagnola, L.A. Posey, M.A. Johnson, J. Chem. Phys., 92 (1990) 3243.

[10] P. Ayotte, M. A. Johnson, J. Chem. Phys., 106 (1997) 811.

[11] T. Maeyama, T. Tsumura, A. Fujii, N. Mikami, Chem. Phys. Lett., 264 (1997) 292.

[12] C.G. Bailey, J. Kim, M.A. Johnson, J. Phys. Chem., 100 (1996) 16782.

[13] C.G. Bailey, M.A. Johnson, Chem. Phys. Lett., 265 (1997) 185.

[14] J. Kim, I. Becker, O. Cheshnovsky, M.A. Johnson, Chem. Phys. Lett., 297 (1998) 90.

[15] P. Ayotte, C.G. Bailey, J. Kim, M.A. Johnson, J. Chem. Phys., 108 (1998) 444.

[16] P. Ayotte, G.H. Weddle, C.G. Bailey, M.A. Johnson, F. Vila, K.D. Jordan, J. Chem. Phys., 110 (1999) 6268.

[17] R.N. Barnett, U. Landman, C.L. Cleveland, J. Jortner, J. Chem. Phys., 88 (1988) 4429.

[18] D.M. Chipman, J. Phys. Chem., 83 (1979) 1657.

[19] R.N. Barnett, U. Landman, S. Dhar, N.R. Kestner, J. Jortner, A. Nitzan, J. Chem. Phys., 91 (1989) 7797.

[20] K.S. Kim, I. Park, S. Lee, K. Cho, J.Y. Lee, J. Kim, J.D. Joannopoulos, Phys. Rev. Lett., 76 (1996) 956.

[21] S. Lee, S.J. Lee, J.Y. Lee, J. Kim, K.S. Kim, I. Park, K. Cho, J.D. Joannopoulos, Chem. Phys. Lett., 254 (1996) 128.

[22] K.S. Kim, S. Lee, J. Kim, J.Y. Lee, J. Am. Chem. Soc., 119 (1997) 9329.

[23] S. Lee, J. Kim, S.J. Lee, K.S. Kim, Phys. Rev. Lett., 79 (1997) 2038.

[24] J. Kim, J.M. Park, K.S. Oh, J.Y. Lee, S. Lee, K.S. Kim, J. Chem. Phys., 106 (1997) 10207.

[25] D.M.A. Smith, J. Smets, Y. Elkadi, L. Adamowicz, J. Chem. Phys., 107 (1997) 5788.

[26] D.M.A. Smith, J. Smets, Y. Elkadi, L. Adamowicz, J. Chem. Phys., 109 (1998) 1238.

[27] D.M.A. Smith, J. Smets, L. Adamowicz, J. Chem. Phys., 110 (1999) 3804.

[28] Y. Bouteiller, C. Desfrançois, J.P. Schermann, Z. Latajka, B. Silvi, J. Chem. Phys., 108 (1998) 7967.

[29] T. Tsurusawa, S. Iwata, Chem. Phys. Lett., 287 (1998) 553.

[30] T. Tsurusawa, S. Iwata, J. Phys. Chem. A, 103 (1999) 6134.

[31] T. Tsurusawa, S. Iwata, in preparation.

[32] M.J. Frisch, G.W. Trucks, H.B. Schlegel, G.E. Scuseria, M.A. Robb, J.R. Cheeseman, V.G. Zakrzewski, J.A. Montgomery, R.E. Stratmann, J.C. Burant, S. Dapprich, J.M. Millam, A.D. Daniels, K.N. Kudin, M.C. Strain, O. Farkas, J. Tomasi, V. Barone, M. Cossi, R. Cammi, B. Mennucci, C. Pomelli, C. Adamo, S. Clifford, J. Ochterski, G.A. Petersson, P.Y. Ayala, Q. Cui, K. Morokuma, D.K. Malick, A.D. Rabuck, K. Raghavachari, J.B. Foresman, J. Cioslowski, J.V. Ortiz, B.B. Stefanov, G. Liu, A. Liashenko, P. Piskorz, I. Komaromi, R. Gomperts, R.L. Martin, D.J. Fox, T. Keith, M.A. Al-Laham, C.Y. Peng, A. Nanayakkara, C. Gonzalez, M. Challacombe, P.M.W. Gill, B.G. Johnson, W. Chen, M.W. Wong, J.L. Andres, M. Head-Gordon, E.S. Replogle, and J.A. Pople., Gaussian 98 (Revision A.5), Gaussian, Inc., Pittsburgh PA, 1998.

[33] J. Kim, K.S. Kim, J. Chem. Phys., 109 (1998) 5886.

Figure captions

Fig. 1. The calculated IR spectra and the optimized structure of tetramer anions. (a) 4W-a, (b) 4W-b and (c) 4W-c. The arrows indicate the bands of the stretching modes in {e}HO bonds. The horizontal axis is the frequency shift $\Delta\nu_{OH}$ in cm^{-1} and the vertical axis is the intensity in KM/Mole. The SEM and VDE are also listed in the figures. The intensity of the strongest band in (c) is 11106 KM/Mole as shown in the figure.

Fig. 2. The calculated IR spectra and the optimized structure of hexamer anions. (a) 6W-a, (b) 6W-b and (c) 6W-c.

Fig. 3. The correlation between VDE and SEM. In addition to the isomers shown in Figs. 1 and 2, the data for Y42 and Y51 in Ref. 23, a linear trimer anion, 3W-a trimer in chapter 2 and a hexamer with a five-membered ring structure and a double proton acceptor water molecule, are plotted together.

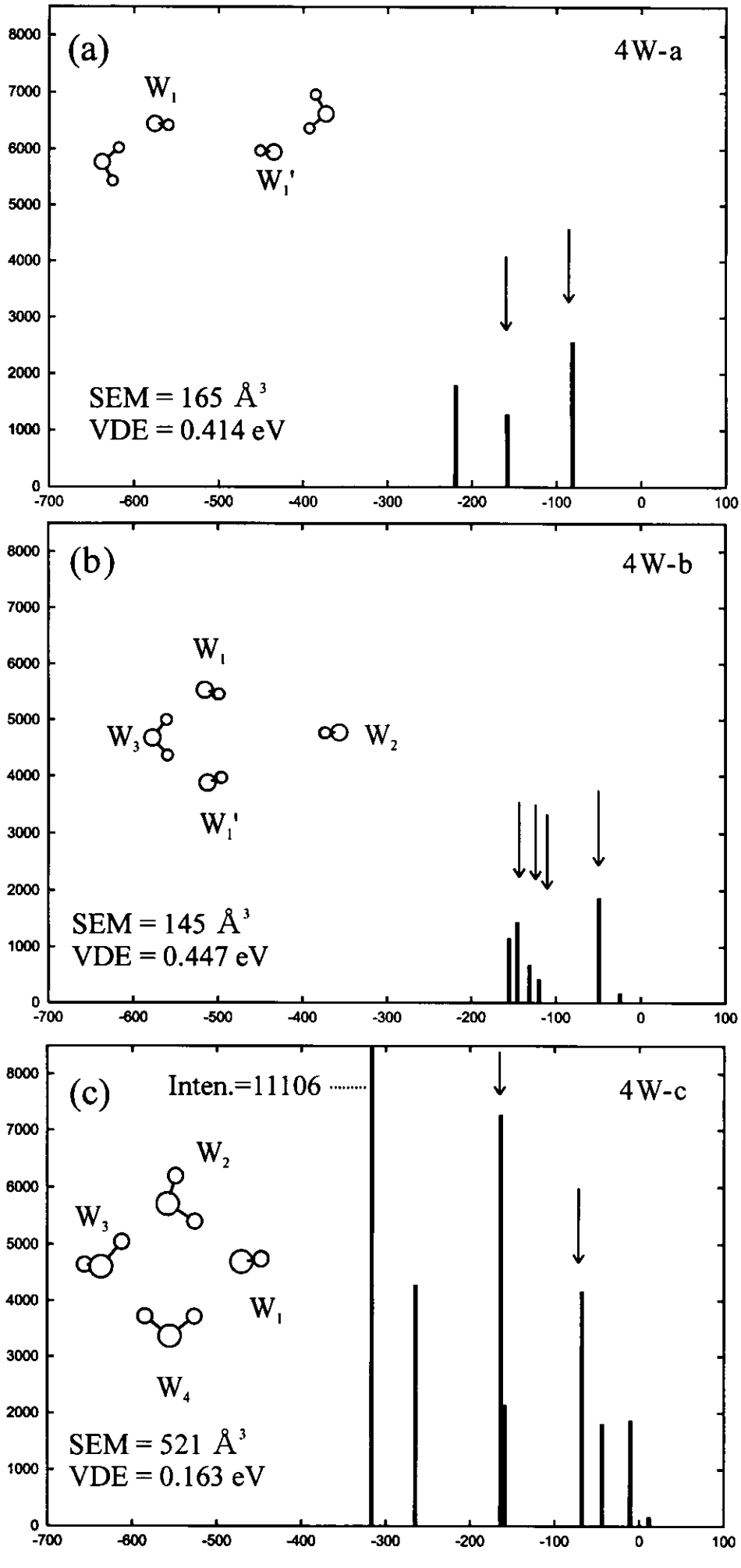
(a)
4W-a
W1
W1'
SEM = 165 Å3
VDE = 0.414 eV
(b)
4W-b
W1
W2
W3
W1'
SEM = 145 Å3
VDE = 0.447 eV
(c)
Inten.=11106
4W-c
W2
W3
W1
W4
SEM = 521 Å3
VDE = 0.163 eV
8000
7000
6000
5000
4000
3000
2000
1000
0
-700
-600
-500
-400
-300
-200
-100
0
100

Figure 1

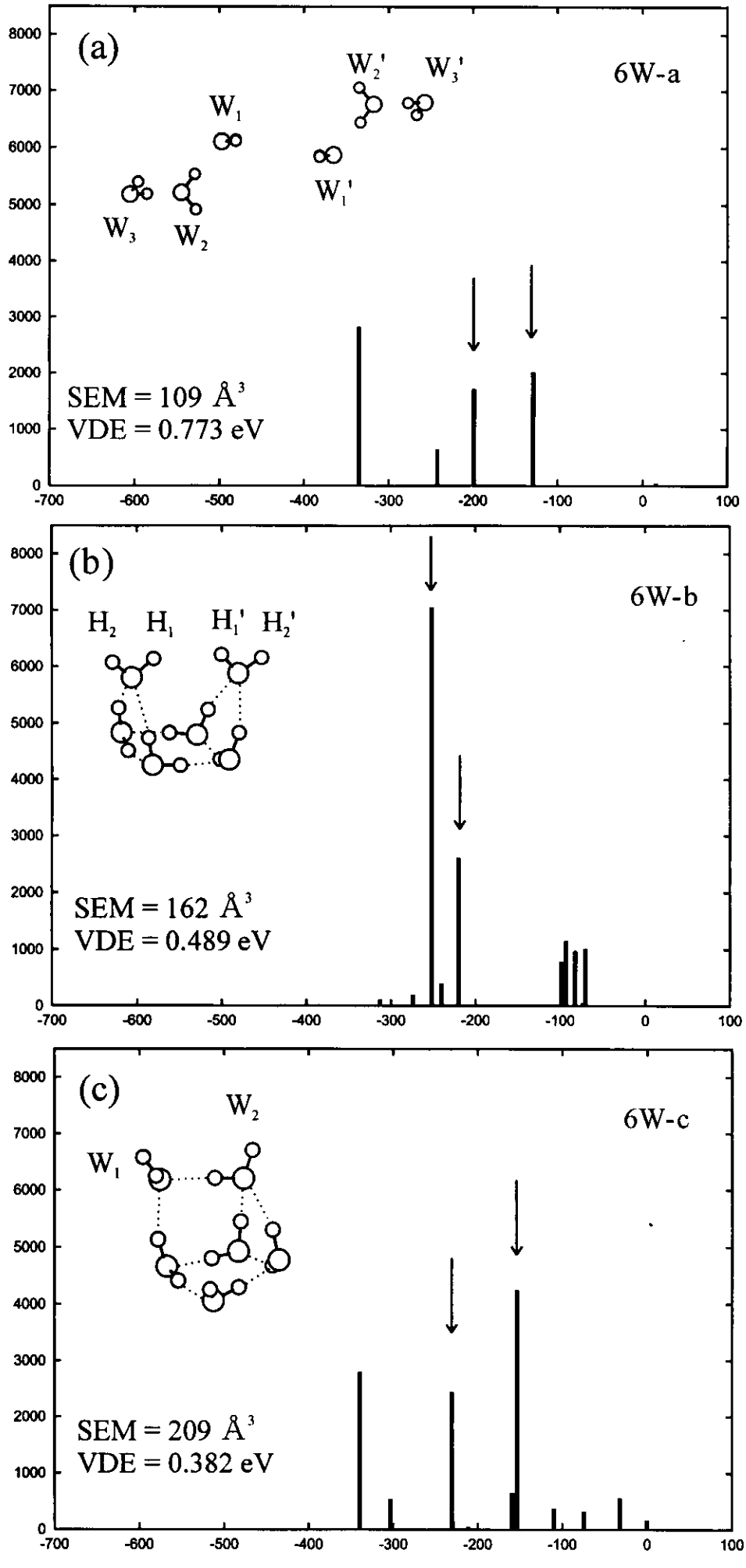
(a)
6W-a
W1
W2'
W3'
W1'
W3
W2
SEM = 109 Å3
VDE = 0.773 eV
(b)
6W-b
H2 H1 H1' H2'
SEM = 162 Å3
VDE = 0.489 eV
(c)
6W-c
W2
W1
SEM = 209 Å3
VDE = 0.382 eV

Figure 2

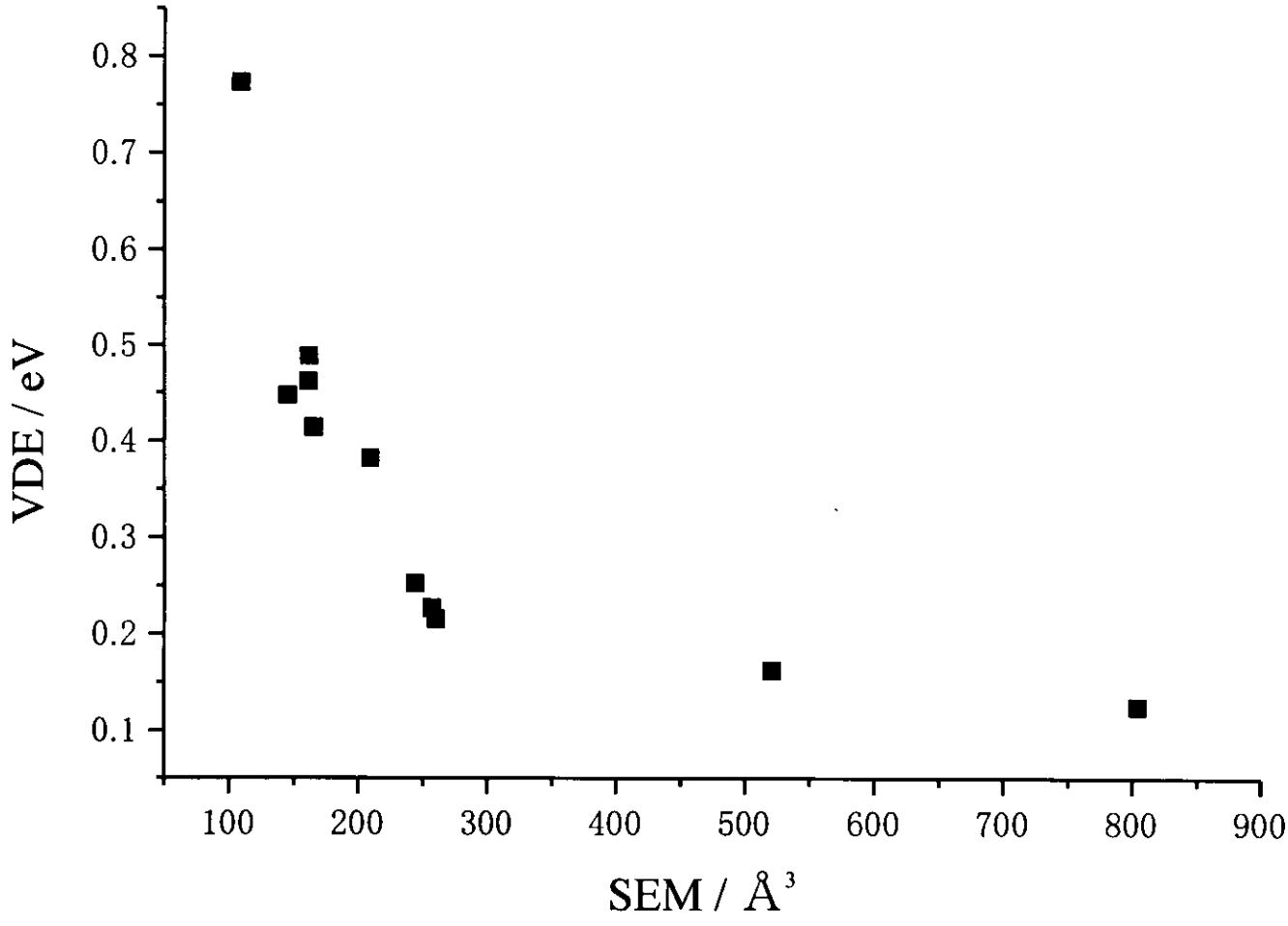
VDE / eV
0.8
0.7
0.6
0.5
0.4
0.3
0.2
0.1
100
200
300
400
500
600
700
800
900
SEM / Å^3

Figure 3

Chapter 4

Theoretical studies of structures and ionization threshold energies of water cluster complexes with a group 1 metal, $M(H_2O)_n$ (M = Li and Na)

Journal of Physical Chemistry A **1998**, *103*, 6134–6141

4.1 Introduction

The ionization threshold energies (ITEs) of water clusters containing a group 1 metal atom, $M(H_2O)_n$ (M=Li, Na and Cs) have been reported by Takasu et al. [1], Hertel et al. [2] and Misaizu et al. [3]. The observed ionization threshold energies of these clusters show several interesting features. For $n \leq 3$, the ITE decreases rapidly as n increases. But for $n \geq 4$, it becomes constant, and the converged value is nearly equal to the ionization energy of bulk water (about 3.2 eV [4]); the value is common for Li, Na and Cs. To explain this behavior, the experimentalists assumed that the solvated metal

atom is completely ionized and screened by four water molecules. In their model, the excess electron is ejected outside the first solvation shell, and the state of the excess electron is not affected by the solvated metal ion. Theoretical calculations were also performed to explore the anomalous features. Barnett et al. [5] showed by the local-spin-density functional method for $Na(H_2O)_n$, that the Na atom becomes ionized at $n = 4$ and that for $n \geq 4$ the structures of $Na(H_2O)_n$ resemble $Na(H_2O)_n^+$ with a Rydberg-like excess electron. Hashimoto and Morokuma (HM) also performed calculations for $Na(H_2O)_n$ using ab initio MO methods [6, 7, 8]. They showed that the most stable structure was the surface-metal structure, where an Na atom sits on the cluster surface. Because this type of structure cannot have more than four water molecules in the first solvation shell, the behavior of the ionization threshold changed at $n = 4$. The excess electron distribution in the surface structure is localized near the Na atom and opposite the water molecules. Hashimoto and Kamimoto (HK) [9, 10] have also reported ab initio calculations for $Li(H_2O)_n$. They showed that the interior-metal structure is most stable, where the metal is surrounded by four water molecules, and that it cannot have more than four water molecules in the first solvation shell. They suggested that this is the origin of the change in the ionization threshold of $Li(H_2O)_n$ at $n = 4$. However, the excess electron density is distributed on and between the water molecules in the second solvation shell, which is different from that in $Na(H_2O)_n$. Most of the theoretical works indicated that the clusters have four water molecules in the first solvation shell and the metal atom becomes ionized at $n = 4$. But until now, the reason why the ionization threshold is independent of the metal element has not been explained, and the reasons for its independence have not been explored.

Recently, I have performed a series of ab initio MO calculations on the water cluster anions, $(H_2O)_n^-$, and showed that the excess electron can be trapped inside water clusters as small as $n = 2, 3$ and 4 [11, 12]. The electron cloud is surrounded by two or more H-O bonds of water molecules, whose structure I denote O-H$\{e\}$H-O hereafter. Kim et al. [13, 14] also found a similar structure in the excess electron of the most stable isomer of $(H_2O)_6^-$. These results suggest the stability of this type of structure for the excess electron, and encourage me to think that the O-H$\{e\}$H-O structure

might be present also in a group 1 metal-water clusters, $M(H_2O)_n$. If $M(H_2O)_n$ is an ion pair with a O-H{e}H-O structure and a solvated metal atomic ion, the ionization energy might not be affected by the metal cation. Furthermore, the structure O-H{e}H-O might remain unchanged when n increases, and consequently the ionization energy could become n-independent.

In this paper, I re-examine $M(H_2O)_n$(M = Li and Na) in a consistent way, keeping a O-H{e}H-O structure in mind. I first describe the geometric structures of the optimized isomers and their relative energies. The isomers are classified by introducing a set of measures to characterize the singly occupied molecular orbital (SOMO). The determining factor of the vertical ionization energy is analyzed. Finally I present a model to explain why the ionization threshold energy converges at an energy beyond $n = 4$, independently on the metal element.

4.2 Computational details

For the geometry optimization, the MP2/6-311++G(d,p) level of approximation is used. In my previous study for water cluster anions, which have a O-H{e}H-O structure [11], I have found it necessary to work at least at the MP2 level of approximation. Some of the isomers determined by Hashimoto and Kamimoto [10] , and by Hashimoto and Morokuma are re-optimized at the MP2 level. The harmonic vibrational frequencies are also calculated to confirm the stable structures, and they will be reported in a separate paper [12]. To estimate the total binding energy, the basis set superposition error (BSSE) has to be corrected. In the present paper I discuss only on the relative energy among the isomers of the same size n. In most cases the energy differences are small, and the identification of the most stable isomer is difficult. All calculations are carried out with Gaussian94 [15] registered at the computer center of Institute for Molecular Science.

Three measures are defined to characterize the electron distribution of the singly occupied molecular orbital (SOMO).

1) SOMO extent measure (SEM): The volume (in $Å^3$) of the sphere, which contains a half of electron

in SOMO. To define the sphere, I first calculate $\psi_{SOMO}(\mathbf{r}_{ijk})$ at the cubic grids $\mathbf{r}_{ijk} = (x_i, y_j, z_k)$ for $i = 1, \cdots, L$, $j = 1, \cdots, M$ and $k = 1, \cdots, N$. The spacings of these grids are fixed as Δx, Δy and Δz. Next, I sort them in descending order such that $|\psi_{SOMO}(1)| \geq |\psi_{SOMO}(2)| \geq \cdots \geq |\psi_{SOMO}(p)| \geq \cdots \geq |\psi_{SOMO}(LMN)|$. Finally, I search the index P such that $\sum_{p=1}^{P} |\psi_{SOMO}(p)|^2 \times \Delta x \Delta y \Delta z \approx 0.5$. The sphere so defined is unique and has a volume $P \times \Delta x \Delta y \Delta z$.

2) R({e}-M) : The distance between the center of the electron density of SOMO ($\mathbf{R}_{\{e\}}$) and the metal atom. $\mathbf{R}_{\{e\}}$ is evaluated as $\mathbf{R}_{\{e\}} = \sum_{ijk} |\psi_{SOMO}(\mathbf{r}_{ijk})|^2 \Delta x \Delta y \Delta z \times \mathbf{r}_{ijk}$.

3) R({e}-H) : The distance between $\mathbf{R}_{\{e\}}$ and the hydrogen atom.

I have also examined the effect of adding a set of diffuse sp type functions on the vertical ionization energy (VIE) and on the SEM of three isomers of $Li(H_2O)_4$ (Li4b, Li4c and Li4e), which correspond to three types of isomer as I will show later. These diffuse functions are added only on the oxygen atom and their exponents are 0.017, 0.003, 0.0006 and 0.00012. As a result, VIEs increase by at most 0.01 eV and are almost converged with 6-311++G(d,p) basis set. SEMs also increase slightly by at most 3 $Å^3$. Because both changes are small and do not influence the following discussion, I have used 6-311++G(d,p) basis set in the present calculation.

4.3 Results and discussion

The optimized structures for $Li(H_2O)_n$ and $Na(H_2O)_n$ for $n = 3$ to 6 are given in Figures 1–4. The surface of the sphere, defined in the previous section, is also shown. The SEM in my definition is the volume of the sphere in the figures. In Table 1 three measures defined above as well as the VIE and the relative isomer energy are summarized. The geometric structures of isomers are classified in terms of the number of water molecules m in the first solvation shell; 'MmW' isomer. The electronic structures of $M(H_2O)_n$ are classified using two measures (SEM and R({e}-M)) into three types, surface (S), semi-internal (I) and quasi-valence (V). The definition is as follows;

1)Surface (S): SEM is larger than 75 $Å^3$. In this type of isomers, an electron is detached from the

metal atom, and the ejected electron is delocalized on the surface of the cluster.

2)Semi-Internal (I): SEM is smaller than or equal to 75 $Å^3$ and R({e}-M) is longer than 2.0 Å. The electron is detached from the metal atom and captured internally by O-H bonds of the water molecules. The structure O-H{e}H-O plays a key role in localizing the ejected electron.

3) Quasi-valence (V): SEM is smaller than 55 $Å^3$ and R({e}-M) is shorter than 2.0 Å. The SOMO electron is not yet completely detached from the metal atom. The SOMO is a sp hybrid orbital, though it is more diffuse than the ordinal valence s and p orbitals. This type of isomers has a larger VIE than those of the other types.

The correlations of SEM with VIE (a) and with R({e}-M) (b) are shown in Figure 5, which demonstrates the appropriateness of the classification.

4.3.1 $M(H_2O)_3$

Three isomers are found for $Li(H_2O)_3$, and two isomers are for $Na(H_2O)_3$ (see Figure 1). Isomer Li3a has C_3 symmetry, and all oxygen atoms lie nearly on a plane. Hydrogen bonds among the water molecules are not formed, because of short Li - O distances. I also found a similar planar C_3 structure for $Na(H_2O)_3$, which turned out to have two imaginary frequencies and collapsed to isomer Na3b by forming a hydrogen bond between a pair of water molecules. Isomers Li3b and Na3b have a pair of hydrogen-bonded water molecules. The difference in the hydrogen bond strength of Li3b and Na3b, which is seen in the metal-oxygen bond distances, results from the ionic radius of Li^+ and Na^+. Isomer Li3a, having no hydrogen bonds, is as stable as isomer Li3b. The electronic structures of Li3a, Li3b and Na3b are of typical surface type; the SEMs are as large as 115 $Å^3$, 95 $Å^3$ and 101 $Å^3$, respectively. In these isomers the metal atom is ionized, and the ejected electron is distributed on the surface of the cluster. One of the interesting findings in the surface type electron is that $\mathbf{R}_{\{e\}}$ is closer to the metal ion than to the hydrogen atoms of water molecules, although some of OH bonds are directed toward {e}, as seen in the figure.

Isomers Li3c and Na3c are of M2W. The energy difference of isomers Li3c and Li3a is as large

as 5.49 kcal/mol. On the other hand, the corresponding difference of Na3c and Na3b is less than 1 kcal/mol. The Na-O bond energy is similar to the hydrogen bond between the first and second shell water molecules, and they are smaller than the Li-O bond energy. The characteristics of isomers of Li3c and Na3c are small SEM, short R($\{e\}$-M) and long R($\{e\}$-H), as is shown in Table 1. The electron in SOMO is bound to the metal atom, and therefore, I classify the isomers quasi-valence type. It might be worth emphasizing that the interaction between $\{e\}$ and HO bonds determines the direction of the second shell water molecule and one of the first shell water molecules.

Hashimoto and Kamimoto (HK) examined isomers of $Li(H_2O)_3$ with several basis sets [10]. Hashimoto and Morokuma (HM) also reported the structures of isomers of $Na(H_2O)_3$ [8]. Some of their isomers are similar to Li3a, Li3b and Na3b. They also found a few isomers of M2W having two hydrogen bonds. The quasi-valence type isomers Li3c and Na3c are not reported, probably because they expected that the isomers of this type are less stable than the isomers having two hydrogen bonds.

4.3.2 $M(H_2O)_4$

The isomers of $Li(H_2O)_4$ and $Na(H_2O)_4$ in Figure 2 have similar structures except the metal-oxygen distances. An exception is Li4a; the counterpart Na4a collapses to Na4b as Na3a does to Na3b. Isomers Li4b and Na4b have C_2 symmetry and have two hydrogen-bonds. Because of a larger ionic radius of the Na^+ ion, the Na-O bonds in Na4b is much longer and weaker than the Li-O bonds in Li4b, and thus the water molecules in Na4b can be reoriented to form stronger hydrogen bonds. The SOMOs of three isomers are of surface type, as their SEMs indicate, although the distances R($\{e\}$-M) are substantially larger than in Li3b and Na3b. Besides, some of R($\{e\}$-H) are short, which suggests stronger OH and $\{e\}$ interaction.

Two pairs of M3W isomers, M4c and M4d, are found in my study. In M4c, the water molecule in the second solvation shell is a double proton-acceptor water molecule; one of OH bonds of the molecule interacts with an electron cloud $\{e\}$. In M4d, a pair of water molecules in the first shell are hydrogen-bonded. The energy difference between M4c and M4d is 1.49 kcal/mol for M=Li and 0.37

kcal/mol for M=Na. The SOMO electron of both M3W isomers is semi-internal, as their SEMs range from 63 $Å^3$ to 75 $Å^3$. There are noticeably short R($\{e\}$-H)s. It should be noticed that even though M4d has the first shell structure of M3b, the electron distribution $\{e\}$ of M4d is different from that of M3b. This implies that the second shell water molecule in M4d substantially reduces the electron distribution $\{e\}$.

One M2W isomer M4e is found for both metals. Both have C_2 symmetry, and a pair of water dimers coordinate to the metal atom. The isomer is less stable than the others. The SEM and R($\{e\}$-M) indicate the character distinct from the other isomers, and the SOMO is a typical quasi-valence orbital. The water molecules in the second shell interact strongly with the electron.

4.3.3 $M(H_2O)_5$ and $M(H_2O)_6$

For $M(H_2O)_5$, three M4W isomers for Li and one for Na are found (Figure 3). There is a double proton-acceptor water molecule in the second shell in Li5a, Li5b and Na5a, which share a similar electronic structure. The SOMO is of semi-internal type, and the ejected electron $\{e\}$ interacts with the double proton-acceptor water molecule and with one of the first shell water molecules. The number of OH bonds strongly interacting with $\{e\}$ in isomer Li5b is two, while it is three in isomer Li5a. This difference comes from the position of the hydrogen bond within the first solvation shell. The energy difference of the isomers, however, is merely 0.50 kcal/mol. The attempt to locate the corresponding isomer Na5b has failed.

There is a large free space in the other side of water molecules in M5a, which suggests that one more water molecule can hydrate to the metal atom; in fact isomers Li6a and Na6a are found as shown in Figure 4. The SEMs become smaller and R($\{e\}$-M) longer than the corresponding M5a. It is, however, worth noticing that three shortest R($\{e\}$-H)s are not much changed; the structure $(OH_2)\{e\}(HO)$ is almost common in M5a and M6a. Most of the M4W form of $M(H_2O)_n$ ($n > 4$) have the structure of M4b as an ion core, which has two strong intra-shell hydrogen bonds of four-membered ring. In M5a, one of the ring is replaced with a six-membered hydrogen bond ring. If two of the four-membered

rings are replaced, it becomes one of the isomers found for $Na(H_2O)_6$ by Hashimoto and Morokuma [8]. It is expected that a similar core structure persists both for $K(H_2O)_n$ and $Cs(H_2O)_n$.

Isomer Li5c is also M4W, and its first shell structure is similar to Li4a. But, the character of the SOMO is changed to semi-internal in my classification; R($\{e\}$-M) becomes longer, and the SEM is as small as 63 $Å^3$. The change of SOMO results from stronger interaction of the ejected electron with the proton acceptor water molecule. The energy difference from the other M4W isomer Li5a is only 0.60 kcal/mol, though the structure is very different.

Two isomers (M5d and M5e) of M3W are examined for $M(H_2O)_5$. The SOMO of both isomers is of semi-internal type. A large R($\{e\}$-M) clearly indicates the ion-pair formation in these isomers. Isomers M5d have three hydrogen bonds, and two OH bonds of the second shell molecules interact with the ejected electron $\{e\}$. On the other hand, isomers M5e have only two hydrogen bonds, but three OHs strongly interact with $\{e\}$. The SEMs are small, in particular, for isomers M5e. There are more isomers of M3W and M2W types expected, with different hydrogen-bonding networks of water molecules.

There are many more isomers in $M(H_2O)_6$ than in $M(H_2O)_5$; some of them are reported by HK for M = Li [10] and HM for M = Na [8]. I have chosen two isomers of M5W and M4W of $M(H_2O)_6$ to examine the structural dependence of the vertical ionization energy. As already mentioned above, isomers M6a are derived from M5a by adding a water molecule at the other side of $\{e\}$. This extra water molecule lengthens R($\{e\}$-M), but the character of SOMO is not much affected, as both SEM and R($\{e\}$-H) are similar to each other in M6a and M5a. Isomers M6b are representatives of M4W; they are derived from isomers M5d of M3W, by adding a water molecule to the metal ion. In Li6b, four of the oxygen atoms in the first shell are nearly tetrahedrally coordinated, while in Na6b they are distorted from the tetrahedral configuration, because of a hydrogen-bond within the first shell. Even with this difference, the characteristic measures of SOMO are very similar to each other as is seen in Table 1. Isomer Li6a is slightly less stable (1.48 kcal/mol.) than isomer Li6b, while isomer Na6a is a little more stable than isomer Na6a. The energy difference is in any case insignificant. Hashimoto and

his coworkers reported several isomers for $M(H_2O)_6$ in their papers. Isomers HK-VIa and HM-m in Figure 4 and Table 1 are their most stable isomers for $Li(H_2O)_6$ [10] and for $Na(H_2O)_6$ [8], respectively. To compare the relative stability, the structures were re-optimized with MP2 /6-311++G(d,p) level of calculations. Isomer Li6b is a little less stable than HK-VIa. It is probably because the latter has two six-membered rings. Isomer Na6a of M4W is slightly more stable than isomer HM-m of M3W. The SOMOs of all isomers are semi-internal, except for HM-m, whose SOMO is quasi-valence in my definition, as a very short R($\{e\}$-M) indicates.

Concluding the subsection, I should emphasize that for $n \geq 4$ there are several (or many) isomers within 2 kcal/mol. The ordering of the calculated stability energy among the isomers might be sensitive to the basis set superposition correction. Experimentally it is most likely that a few of isomers coexist in the molecular beam, as was recently found in $(H_2O)_6^-$[16] and $Mg^+(H_2O)_n$[17]

4.3.4 Vertical ionization energies (VIEs), and their size- and metal-dependencies

Table 1 summarizes the calculated VIEs, which are evaluated by taking the difference of MP2 energies of the neutral and cation clusters at the optimized geometry for the neutral cluster. Before discussing the calculations, it is worth noticing what is experimentally known. Photoelectron spectra have not been measured for these neutral clusters because of the difficulty in size-selection. Instead, the threshold photon energy, where the ions start to be detected in the mass spectrometer, is experimentally determined. The ITE would be close to the VIE, only if the geometries of the initial (neutral) and final (cation) clusters were similar to each other. In this case, both should be close to the adiabatic ionization energy. In the clusters I are studying, the cation clusters $M^+(H_2O)_n$ might be more strongly bound than the corresponding neutral clusters. More importantly, the interaction between the electron $\{e\}$ and the OH bonds influences the geometric structures of hydrated water molecules in the neutral clusters, as I have seen in Figures 1 - 4. Therefore, it is expected that VIE will be larger than the ITE in most cases. There is another complication; if a few isomers coexist in the experimental beam condition, the observed ITE is determined by the isomer which has the smallest ITE. Table 1

(also the papers of HK and HM) shows that the energy difference among the isomers is small, and that the number of possible isomers increases with the size of clusters. So the direct comparison of the calculated VIE with the observed ITE is not straightforward. With these reservation, the trends in the calculated VIE are still informative in exploring the experimentally observed features in the ITE.

At a glance, the VIEs in Table 1 are almost size- and metal-independent; the values range from 3.3 to 4.0 eV. In Figure 5, the correlation between SEM and VIE (a) and between SEM and R(M-$\{e\}$) (b) is shown. Distinctively the isomers of quasi-valence type (V) SOMO, M3c and M4e(M=Li and Na), have larger VIE, smaller SEM and shorter R(M-$\{e\}$) than the others. The VIE of M4e is larger than that of M3c, which is contrary to the experimental trends in ITE. The VIE decreases almost linearly with the SEM, except for HM-m. These isomers, except for Na3c, are less stable than the other isomers. Thus, I may be able to exclude these isomers as candidates for the clusters detected in the experiments.

In Figure 5, the isomers of surface type (S) SOMO, Li3a, M3b, Li4a and M4b, are clearly distinguished from the others. They have almost same VIE; the VIEs of $M(H_2O)_4$ are slightly smaller than those of $M(H_2O)_3$. Experimental ITEs are 3.36 eV for $Li(H_2O)_3$ [1], 3.25 - 3.3 eV for $Na(H_2O)_3$ [2], 3.12 eV for $Li(H_2O)_4$ [1] and 3.17 eV for $Na(H_2O)_4$ [2]. The calculated VIEs for $M(H_2O)_3$ are close to the experimental ITEs, although a slight difference in the experimental ITE of Li and Na is not reproduced in the calculations. The geometric structures of these isomers are expected not to be changed by the ionization, and the VIE should be close to the adiabatic and threshold ionization energies. The calculated VIE difference of surface type $M(H_2O)_3$ and $M(H_2O)_4$ is nearly 0.1 eV or less than that, which is slightly smaller than the experimental one. Among the isomers of surface type, isomer Na4b may be classified as an intermediate to semi-internal type, as Figure 5 shows. Two of water molecules interacting with $\{e\}$ are the proton-acceptors in the hydrogen bonds, and their hydrogen atoms become more positive. Because of stronger OH-$\{e\}$ interaction, the SEM is reduced. In larger clusters, the hydrogen-bond network evolves, and the surface type SOMO is not possible to exist.

As Figure 5(a) shows, the VIEs of isomers having the semi-internal (I) type SOMO range from 3.3 to 3.5 eV, independently of the metal element and the size of clusters; the exception is isomers M5e, whose VIE is 3.7eV; the reason for this will be discussed below. Even though isomers of the (I) type generally have a restricted range of VIE, SEM and R(M-$\{e\}$), the correlation among them is not so straightforward. It is because the structure of water molecules surrounding $\{e\}$ does play a key role in determining both VIE and SEM that I have denoted the structure O-H$\{e\}$H-O. To analyze the determining factors of the VIE, more careful examination of the geometric and electronic structures of the clusters is required.

One of characteristics in the isomers of semi-internal type is the similarity of the structure of the corresponding isomer $Li(H_2O)_n$ and $Na(H_2O)_n$. The structures around the ejected electron $\{e\}$ of the corresponding pairs (Li4c, Na4c), (Li4d, Na4d), (Li5a, Na5a), (Li5d, Na5d), (Li5e, Na5e), (Li6a, Na6a) and (Li6b, Na6b) resemble each other, although the difference in the ionic radii causes the structural change around the metal atom ion and the distance R(M-$\{e\}$). Their structures have a common form of $M^+(H_2O)_m \cdot (H_2O)_l \cdot (H_2O)^-_{n-m-l}$ where the metal atom is ionized and becomes a hydrated ion $M^+(H_2O)_m$ (m = 3-5) in the clusters . The water cluster $(H_2O)_{n-m-l}$ traps an ejected electron and becomes a water cluster anion $(H_2O)^-_{n-m-l}$, which determines the shape of the SOMO, as are seen in the figures. The structure O-H$\{e\}$H-O is the essential part of the anion part. The energy required to ionize an electron is, however, governed not only by the anion part but also by the hydrated metal ion $M^+(H_2O)_m$. The potential (V_{SOMO}) on the SOMO electron could conceptually be written as $V_{SOMO} = V^{HMI}_{SOMO} + V^{WC}_{SOMO}$, where V^{HMI}_{SOMO} is a long range potential of the hydrated metal ion (HMI), and V^{WC}_{SOMO} is the short range potential of the water cluster (WC) $(H_2O)_{n-m-l}$. Because of these two factors, the correlation of SEM with VIE and with R(M-$\{e\}$), shown in Figure 5, looks somewhat weak. Nevertheless, the SEM and VIE of the pairs (Li5a, Na5a), (Li5d, Na5d), (Li5e, Na5e) and (Li6b, Na6b) are close to each other. The common feature among these pairs is that the pair has either long R(M-$\{e\}$) or nearly equal R(M-$\{e\}$). To examine the determining factors of the electronic structure of O-H$\{e\}$H-O and VIE more in detail, I analyze a few examples below.

Isomers M6b of M4W are derived from isomers M5d of M3W; in the former an extra water molecule hydrates to the metal ion. In all of these four isomers there are a very short ($\leq$ 1.23Å) and a short ($\leq$ 1.88Å) R(H-{e})s. Besides, their SEMs are also close to each other (ranging from 48 Å^3 to 53 Å^3). So, the local structure of O-H{e}H-O in M6b are similar to that in M5d. On the other hand, R({e}-M)s become longer in M6b than in M5d, which reduce V_{SOMO}^{HMI}, resulting in smaller VIE by 0.15 eV in M6b than in M5d. The pair (Li4c, Li5b) is another example of this type; they share the similar O-H{e}H-O structure, but VIE of Li5b is 0.20eV smaller than that of Li4c.

Isomers M6b can be also regarded as derivatives of M5a; both have a M4W structure of the hydrated metal ion $M^+(H_2O)_m$. In M6b, a water molecule is added in the second shell, which causes the rearrangement of the hydrogen bonds in the cluster. As a result, the surrounding structure of the metal ion and the O-H{e}H-O structure undergo large changes. But, the calculated VIEs are all nearly equal to each other (3.36 - 3.37 eV). I may be able to interpret this apparent size- and metal-independence as a result of the cancellation of V_{SOMO}^{HMI} and V_{SOMO}^{WC}. Because R(M-{e}) in M6b is longer than in M5a, V_{SOMO}^{HMI} is weaker in M6b. On the other hand, a short R(H-{e}) and smaller SEM in M6b suggest stronger {e}-HO interaction and larger V_{SOMO}^{WC} than in M5a. A OH bond of the newly added water molecule leads to the stronger interaction; the water molecule is a proton-acceptor molecule in the hydrogen-bond, and the hydrogen is more positively charged. Besides, the molecule can freely rotate to maximize the interaction with {e}. As a result, the SEMs of M6b become substantially smaller and V_{SOMO}^{WC} larger than those of M5a. Two opposite effects are canceled out, and in effect the VIEs of M6band M5a become nearly equal to each other.

I have seen the SEM is an appropriate measure to characterize the electronic structure of the ejected electron {e} and the O-H{e}H-O structure. Three factors can be identified in determining the O-H{e}H-O structure and V_{SOMO}^{WC}, and therefore its SEM. One is the strength of the bond dipole of the O-H bonds which directly interact with the ejected electron. It is known that as a hydrogen bond chain becomes longer, the charge on the terminal hydrogen atom becomes more positive and consequently the bond dipole of O-H bond becomes larger as mentioned above. It is also known

that the hydrogen atoms of the proton-acceptor water molecules are more positively charged. This is particularly true for the double proton-acceptor molecule [18]. The larger bond dipoles of O-H bonds make SEM smaller. The examples are seen in the SEMs of pairs of isomers; Li5a(67 $Å^3$) and Li6b(53 $Å^3$), Na5a(65 $Å^3$) and Na6b(53 $Å^3$), Li4c(63 $Å^3$) and Li5d(51 $Å^3$), and Na4c(69 $Å^3$) and Na5d(48 $Å^3$). As the cluster size of semi-internal electron type becomes large and the hydrogen bond chain becomes long, the bond dipole of O-H bonds in the O-H{e}H-O structure become large. As a result, the SEM becomes smaller. Another factor is the number of OH bonds in the O-H{e}H-O structure. The SEM becomes smaller as the number of surrounding OH bonds increases. An example is the SEM of Li5e and Na5e, which have three OH bonds in the O-H{e}H-O structure; two of them are those of the proton-acceptor molecules. Their SEMs are as small as 36 $Å^3$. Because of the small SEM, their VIEs are as large as 3.70 eV, and in Figure 5(a) their points are located far from those of the other surface type isomers. The relative orientation of O-H bonds also plays a role. For example, when two dipoles of the opposite direction are collinear, the electrostatic potential well between the dipoles becomes the deepest. The factor may have little effect in the present cases, but it might play a role in the pure water cluster ions.

In my present level of calculations and with the restricted experimental data available, I cannot identify the experimentally-detected isomers, which have nearly equal ionization threshold energy for $n \geq 4$ of $M(H_2O)_n$ (M = Li and Na). From the above results, I might, however, be able to deduce the working hypothesis for further studies. The ion-pair structure, $M^+(H_2O)_m \cdot (H_2O)_l \cdot (H_2O)^-_{n-m-l}$, is the basic unit of the clusters of $n > 5$; $m = 3, 4$ or 5. The most probable m is 4. Among the isomers I have studied, M4b, M5a, and M6b, all of which have a M4W core, explain the observed features; the convergence and the metal-independence of VIE. They are the most stable or close to the most stable in energy. The metal independence of VIE results from the ion-pair structure as the experimentalists thought. The convergence of VIE is attained by the cancellation of two factors $V^{HMI}_{SOMO} + V^{WC}_{SOMO}$. In large n, R(M-{e}) is long, and consequently the electrostatic potential V^{HMI}_{SOMO} becomes weaker. At the same time, the hydrogen bond chain becomes longer and therefore the interaction between the

ejected electron and the terminal O-H bonds becomes stronger, and V_{SOMO}^{WC} becomes larger.

4.4 Conclusion

I have investigated the water clusters containing a group 1 metal atom $M(H_2O)_n$ (M=Li and Na) for $n = 3 - 6$ with ab initio MO methods. These isomers are classified into three types, and among these types of clusters the semi-internal electron type isomers have the ion-pair structure, $M^+(H_2O)_m \cdot (H_2O)_l \cdot (H_2O)^-_{n-m-l}$, in the clusters $M(H_2O)_n$, and possibly determine the features of the observed ITE. The structure of $(H_2O)^-_{n-m-l}$ part contains the O-H$\{e\}$H-O structure, and the structure around the ejected electron is determined by the interaction within the O-H$\{e\}$H-O structure. The calculations indicate that there are a few isomers of nearly equal stabilization energy. The number of those isomers increases substantially with n. Photoelectron spectra and vibrational spectra are more informative than ionization threshold spectra for the structures of the isomers. More theoretical work is in progress [12]. In the present study, I have reached a model to explain the observed convergence of ITEs at $n = 4$ and their metal-independence. I cannot, however, say anything yet about why the converged value is the VIE of bulk water. To understand it, further extensive theoretical studies are required.

Acknowledgement

The present work was partially supported by the Grant-in-Aids for Scientific Research (No.09304057) by the Ministry of Education, Science, Sports, and Culture, Japan, and by Research and Development Applying Advanced Computational Science and Technology, Japan Science and Technology Corporation (ACT-JST). A part of calculations was carried out at the Computer Center of the Institute for Molecular Science. The authors thank Prof. Sutcliffe for reading the manuscript.

Bibliography

[1] Takasu, R.; Misaizu, F.; Hashimoto, K.; Fuke, K. J. Phys. Chem. **1997**, A101, 3078.

[2] Hertel, I.V.; Hüglin, C.; Nitsch, C.; Schulz, C.P. Phys. Rev. Lett. **1991**, 67, 1767.

[3] Misaizu, F.; Tsukamoto, K.; Sanekata, M.; Fuke, K. Chem. Phys. Lett. **1992**, 188, 241.

[4] Coe, J.V.; Lee, G.H.; Eaton, J.G.; Arnold, S.T.; Sarkas, H.W.; Bowen, K.H.; Ludewigt, C.; Haberland, H.; Worsnop, D.R. J. Chem. Phys. **1990**, 92, 3980.

[5] Barnett, R. N.; Landman, U. Phys. Rev. Lett. **1993**, 70, 1775.

[6] Hashimoto, K.; He S.; Morokuma, K. Chem. Phys. Lett. **1993**, 206, 207.

[7] Hashimoto, K.; Morokuma, K. Chem. Phys. Lett. **1994**, 223, 423.

[8] Hashimoto, K.; Morokuma, K. J. Am. Chem. Soc. **1994**, 116, 11436.

[9] Kamimoto, T.; Hashimoto, K. Structures and dynamics of clusters; Kondow, T., Kaya, K., Terasaki, A., Eds.; Universal Academy Press: Tokyo, 1996; pp 563-572

[10] Hashimoto, K.; Kamitomo, T. J. Am. Chem. Soc. **1998**, 120, 3560.

[11] Tsurusawa, T.; Iwata, S. Chem. Phys. Lett. **1998**, 287, 553.

[12] Tsurusawa, T.; Iwata, S. J. Chem. Phys. in press.

[13] Kim, K. S.; Lee, S.; Kim, J.; Lee, J. Y. J. Am. Chem. Soc. **1997**, 119, 9329.

[14] Lee, S.; Kim, J.; Lee, S. J.; Kim, K. S. Phys. Rev. Lett. **1997**, 79, 2038.

[15] Gaussian 94 (Revision E.2), M.J. Frisch, G.W. Trucks, H.B. Schlegel, P.M.W. Gill, B.G. Johnson, M.A. Robb, J.R. Cheeseman, T.A. Keith, G.A. Petersson, J.A. Montgomery, K. Raghavachari, M.A. Al-Laham, V.G. Zakrzewski, J.V. Ortiz, J.B. Foresman, C.Y. Peng, P.Y. Ayala, M.W. Wong, J.L. Andres, E.S. Replogle, R. Gomperts, R.L. Martin, D.J. Fox, J.S. Binkley, D.J. Defrees, J. Baker, J.P. Stewart, M. Head-Gordon, C. Gonzalez and J.A. Pople, Gaussian, Inc., Pittsburgh PA, 1995.

[16] Bailey, C.G.; Kim, J.; Johnson, M.A. J. Phys. Chem. **1996**, 100, 16782.

[17] Watanabe H.; Iwata S. J. Chem. Phys. **1998**, 108, 10078.

[18] Watanabe H.; Aoki M.; Iwata S. Bull. Chem. Soc. Jpn. **1993**, 66, 3245.

Figure caption

Figure 1. The optimized structures for $Li(H_2O)_3$ and $Na(H_2O)_3$. The surface of the sphere, inside of which a half of the SOMO electron is contained, is drawn. The hydrogen bonds are shown by dotted lines. The metal-oxygen bond lengths and the hydrogen bond lengths are given in angstrom. The hydrogen bond lengths are put in parentheses.

Figure 2. The optimized structures for $Li(H_2O)_4$ and $Na(H_2O)_4$.

Figure 3. The optimized structures for $Li(H_2O)_5$ and $Na(H_2O)_5$.

Figure 4. The optimized structures for $Li(H_2O)_6$ and $Na(H_2O)_6$.

Figure 5. (a)The correlation between SEM(SOMO extent measure) and VIE (Vertical ionization energy). (b)The correlation between SEM and R(M-$\{e\}$). The broken lines indicate the criteria for classification of isomers.

TABLE 1: The distance between $R_{\{e\}}$ and the metal atom, the shortest four distances between $R_{\{e\}}$ and the hydrogen atoms, SEM, VIE and ΔE_{ISO}

	Type	MnW	R({e}-M)[a]	R({e}-H)[a]	SEM[b]	VIE[c]	ΔE_{ISO}[d]
Li3a	S	M3W	1.50	2.42,2.42,2.42,2.85	115	3.39	0.00
Li3b	S	M3W	1.69	1.76,1.96,2.11,2.17	95	3.43	0.09
Na3b	S	M3W	1.65	2.03,2.33,2.42,2.84	101	3.40	0.00
Li3c	V	M2W	1.41	2.63,2.81,3.06,3.33	40	3.78	5.49
Na3c	V	M2W	1.34	3.05,3.22,3.32,3.84	48	3.68	0.93
Li4a	S	M4W	2.13	1.74,1.78,2.29,2.47	96	3.31	0.00
Li4b	S	M4W	2.21	1.34,1.34,2.44,2.44	93	3.30	0.09
Na4b	S	M4W	2.68	1.39,1.39,2.48,2.48	83	3.36	0.00
Li4c	I	M3W	2.71	1.48,1.66,2.68,2.90	63	3.53	2.77
Na4c	I	M3W	2.94	1.48,1.60,2.77,3.02	69	3.40	1.58
Li4d	I	M3W	2.55	1.07,1.24,2.23,2.85	75	3.42	4.26
Na4d	I	M3W	2.49	1.17,2.08,2.21,3.04	63	3.55	1.95
Li4e	V	M2W	1.90	1.98,1.98,2.95,2.95	28	3.97	9.05
Na4e	V	M2W	1.92	2.12,2.12,3.18,3.18	36	3.90	3.01

[a] In Å. [b] In $Å^3$. [c] In eV. [d] In kcal/mol.

TABLE 1 (cont.): The distance between $R_{\{e\}}$ and the metal atom, the shortest four distances between $R_{\{e\}}$ and the hydrogen atoms, SEM, VIE and ΔE_{ISO}

	Type	MnW	R({e}-M)[a]	R({e}-H)[a]	SEM[b]	VIE[c]	ΔE_{ISO}[d]
Li5a	I	M4W	2.99	1.52,1.59,1.82,2.90	67	3.36	0.00
Na5a	I	M4W	3.47	1.49,1.57,1.95,3.01	65	3.37	0.00
Li5b	I	M4W	2.98	1.53,1.58,2.75,2.83	62	3.33	0.50
Li5c	I	M4W	2.51	1.62,1.92,2.01,2.53	63	3.48	0.60
Li5d	I	M3W	3.34	1.16,1.73,2.70,2.74	51	3.50	3.42
Na5d	I	M3W	3.40	1.23,1.78,2.74,2.80	48	3.51	2.19
Li5e	I	M3W	3.12	1.51,1.70,2.01,2.70	36	3.72	4.87
Na5e	I	M3W	3.18	1.61,1.72,2.00,2.98	36	3.70	3.77
Li6a	I	M5W	3.27	1.38,1.57,1.87,2.70	66	3.34	2.66
Na6a	I	M5W	3.69	1.25,1.74,1.97,2.77	61	3.44	0.00
Li6b	I	M4W	3.73	1.07,1.76,2.60,2.67	53	3.35	1.18
Na6b	I	M4W	4.05	1.02,1.88,2.53,2.75	53	3.37	0.57
HK-VIa	I	M4W	3.15	1.52,1.58,1.71,3.01	55	3.49	0.00
HM-m	V	M3W	1.38	3.59,3.59,3.59,3.96	52	3.35	0.57

[a] In Å. [b] In $Å^3$. [c] In eV. [d] In kcal/mol.

(*Li3a*:C_3)

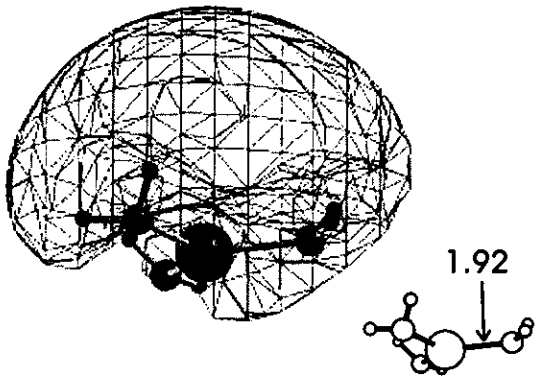

(*Li3b*)

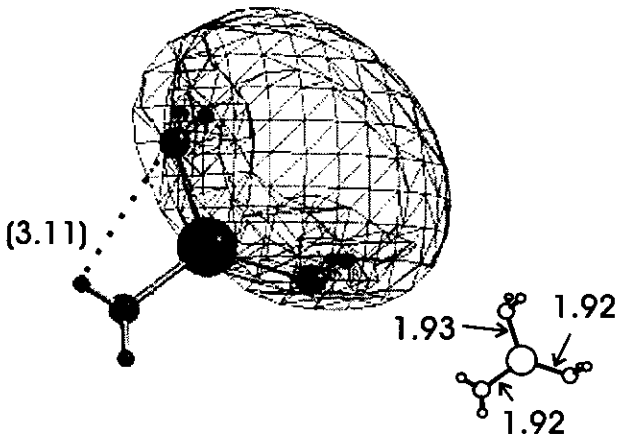

(*Li3c*)

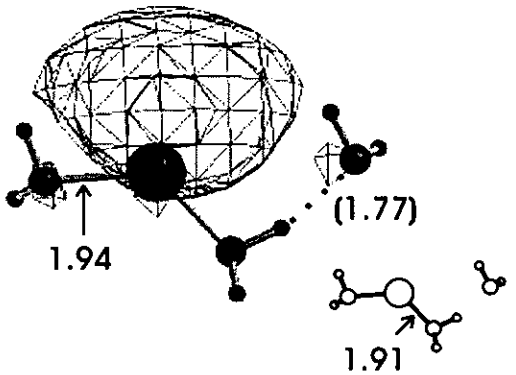

(*Na3b*)

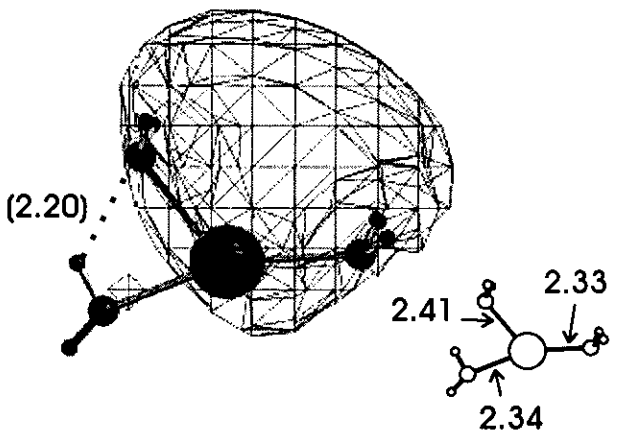

(*Na3c*)

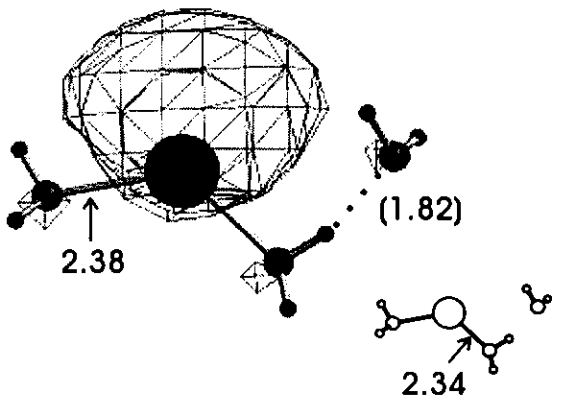

Figure 1

(*Li4a*)

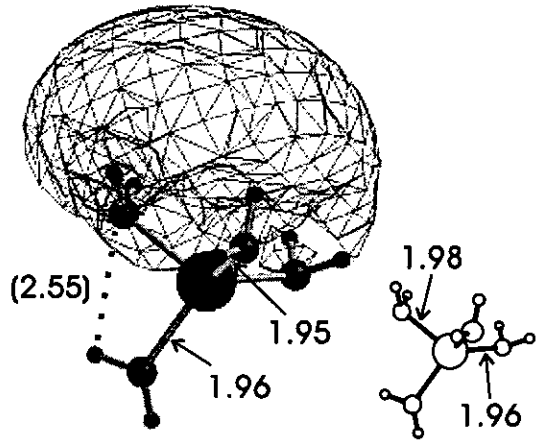

(*Li4b*:C_2)

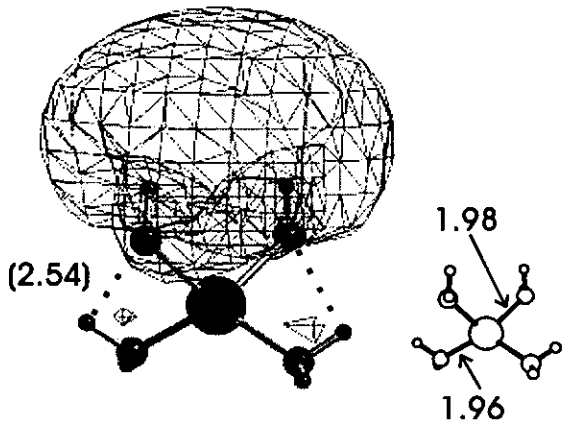

(*Li4c*)

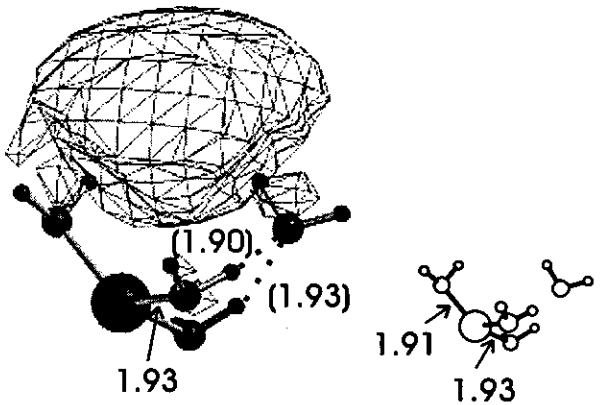

(*Na4b*:C_2)

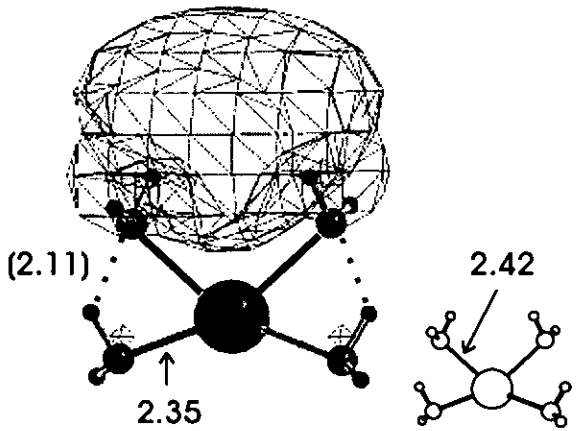

(*Na4c*)

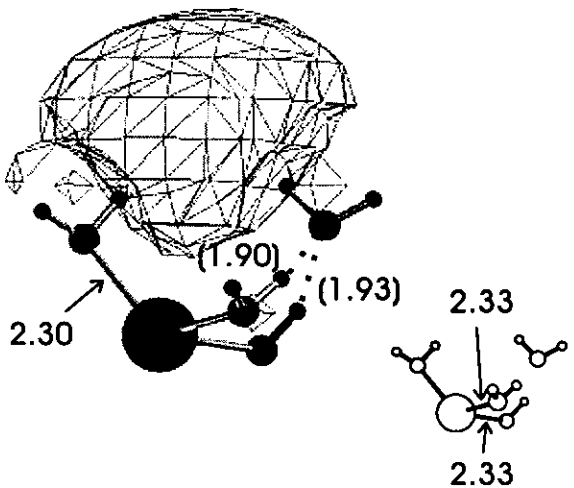

Figure 2 (1/2)

(*Li4d*)

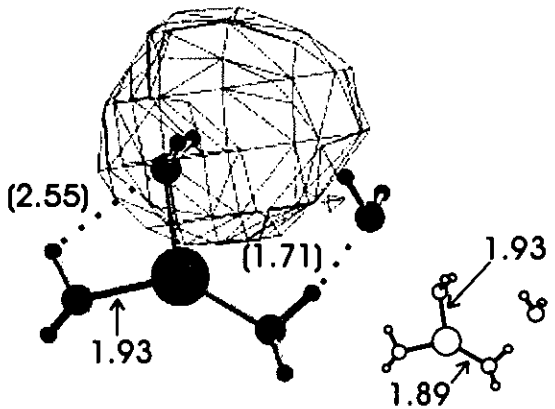

(*Li4e*:C_2)

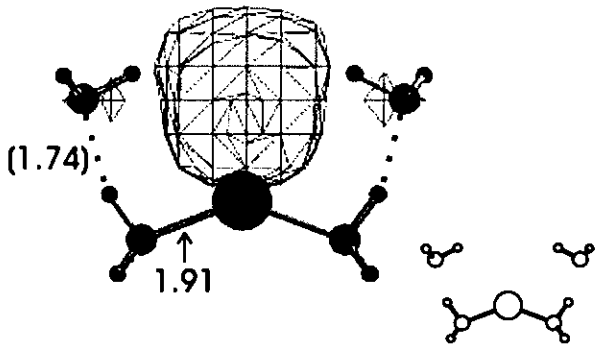

(*Na4d*)

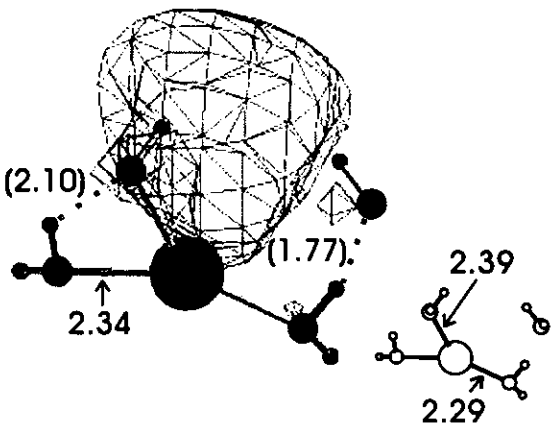

(*Na4e*:C_2)

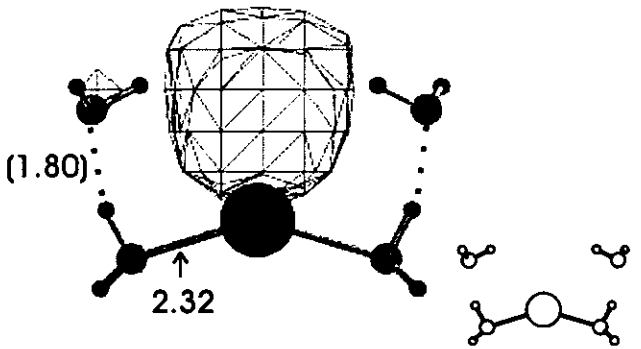

Figure 2 (2/2)

(*Li5a*)

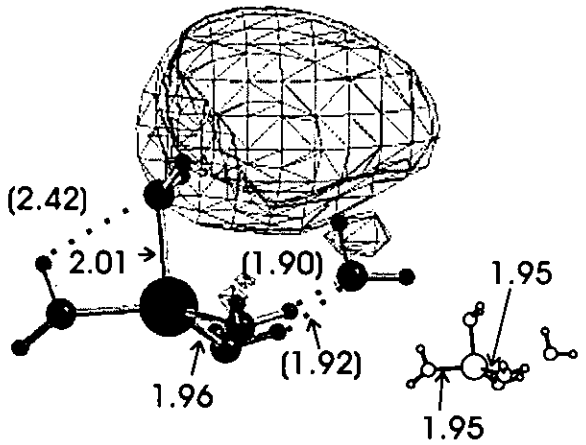

(*Li5b*)

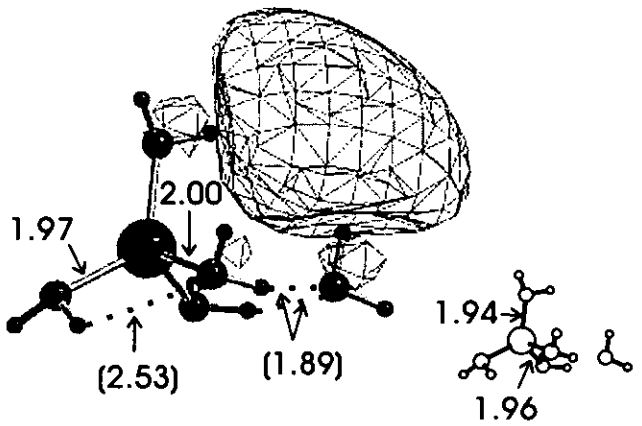

(*Li5c*)

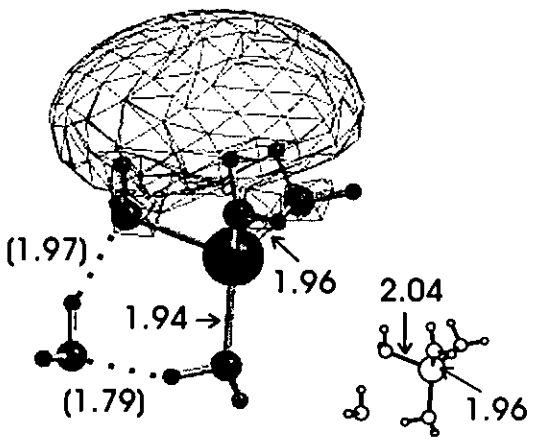

(*Na5a*)

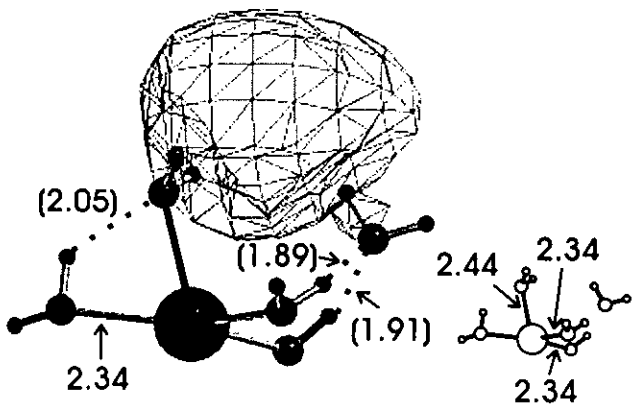

Figure 3 (1/2)

(*Li5d*)

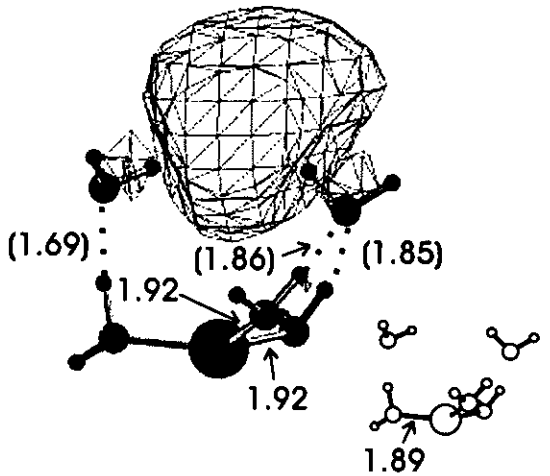

(*Li5e*)

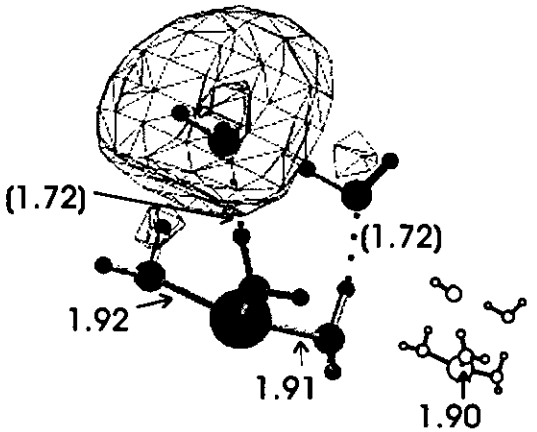

(*Na5d*)

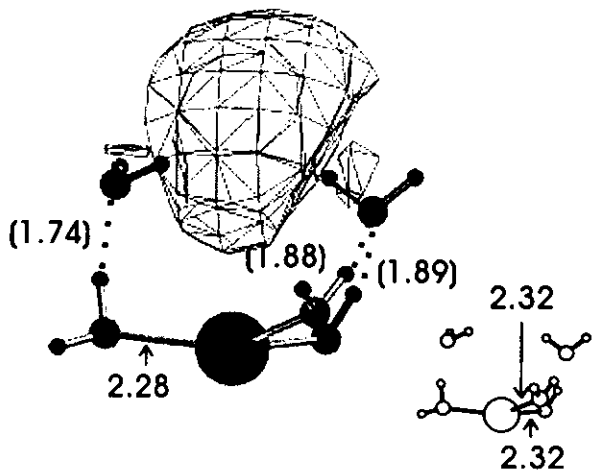

(*Na5e*)

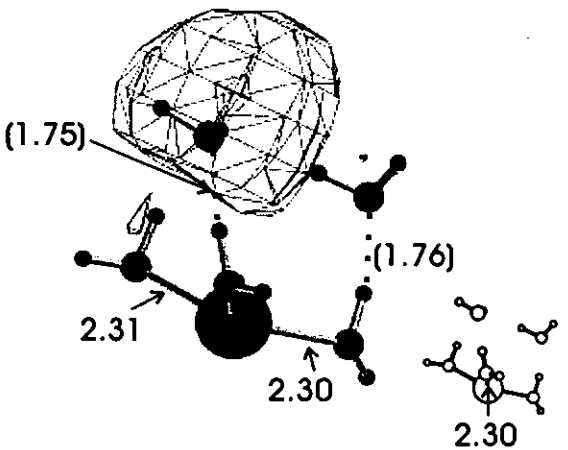

Figure 3 (2/2)

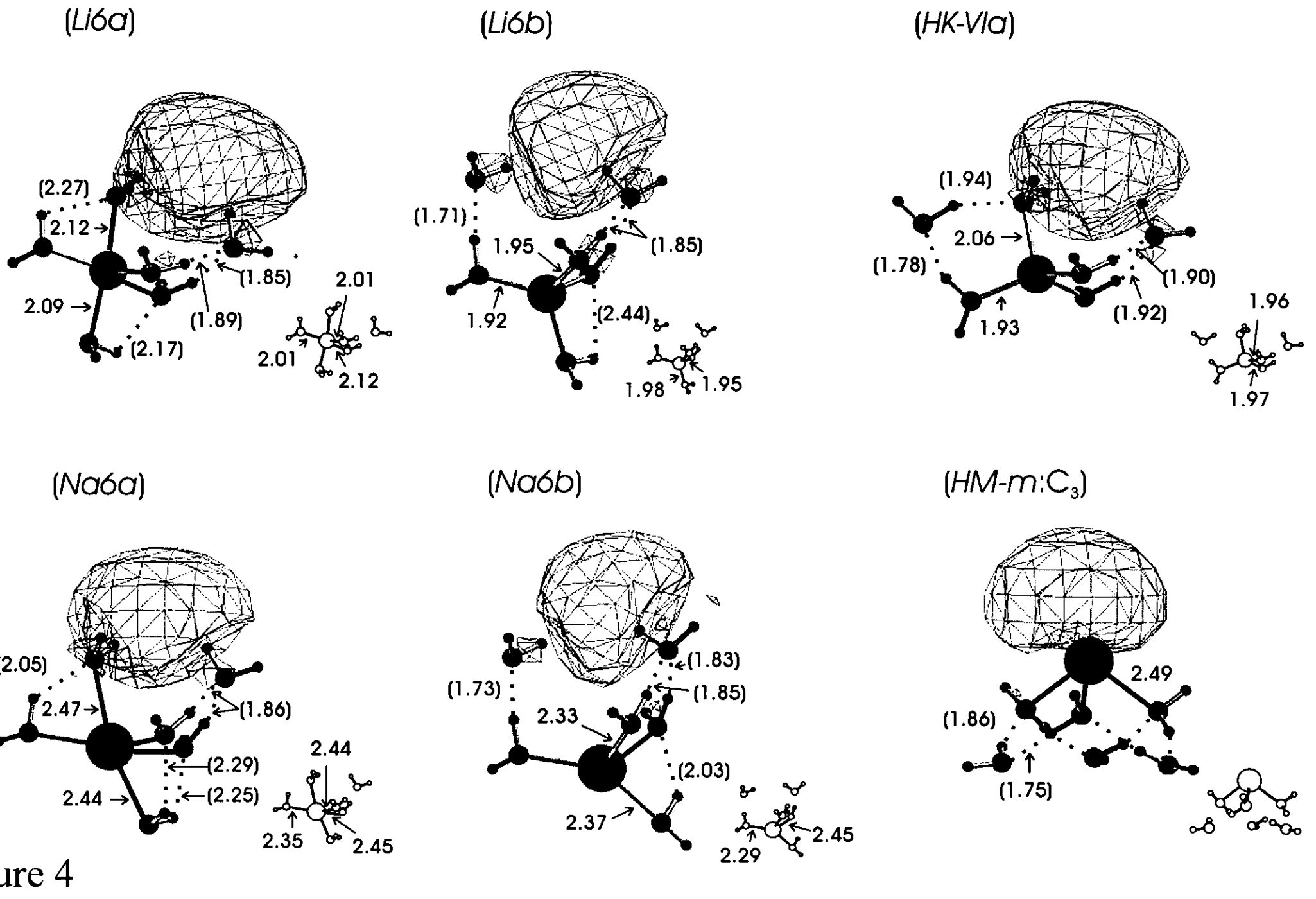
(Li6a)
(2.27)
2.12
(1.85)
2.09
(1.89)
(2.17)
2.01
2.01
2.12
(Li6b)
(1.71)
1.95
(1.85)
1.92
(2.44)
1.98
1.95
(HK-Vla)
(1.94)
2.06
(1.78)
(1.90)
1.93
(1.92)
1.96
1.97
(Na6a)
(2.05)
2.47
(1.86)
(2.29)
2.44
(2.25)
2.44
2.35
2.45
(Na6b)
(1.83)
(1.73)
(1.85)
2.33
(2.03)
2.37
2.29
2.45
(HM-m:C3)
2.49
(1.86)
(1.75)

Figure 4

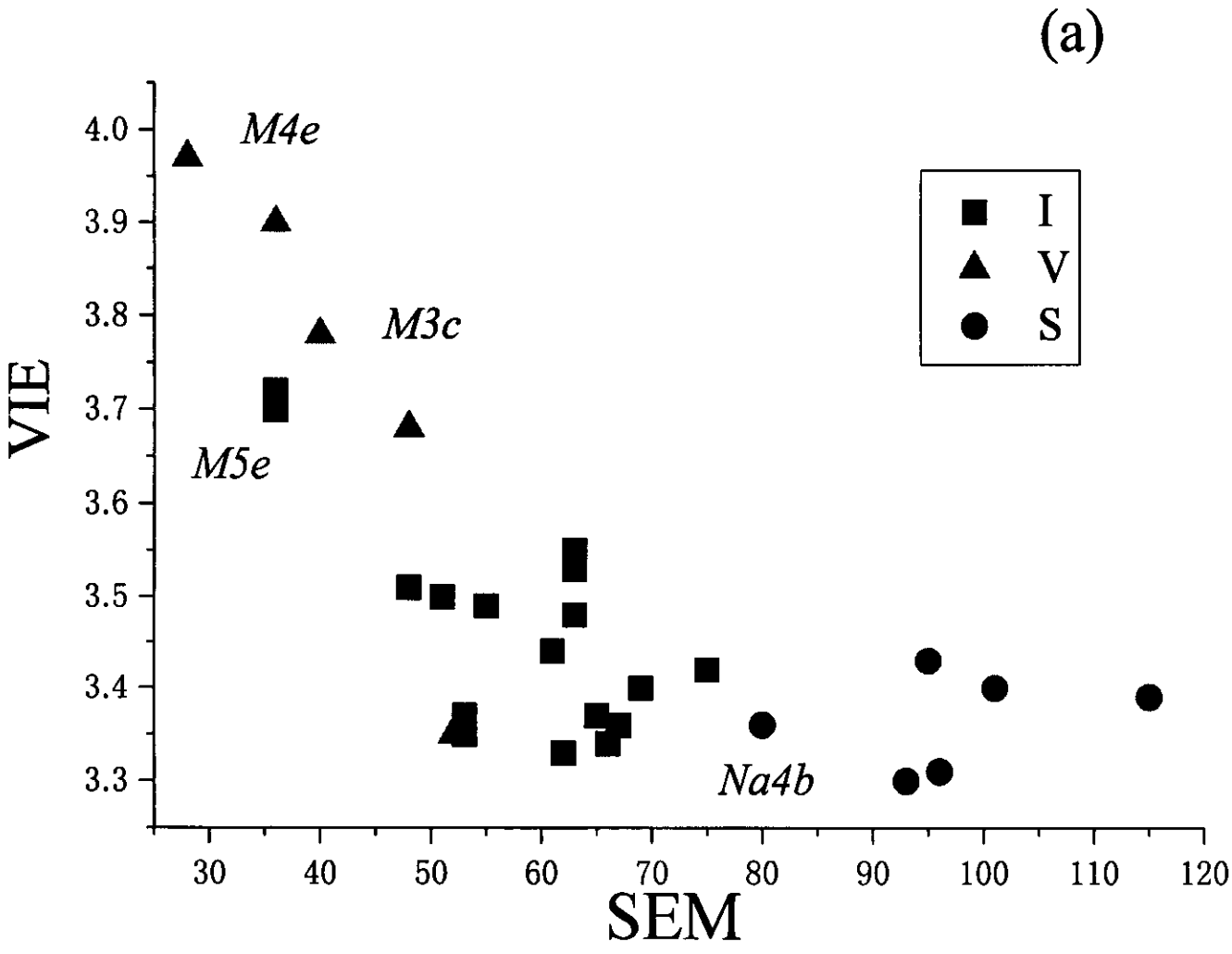
(a)
M4e
M3c
M5e
Na4b
I
V
S
VIE
SEM
4.0
3.9
3.8
3.7
3.6
3.5
3.4
3.3
30
40
50
60
70
80
90
100
110
120

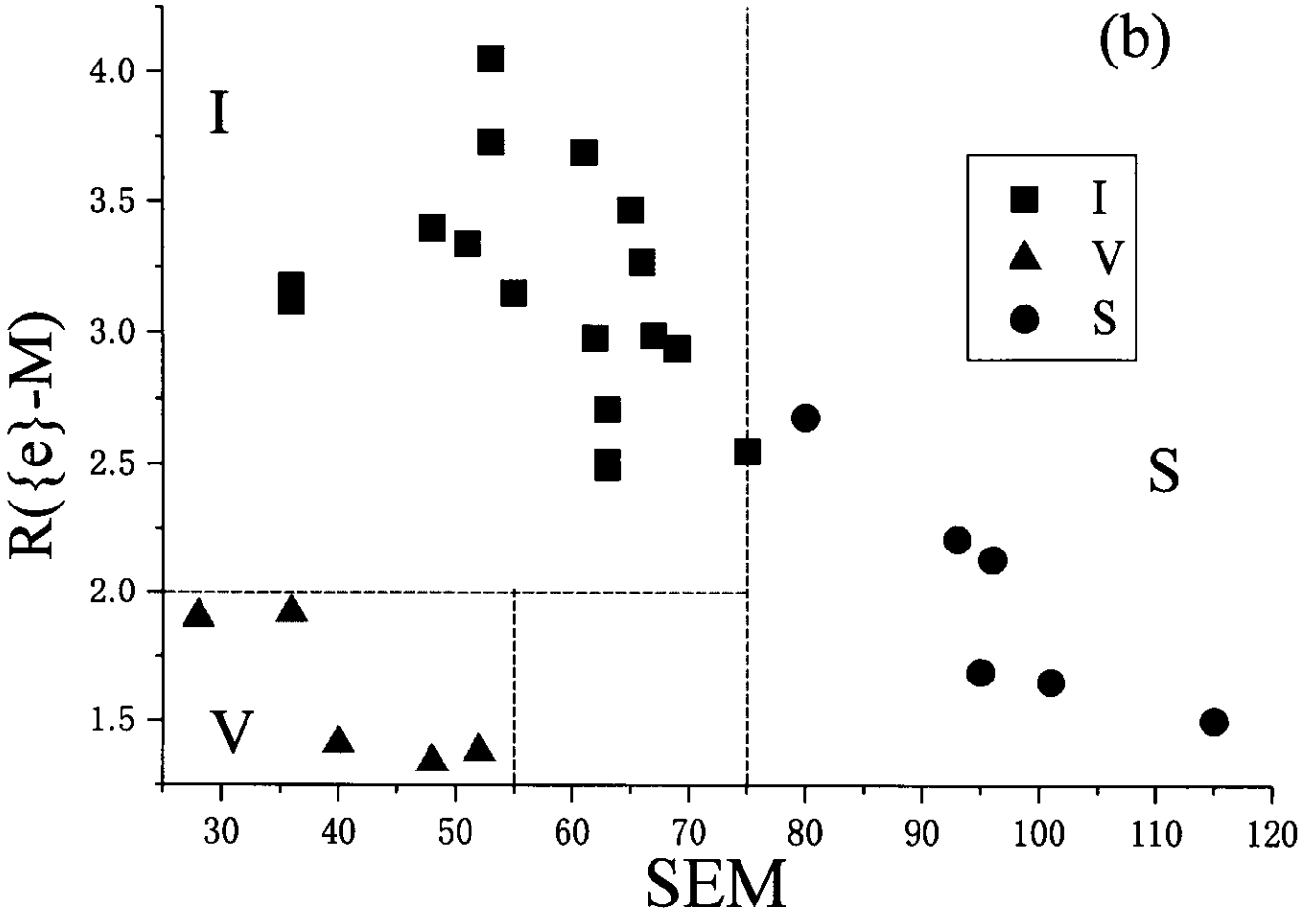
(b)
I
V
S
I
V
S
R({e}-M)
SEM
4.0
3.5
3.0
2.5
2.0
1.5
30
40
50
60
70
80
90
100
110
120

Figure 5

Chapter 5

Electron-hydrogen bonds and OH harmonic frequency shifts in water cluster complexes with a group 1 metal atom, $M(H_2O)_n$ (M = Li and Na)

Journal of Chemical Physics, in press

5.1 Introduction

In recent years, there have been extensive experimental and theoretical studies on the water cluster complexes with a metal atom and with its ion [1]. In my recent paper[2] I reported that the group 1 metal atom - water cluster complexes $M(H_2O)_n$ form an ion pair structure $M^+(H_2O)_n^-$ for $n \geq 4$. The water anion part has a structural unit similar to the one found in water cluster anions $(H_2O)_n^-$ in my previous studies. [3, 4] The water cluster anions have also been one of hot subjects in physics and chemistry of molecular clusters.[5, 6, 7, 8, 9, 10, 11, 12, 13, 14] For small size of water cluster anions

such as dimer, trimer and tetramer anions, it has been believed that a chain of hydrogen bonded network forms the backbone structure, which has a large dipole moment enough to bind an electron; it is called the dipole bound electron. In my papers, in addition to the anions having the dipole bound electron, I have found the other type of anions even for n = 2, 3, 4 and 6. The excess electron in these anions is trapped between water molecules, and is surrounded by more than two OH bonds. Importantly, in these anions, when the excess electron is removed, the clusters are broken. It is this type of the structural unit that I found in the anion part of the ion pair $M^+(H_2O)_n^-$. I called it a OH{e}HO structure, and the bonds in the structure can be called electron-hydrogen bonds. It turns out that the OH{e}HO structure plays a key role in determining the characteristics in the ionization energy of $M(H_2O)_n$, M = Li and Na. It has been known [15, 16, 17] that the ionization threshold energy (ITE) of $M(H_2O)_n$ for M = Li, Na and Cs shows characteristic size dependence; (1) ITEs rapidly decrease with increasing n up to n = 4 and then become constant for $n \geq 4$. (2) The n dependencies of their ITEs are independent of the metal element contained in the clusters. (3) Those limiting values are close to the estimated photoelectric threshold of bulk ice. In my paper,[2] after extensive search of possible isomers with the MP2/6-311++G(d,p) level of approximation, I presented a model structure $M^+(H_2O)_m \cdot (H_2O)_{n-m-l} \cdot (H_2O)_l^-$ for the ion pair. This model explained the first two characteristics mentioned above. The water cluster anion part, $(H_2O)_l^-$, has a OH{e}HO structure, and the ITE of the clusters is mostly governed by this structural unit.

By looking back the past research on water clusters interacting with a negatively charged atom or molecule, I can find the structures similar to the OH{e}HO structure. One of the examples is the $X^- \cdot (H_2O)_n$ (X = F, Cl, Br, I and Cu) [1, 18, 19, 20, 21, 22] complexes, in which the so-called ion-internal isomers become more stable for larger n than the ion-surface isomers. In particular, for X = F, the observed vibrational spectrum for n = 3 shows only the ion-HO hydrogen bonds. [21] The model studies of the solvated electron in liquid water and methanol [23, 24, 25, 26, 27, 28] are the other examples, where the geometric configurations of water (methanol) molecules were assumed; therefore, the effects of the solvated electron on the intramolecular potential of solvent molecules were

not fully taken into account.

In the present work, I scrutinize the excess electron-HO interaction in the anion part of $M(H_2O)_n$ and show the uniqueness of the electron distribution which is localized by the surrounding OH bonds and has no positive charge near the center of the distribution. In particular, I examine how the surrounding OH bonds are changed when they interact with the excess electron. The harmonic frequencies are calculated for many isomers of $M(H_2O)_n$ (M = Li and Na) as well as for water cluster anions $(H_2O)_n^-$.[4] The strong correlation between the frequency shifts and a few geometric parameters are found; if the infrared absorption and Raman scattering spectra are measured, they help identifying the detected isomers. The magnitude of the shift indicates that the electron-HO interaction in the OH{e}HO structure is as strong as the ordinal hydrogen bonds and that the characteristics of the OH{e}HO structure in $M(H_2O)_n$ are found to be the same in $(H_2O)_n^-$. I call the electron-HO interaction in this structure the electron-hydrogen bond as I call $X^-(H_2O)_n$ the ion-hydrogen bond.

Finally I will discuss the similarity and difference in the electron-hydrogen bond and the ordinal hydrogen bond, and will comment on the ubiquitousness of the electron-hydrogen bond and the chemical and physical implications of a "trapped electron" under a potential field corporately created by a few OH bonds.

5.2 Computational Details

The harmonic frequencies were calculated for the isomers reported in my previous paper.[2] The UHF MP2/6-311++G(d,p) level of approximation was used both in the geometry optimization and in the harmonic frequency calculation. In the previous work, I confirmed that the basis set used was large enough to describe the diffuse electron ejected from the metal atom and also the MP2 level of the electron correlation treatment was required. Gaussian 98 program package [29] registered at the computer center of Institute for Molecular Science was used. For n = 3 and 4, the harmonic frequencies were calculated with the analytical derivative method. For n = 5 and 6, because of the

time limit even for the largest job class on NEC SX-3 in our computer center, I had to employ the numerical derivative method, which allowed me to restart the job a few times.

5.3 Results and Discussion

In the previous paper[2], I reported 15 isomers for $Li(H_2O)_n$ and 11 isomers for $Na(H_2O)_n$ for n = 3–6. There are more isomers for $n \geq 4$ than I reported. To classify the isomers, three measures, SEM, R({e}···M) and R({e}···H), are introduced. The SEM (SOMO extent measure) is defined as the volume (in $Å^3$) of a sphere which contains a half of electron density in the singly occupied molecular orbital (SOMO). The lengths, R({e}···M) and R({e}···H), are defined as the distances from the center of the SOMO density $\mathbf{R}_{\{e\}}$ to a metal atom and to a hydrogen atom, respectively. Using SEM and R({e}···M), the SOMO of the clusters is classified into three types: (1) Surface type: SEM > 75 $Å^3$ (2) Quasi-valence type: SEM < 50 $Å^3$ and R({e}···M) < 2.0 Å (3) Semi-internal type: SEM ≤ 75 $Å^3$ and R({e}···M) > 2.0 Å.

5.3.1 The frequency shifts of the OH stretching modes

To scrutinize the bonding nature between the electron and OH bonds, I calculated the harmonic frequencies of OH stretching modes, and examined the correlation between the shift $\Delta\nu_{OH}$ of the stretching frequency and the OH bond length and between $\Delta\nu_{OH}$ and the distance R({e}···H).

Figures 1 and 2 show the calculated infrared spectra for some typical isomers. The structure of the isomer is inserted in each figure. The sphere of the electron cloud contains a half of the SOMO electron. The abscissa of the figure is the shift $\Delta\nu_{OH}$, defined as

$$\Delta\nu_{OH} = \nu_{OH} - (\nu_{OH}^{free,sym} + \nu_{OH}^{free,anti})/2,$$

where $\nu_{OH}^{free,sym}$ and $\nu_{OH}^{free,anti}$ are the symmetric and anti-symmetric harmonic frequencies of a single water molecule calculated with the same level of approximation as for the complexes.

Figure 1 shows the representative spectra of three types of isomers for both Li and Na complexes;

(a) and (b) for the surface type, (c) and (d) for the quasi-valence type, and (e) and (f) for the semi-internal type. Depending on which OH is mostly vibrating in each normal mode, the sticks are shaded. At the first sight it is evident that almost no difference is found in the spectra of the Li and Na complexes, independent of the types of the isomers. In particular, the spectra of Li4b (Fig. 1(a)) and of Na4b (Fig. 1(b)), both of which are of the surface type, are almost identical. The structure has a C_2 axis. A very strong IR band at $\Delta\nu_{OH} = 360$ cm^{-1} is an antisymmetric mode (symmetry b) of two OH bonds which interact with the ejected surface electron. The symmetric mode (symmetry a) has a weak intensity and slightly smaller $|\Delta\nu_{OH}|$ than the antisymmetric mode. This strong IR band around 350 cm^{-1} is characteristic of the surface type as is also seen in the spectrum of Li3b, shown in Fig. 2(a). When there is no symmetry in the cluster, more than one strong IR mode of HO bonds interacting with the electron ({e}HO bond) are found in the calculated IR spectrum for the surface type isomers. The number of the strong IR modes of the {e}HO bond depends on the number of the {e}HO bonds and on the symmetry of the cluster. Because the electron distribution in the surface type is very diffuse, the OH stretching motion induces a large change in the distribution and thus the large change in the total dipole moment. Hashimoto and Morokuma have shown the spectral patterns for $Na(H_2O)_4$.[30] In their paper, because the electron correlation is not included in geometry optimization and the frequency calculation, $|\Delta\nu_{OH}|$ is about one half of my values, but the features of the spectral pattern is similar to those of the surface type.

The shifts $\Delta\nu_{OH}$ in the quasi-valence type, Li4e and Na4e, shown in Figs. 1(c) and (d), are 300 to 250 cm^{-1}. The shift for the hydrogen-bonded OH bonds to the second shell water molecule is much larger in this type, which is in contrast with the corresponding shift in the surface type. The IR intensity for the {e}HO bond modes is weaker than in the case of the surface type, because the SOMO electron distribution is mostly bound by the metal ion, and not so much affected by the OH stretching motion.

The calculated IR spectra for the semi-internal type are distinct from the other types; the IR bands of both OH, the one interacting with the electron {e}, and the one hydrogen-bonded to the

water molecule, shift by as large as 600 to 300 cm^{-1}. The typical examples are found in the spectra of Li5d and Na5d in Figs. 1(e) and (f). The other examples are shown in Figs. 2(b), (c) and (d). In the spectra of Li5d and Na5d, a pair of OH modes shift downward; one of them is the stretching mode of the {e}HO bond, and the other is the mode of the OH bond of the first shell water molecule which is hydrogen-bonded to the second shell water molecule. The ordering of these two modes is different in Li5d and Na5d, which results from the difference in the metal ion-oxygen distance. The strongest and most downward shifted band in Figs. 2(b) and (c) is typical of the {e}HO mode of the double proton acceptor water molecule. In Fig. 2(d) the similar type band is found, though the intensity is not much strong.

5.3.2 The correlation of the shift $\Delta\nu_{OH}$ with the lengthening of OH bonds in hydrogen bonds and in OH{e}HO structure

As seen in Figs. 1 and 2, the calculated downward shifts of the harmonic frequencies of OH bonds are as large as those of the hydrogen bonded OH bonds. It is well known that the OH bond lengths of water molecules are lengthened when the OH bond is hydrogen bonded. As the basicity of the proton acceptor increases, the OH bond is lengthened in conjunction with the downward shift of the OH vibrational frequency. Figure 3 shows the similar correlation found in the OH{e}HO structure. In the figure the shift $\Delta\nu_{OH}$ both for the hydrogen bonded OH bond and for the {e}HO bond are all together plotted against the OH bond length. It is clear that all plotted data points are almost indistinguishable among the hydrogen bonded OH bonds and the {e}HO bonds in the Li and Na water clusters. The plots demonstrate that the {e}HO bonds are very similar with the ordinal hydrogen bonds in its character. The similar correlation was found in the harmonic frequency shifts in pure water cluster anions.[4]

For the hydrogen bonds, the hydrogen bond distance R(O$\cdots$H) is another measure to see the strength of the hydrogen bonds. In the OH{e}HO structure, the distance between the center of the electron distribution {e} ($\mathbf{R}_{\{e\}}$) and the H atom, R({e}$\cdots$H), will be used in place of R(O$\cdots$H).

In Fig. 4 the correlation of the OH frequency shifts with the distances R(O$\cdots$H) and R({e}$\cdots$H) is plotted. The data for hydrogen bonds are plotted as shaded circle (HB in the legend). In the hydrogen bonds, although the distance R(O$\cdots$H) converges almost at 1.7 Å, the strong correlation of the shifts with R(O$\cdots$H) is evident. In the OH{e}HO structure, two linear relations (I and II) are found. As I will discuss later, these correspond to two distinguishable types of the conformation of the center of {e} and {e}OH bonds. In the plots the types of the electron distribution {e} are distinguished by square marks for surface type, triangle marks for quasi-valence type, and circle marks for semi-internal type. The metal dependence is shown by filled marks for $Na(H_2O)_n$ and by the open marks for $Li(H_2O)_n$, but it is indistinguishable in the plots. I can notice a few characteristics in the plots. All of the triangle marks are close to the line II. Most of the square marks are also close to the line II, but these points are more scattered than the triangle marks, and some of the square marks at small $\Delta\nu_{OH}$ fall on the line I. The circle marks are found only below $\Delta\nu_{OH} = -220$ cm^{-1}, and fall on both the lines I and II.

To explore the causes of two types of linear relations in the plots, I have to analyze the geometric conformation of the SOMO electron {e} and water molecules in the clusters. In Fig. 5, five types of the relative conformations of the SOMO electron {e}, and water molecules and the metal ion are shown. In the first two types A and B, the OH bonds of the second shell water molecules interact with the electron {e}. In the quasi-valence type isomers, the interacting site of OH bonds and the electron {e} has conformation B as is seen in Li4e and Na4e (Figs. 1(c) and (d)), and the shifts $|\Delta\nu_{OH}|$ are not large. R({e}$\cdots$H) is longer than 2.0 Å and their corresponding points are on the line II. Conformation B is also found in the semi-internal isomers as in the left part of Li5d and Na5d (Figs. 1(e) and (f)), but the shifts are on line I. In general, the shifts of conformation B in the semi-internal type isomer are on I. In conformation B, the water molecule interacting with the electron {e} are the single proton acceptor molecule in the second shell.

The right part of Li5d and Na5d is typical of conformation A. The other examples are found in Li4c, Li5a and Li6b in Fig. 2. Their shifts $|\Delta\nu_{OH}|$ are large and on line I. The water molecule interacting

with the electron {e} in conformation A is the double proton acceptor molecule in the second shell. They are mostly found in the semi-internal type of {e}. In the ordinal hydrogen bonds, it is known that the double proton acceptor water molecule forms a strong hydrogen bond; the polarization of the OH bonds of the molecule are induced by two hydrogen bonds to the oxygen atom. Similarly in the {e}HO bonds the double proton acceptor molecules strongly interact with the electron {e}; most of the points on line I for $\Delta\nu_{OH} < -350$ cm^{-1} correspond to this type of interaction. The largest shift is as large as -565 cm^{-1} in Li6b (Fig. 2(d)), where the OH bond directs linearly toward the center of the electron {e} and the distance R({e}$\cdots$H) is 1.07 Å. In conformation C, similar to the conformation A, the OH bond of the first shell molecule directs linearly toward the center of the electron {e}; the example is found in the left side of Li4c (Fig. 2(b)). Their shifts are on line I.

In conformation D, both OHs in a water molecule are directed toward the electron {e}, although these are not in equal proportion. In contrary to the conformation C, the OH bonds do not direct toward the center of the electron {e}. In conformation E, more than one OH bond interact with the {e}, but none of them directs toward the center of {e}. The examples of conformation E are Li4b and Na4b in Fig. 1, and Li3b in Fig. 2(a); all of them are of the surface type. The shift $|\Delta\nu_{OH}|$ for the surface type clusters are at most 330 cm^{-1} and R({e}$\cdots$H) are longer than 1.75 Å. Exceptions are for M4b isomers in Figs. 1(a) and (b), in which the shifts $|\Delta\nu_{OH}|$ are as large as 365 cm^{-1} and R({e}$\cdots$H) are as short as 1.34 Å. The example of conformation D is the left part of Li5a in Fig. 2(c). The data points on line II for R({e}$\cdots$H) < 2.0Å are those of conformations D and E.

5.3.3 Spectral patterns for OH stretching mode in the clusters

As seen in Figs. 1 and 2, the calculated IR spectrum reflects the geometric and electronic structures of the cluster. Therefore, in order to identify the isomers detected in the experiments, the vibrational spectroscopy is expected to be very informative as was in the previous studies of water clusters with a phenol,[31] a benzene [32] or halogens.[1] In $M(H_2O)_n$, both ordinal hydrogen bonds and {e}HO bonds co-exist, and therefore, the spectrum might be congested. In some isomers the shifts of the OH

modes of the hydrogen bonds are larger than those of the {e}HO bonds, and in the others the order is reversed. And furthermore, the IR intensity of both the {e}HO modes and the hydrogen bonded OH modes are comparable.

By examining many calculated spectra, I have found two regular spectral patterns which reflects the relative conformations A and B in Fig. 5. As shown in Fig. 6, conformation A has three strong IR bands; the one with a larger shift is the mode of the {e}HO bond and the other two are the hydrogen bonded OH modes. Because in this type of conformation the water molecule of the {e}HO bond is a double proton acceptor, the {e}$\cdots$HO interaction is strong, and therefore the shift is large. On the other hand, in conformation B, one of the OH bonds of a single proton acceptor water molecule interacts with the electron {e}, and the interaction is weaker than in conformation A. The shift of the hydrogen bonded OH mode is larger than that of the {e}HO mode, and the spectral pattern becomes as shown in the lower part of Fig. 6. Typical examples are seen in the spectra of Li4e and Na4e (Figs. 1(c) and (d)), both of which have two equivalent configurations B. Most of the clusters, however, have two non-equivalent water molecules interacting with the electron {e}. For instance, isomers Li5d and Na5d (Figs. 1(e) and (f)) have conformations A and B, and therefore, the spectra are the sum of these two patterns. These regularities might be helpful in future experimental studies.

5.3.4 Similarity and difference with the hydrogen bond

I have already emphasized the similarity of the {e}$\cdots$HO interaction with the hydrogen bonds. The X$\cdots$HO interaction of the ion-hydrogen bonds in $X^-(H_2O)_n$ complexes, X = F, Cl, Br, I, and Cu,[1] might more closely resemble the {e}$\cdots$HO interaction than the O$\cdots$HO interaction in the ordinal hydrogen bonds. Therefore, I might call the {e}$\cdots$HO interaction 'electron-hydrogen bond'. There are very important differences in the electron-hydrogen bond from the ordinal hydrogen bond and the ion-hydrogen bond. In the former, there is no nuclear center near the center of the negative charge, which attracts the OH bonds. Besides, always more than one OH bonds are attached to an electron to form the OH{e}HO structure. In fact, the electrostatic potential created corporately by two or more

OH bonds of water molecules traps the electron, and in turn, the OH bonds are strongly polarized by the negative charge and are attracted to it. The interrelation between the electron distribution {e} and OH bonds is essential to form the stable OH{e}HO structure.

5.4 Conclusion

In the present paper, I calculated the harmonic vibrational frequencies of the $M(H_2O)_n$ cluster and found the strong correlation between the lengthening of OH bond length and the down-shift of OH frequency as is known in the hydrogen bonding systems. Thus, I call the {e}$\cdots$HO interaction in the clusters an electron-hydrogen bond. This bond is unique in the sense that no positive charge exists at the center of the electron distribution which binds the OH bonds. The electron itself is localized under the electrostatic field created corporately by a few OH bonds. The self-consistent type mutual action between the localization of the electron and the polarization of OH bonds is essential in this bond. The electron-hydrogen bond also plays an important role in the water cluster anions.

By examining the correlation between the harmonic frequency shifts and the distance R({e}$\cdots$H), I found two types of {e}$\cdots$HO interactions. When an OH bond is enough polarized by the hydrogen bond network, the OH bond and the center of the electron $\mathbf{R}_{\{e\}}$ line up almost colinearly, and the interaction between the electron {e} and the OH bond becomes stronger. In the other types of conformations, the OH bonds direct toward $\mathbf{R}_{\{e\}}$ slantwise.

In the ion-pair complexes, $M^+(H_2O)_n^-$, and also in some of the isomers of water cluster anions, the electron-hydrogen bonds and the structural unit OH{e}HO determine the geometric structure of the whole cluster. There are other cases where a kind of OH{e}HO structures might be stable or quasi-stable as a resonant state. In liquids and glassy solutions, and in polymers, the hydrogen bonds and the other stronger bonds determine the backbone of the structure, in which some of the OH bonds (or the other polar bonds XH) are not hydrogen bonded and exist as dangling bonds. If a few of those dangling OH (or XH) bonds would happen to face toward each other, they could generate the

electrostatic field enough to trap an electron permanently or temporally. The solvated electron is one of the examples, and the trapped electrons in γ-irradiated amorphous organic solids at 77 K observed in the near IR region might be the other examples.[33, 34] More systematic and thorough researches on the light of electron-hydrogen bond and XH{e}HY structures are required.

Acknowledgement

I am grateful to Prof. K. Hashimoto for his critical comments throughout the research. The present work was partially supported by the Grant-in-Aids for Scientific Research (No.11640518 and 11166270) by the Ministry of Education, Science, Sports, and Culture, Japan, and by Research and Development Applying Advanced Computational Science and Technology, Japan Science and Technology Corporation (ACT-JST). A part of calculations was carried out at the Computer Center of the Institute for Molecular Science.

Figure Caption

Figure 1.

The theoretical infrared absorption spectra of representative isomers of surface type (a and b), quasi-valence type (c and d), and semi-internal type (e and f) of $M(H_2O)_n$, M = Li and Na. The naming of the isomers is given in the previous paper.[2] The standard of the shift $\Delta\nu_{OH}$ is defined in text. The structure and the shape of SOMO are inserted in the spectra. The shaded region of the SOMO sphere contains a half of electron. The stick IR bands are assigned to the modes shown at the bottom of the figure.

Figure 2.

The theoretical infrared absorption spectra of some of the isomers of $Li(H_2O)_n$. See the caption for Fig. 1.

Figure 3.

The correlation of the harmonic frequency shift $\Delta\nu_{OH}$ with the OH bond length. Both of OHs, hydrogen bonded (HB) and interacting with the electron {e} ({e}HO), are included in the plots. The filled square and triangle marks are for the hydrogen bonded OH in the clusters, and the open square and triangle marks are for the OH bonds interacting with {e}.

Figure 4.

The correlation of the harmonic frequency shift $\Delta\nu_{OH}$ with the distance $R(X\cdots H)$ between the hydrogen atom and either the center of the electron {e}, $\mathbf{R}_{\{e\}}$, or the proton accepting oxygen atom O of the neighboring water molecule.

Figure 5.

Five types of model geometric conformations of the electron {e} and water molecules.

Figure 6.

One-to-one correspondence of the model conformations with the IR spectral patterns.

Bibliography

[1] K. Fuke, K. Hashimoto, and S. Iwata, Adv. Chem. Phys. **110**, 431 (1999).

[2] T. Tsurusawa and S. Iwata, J. Phys. Chem. **103**, 6134 (1999).

[3] T. Tsurusawa and S. Iwata, Chem. Phys. Lett. **287**, 553 (1998).

[4] T. Tsurusawa and S. Iwata, Chem. Phys. Lett. **315**, 433 (2000).

[5] K. S. Kim, I. Park, S. Lee, K. Cho, J. Y. Lee, J. Kim, and J. D. Joannopoulos, Phys. Rev. Lett. **76**, 956 (1996).

[6] S. Lee, S. J. Lee, J. Y. Lee, J. Kim, K. S. Kim, I. Park, K. Cho, and J. D. Joannopoulos, Chem. Phys. Lett. **254**, 128 (1996).

[7] K. S. Kim, S. Lee, J. Kim, and J. Y. Lee, J. Am. Chem. Soc. **119**, 9329 (1997).

[8] J. Kim, J. M. Park, K. S. Oh, J. Y. Lee, S. Lee, and K. S. Kim, J. Chem. Phys. **106**, 10207 (1997).

[9] S. Lee, J. Kim, S. J. Lee, and K. S. Kim, Phys. Rev. Lett. **79**, 2038 (1997).

[10] P. Ayotte and M. A. Johnson, J. Chem. Phys. **106**, 811 (1997).

[11] P. J. Campagnola, L. A. Posey, and M. A. Johnson, J. Chem. Phys. **92**, 3243 (1990).

[12] L. A. Posey and M. A. Johnson, J. Chem. Phys. **89**, 4807 (1988).

[13] J. Kim, I. Becker, O. Cheshnovsky, and M. A. Johnson, Chem. Phys. Lett. **297**, 90 (1998).

[14] L. A. Posey, P. J. Campagnola, M. A. Johnson, G. H. Lee, J. G. Eaton, and K. H. Bowen, J. Chem. Phys. **91**, 6536 (1989).

[15] I. V. Hertel, C. Hüglin, C. Nitsch, and C. P. Schulz, Phys. Rev. Lett. **67**, 1767 (1991).

[16] F. Misaizu, K. Tsukamoto, M. Sanekata, and K. Fuke, Chem. Phys. Lett. **188**, 241 (1992).

[17] R. Takasu, F. Misaizu, K. Hashimoto, and K. Fuke, J. Phys. Chem. **A101**, 3078 (1997).

[18] J. E. Combariza and N. R. Kestner, J. Chem. Phys. **100**, 2851 (1994).

[19] S. Xantheas, J. Phys. Chem. **100**, 9703 (1996).

[20] P. Ayotte, G. H. Weddle, J. Kim, and M. A. Johnson, J. Am. Chem. Soc. **120**, 12361 (1998).

[21] O. M. Cabarcos, C. J. Weinheimer, J. M. Lisy, and S. S. Xantheas, J. Chem. Phys. **110**, 5 (1999).

[22] C.-G. Zhan and S. Iwata, Chem. Phys. Lett. **232**, 72 (1995).

[23] T. Clark and G. Illing, J. Am. Chem. Soc. **109**, 1013 (1987).

[24] H. Tachikawa and M. Ogasawara, J. Phys. Chem. **94**, 1746 (1990).

[25] C. A. Naleway and M. E. Schwartz, J. Phys. Chem. **76**, 3905 (1972).

[26] J. Schnitker and P. J. Rossky, J. Chem. Phys. **86**, 3471 (1987).

[27] L. Turi, A. Mosyak, and P. J. Rossky, J. Chem. Phys. **107**, 1970 (1997).

[28] H. Shiraishi and K. Ishigure, J. Chem. Phys. **88**, 4637 (1988).

[29] *Gaussian 98 (Revision A.2)*, M. J. Frisch, G. W. Trucks, H. B. Schlegel, G. E. Scuseria, M. A. Robb, J. R. Cheeseman, V. G. Zakrzewski, J. A. Montgomery, R. E. Stratmann, J. C. Burant, S. Dapprich, J. M. Millam, A. D. Daniels, K. N. Kudin, M. C. Strain, O. Farkas, J. Tomasi, V. Barone, M. Cossi, R. Cammi, B. Mennucci, C. Pomelli, C. Adamo, S. Clifford, J. Ochterski, G. A. Petersson, P. Y. Ayala, Q. Cui, K. Morokuma, D. K. Malick, A. D. Rabuck, K. Raghavachari,

J. B. Foresman, J. Cioslowski, J. V. Ortiz, B. B. Stefanov, G. Liu, A. Liashenko, P. Piskorz, I. Komaromi, R. Gomperts, R. L. Martin, D. J. Fox, T. Keith, M. A. Al-Laham, C. Y. Peng, A. Nanayakkara, C. Gonzalez, M. Challacombe, P. M. W. Gill, B. G. Johnson, W. Chen, M. W. Wong, J. L. Andres, M. Head-Gordon, E. S. Replogle, and J. A. Pople, Gaussian, Inc., Pittsburgh PA, 1998.

[30] K. Hashimoto and K. Morokuma, Chem. Phys. Lett. **223**, 423 (1994).

[31] H. Watanabe and S. Iwata, J. Chem. Phys. **105**, 420 (1996).

[32] S. Y. Fredericks, J. M. Pedulla, K. D. Jordan, and T. S. Zweir, Theor. Chem. Acc. **96**, 51 (1997).

[33] T. Shida, S. Iwata, and T. Watanabe, J. Phys. Chem. **76**, 3683 (1972).

[34] T. Shida, S. Iwata, and T. Watanabe, J. Phys. Chem. **76**, 3691 (1972).

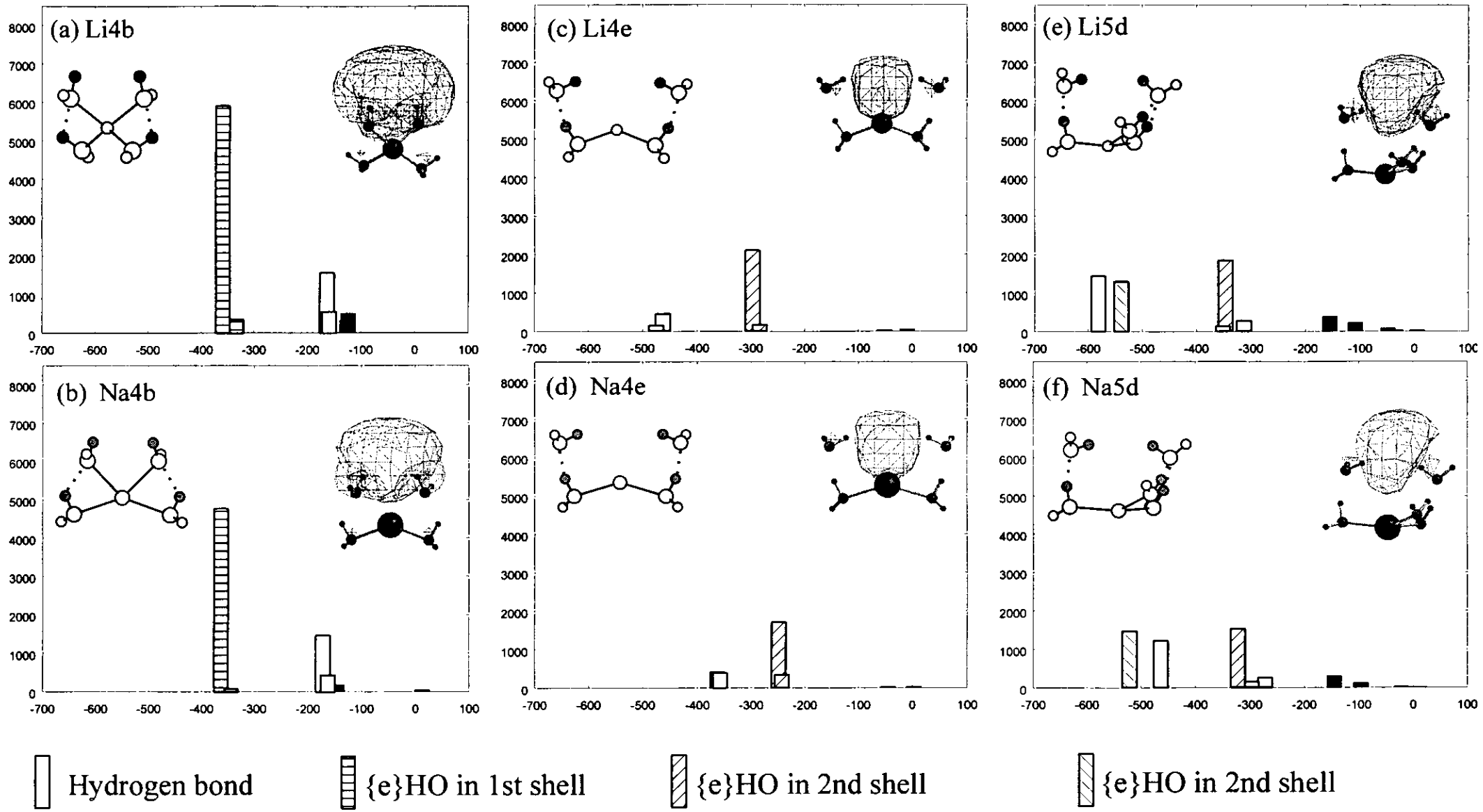
(a) Li4b
(b) Na4b
(c) Li4e
(d) Na4e
(e) Li5d
(f) Na5d
Hydrogen bond
{e}HO in 1st shell
{e}HO in 2nd shell
{e}HO in 2nd shell

Fig.1

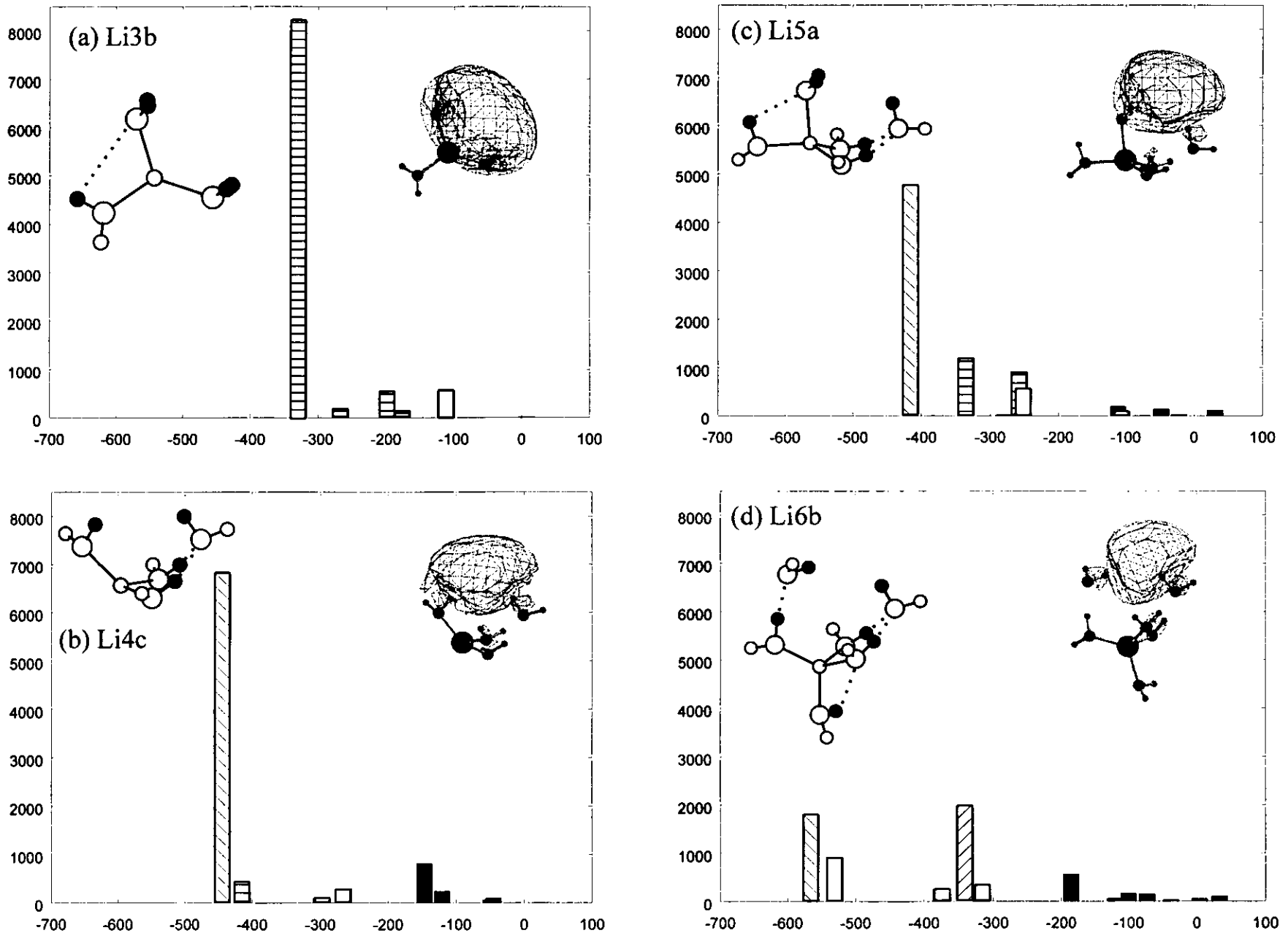
(a) Li3b
(c) Li5a
(b) Li4c
(d) Li6b
8000
7000
6000
5000
4000
3000
2000
1000
0
-700
-600
-500
-400
-300
-200
-100
0
100

Fig.2

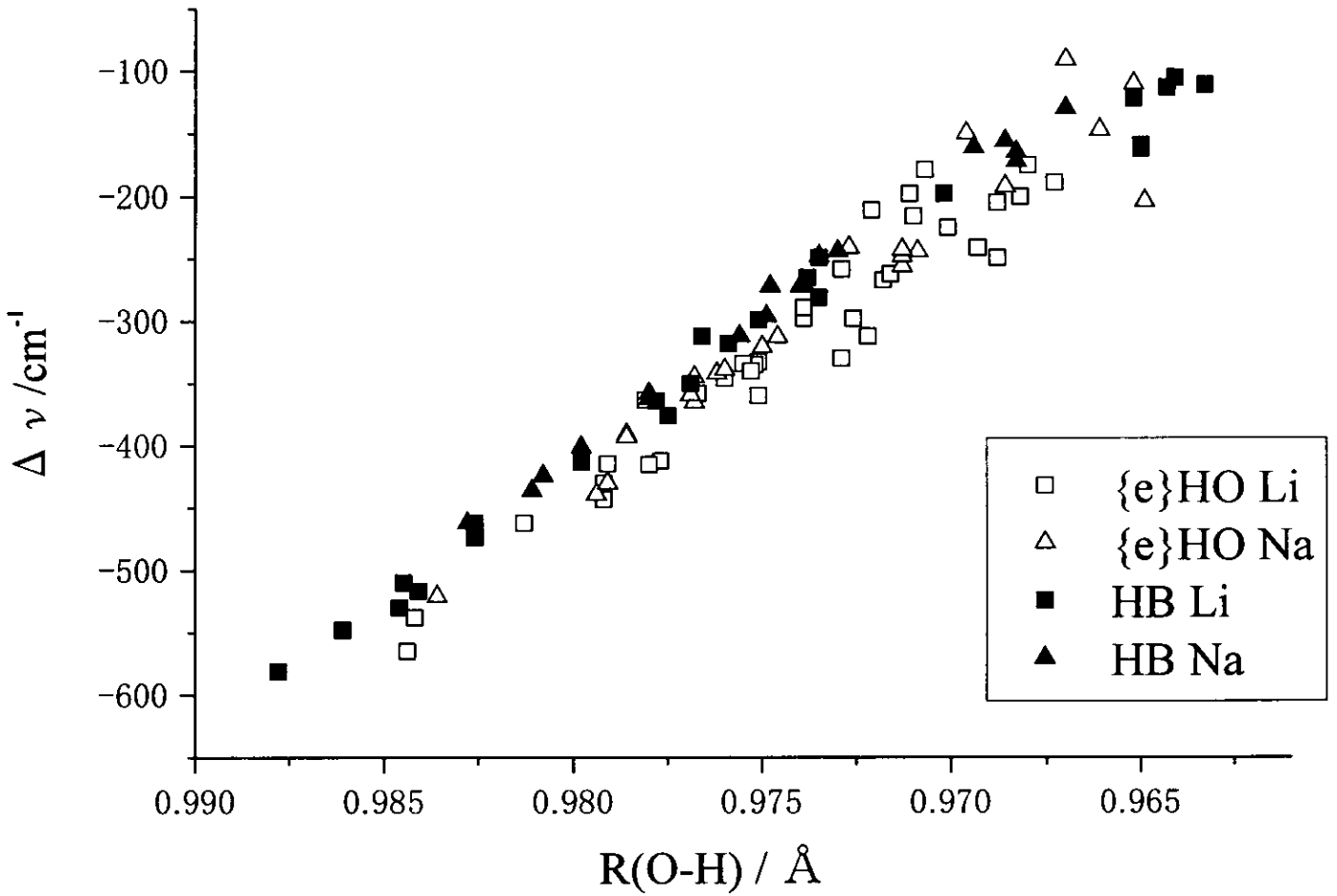
−100
−200
−300
−400
−500
−600
Δ ν /cm⁻¹
0.990
0.985
0.980
0.975
0.970
0.965
R(O-H) / Å
{e}HO Li
{e}HO Na
HB Li
HB Na

Fig.3

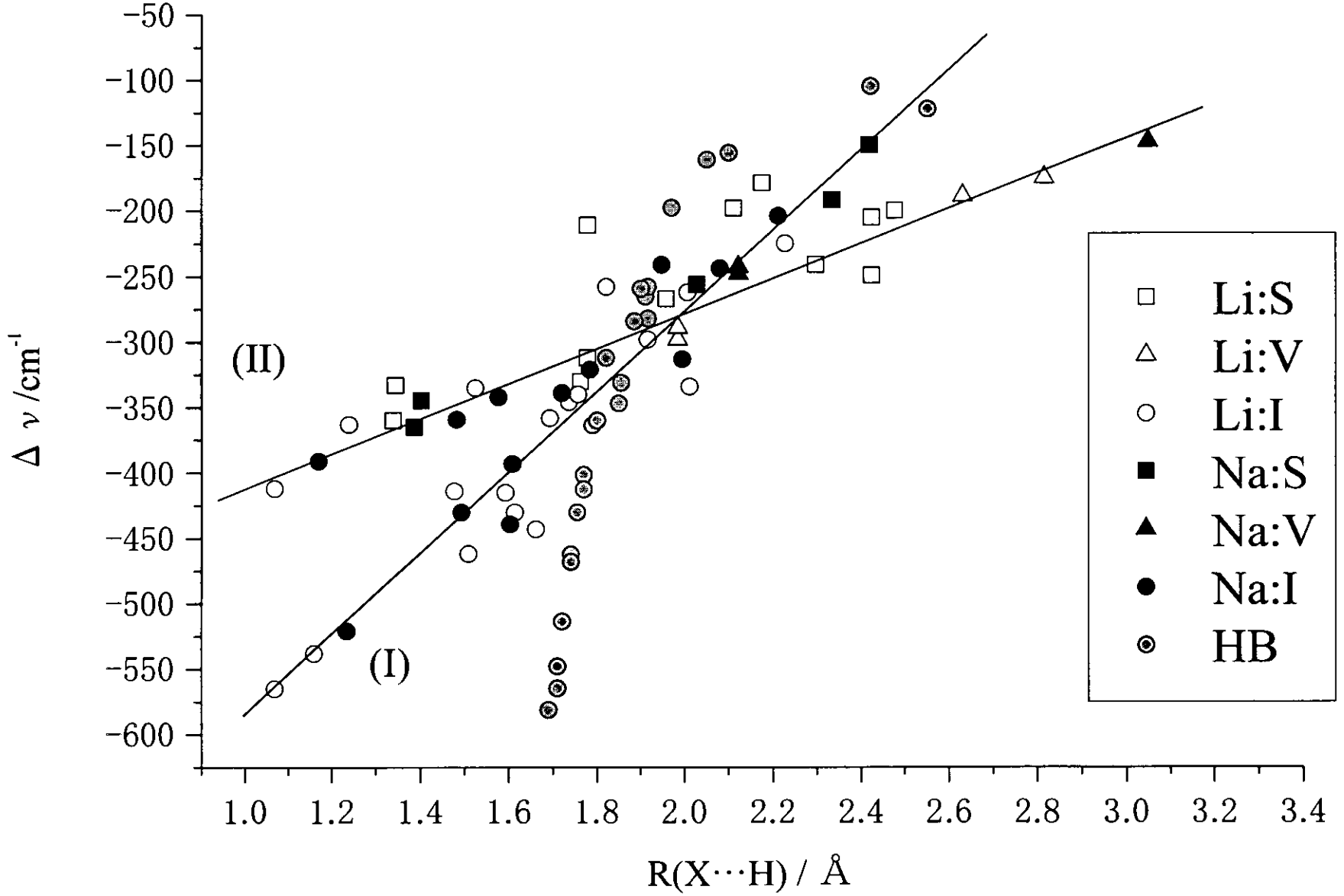
−50
−100
−150
−200
−250
−300
−350
−400
−450
−500
−550
−600
Δ ν /cm⁻¹
(II)
(I)
Li:S
Li:V
Li:I
Na:S
Na:V
Na:I
HB
1.0
1.2
1.4
1.6
1.8
2.0
2.2
2.4
2.6
2.8
3.0
3.2
3.4
R(X···H) / Å

Fig.4

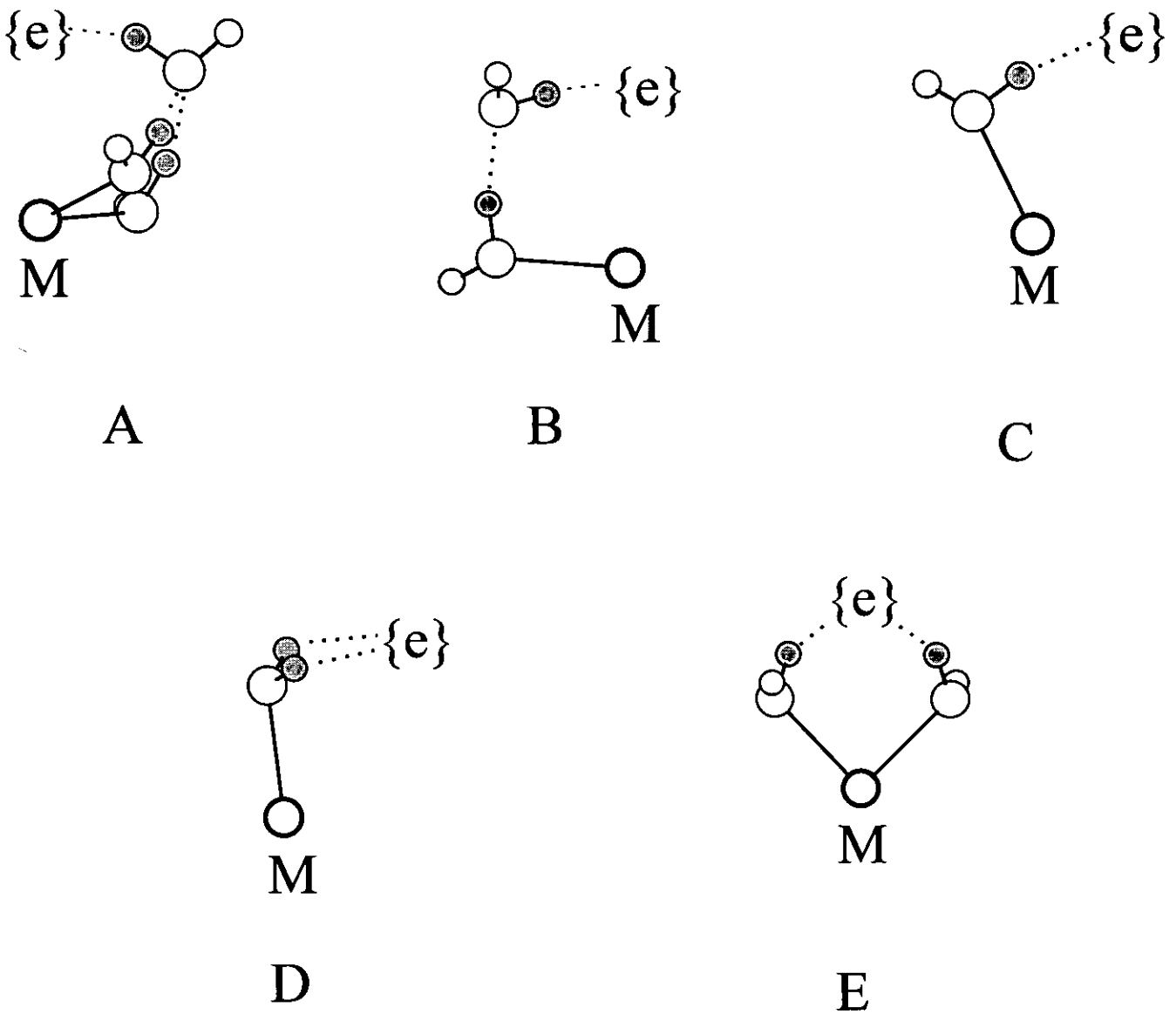

Fig.5

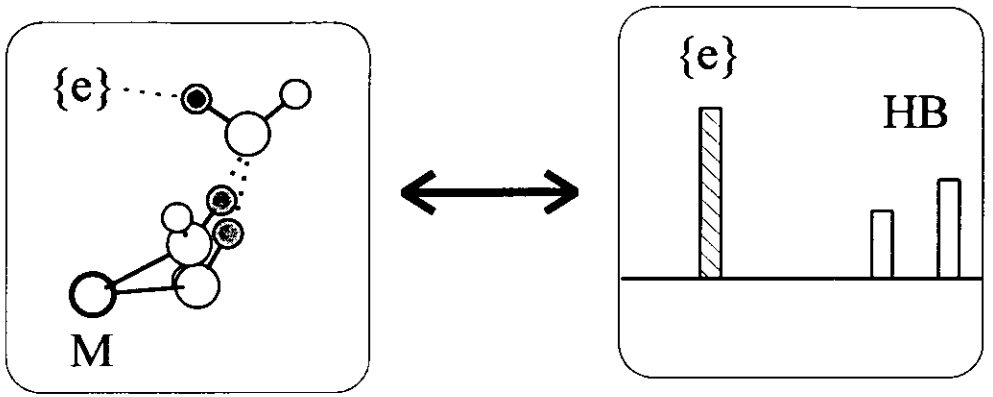

Double proton acceptor water molecule (Configuration A)

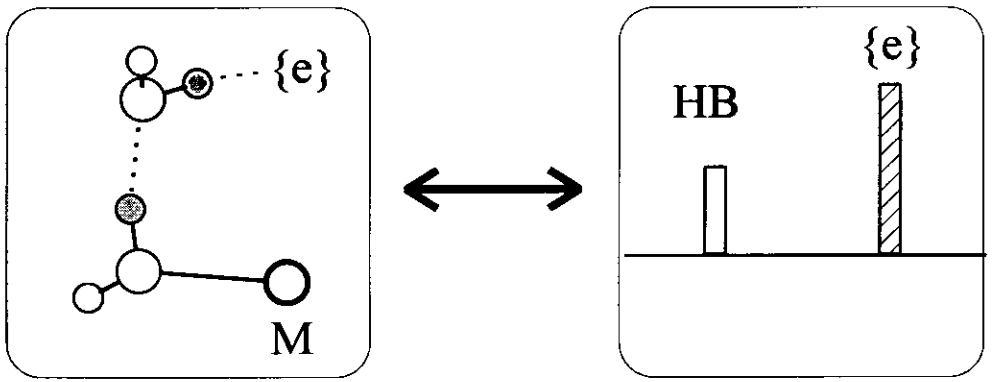

Single proton acceptor water molecule (Configuration B)

Fig.6

Acknowledgement

The contents of the present thesis are the summaries of the author's works at Professor Iwata's group in the Institute for Molecular Science. I wish to acknowledge Professor Iwata for his helpful discussion and guidance. I also wish to acknowledge Professor Kenro Hashimoto for his critical comments throughout the research.

I wish to thank Professor Seiichiro Ten-no, Dr. Tsutomu Ikegami, Dr. Katsuhiko Satoh and Dr. Feiwu Chen for their fruitful discussion. I also thank Mr. Tadayosi Suzuki, Mr. Kazutosi Okada and Dr. Tomohiro Hashimoto for his help for using computers. I wish to thank Professor Jan Hrušák, Dr. Andreas Fiedler and Dr. Pradipta Bandyopadhyay for their helpful discussion and encouragement of the research. I wish to thank Professor Fernando Ornellas for his kind advice and I wish to acknowledge Mrs. Emilia Ornellas for her kind English lesson. I wish to thank Professor Sutcliffe for reading the manuscript and his kind suggestion. I thank all members of theoretical division.

Finally, I wish to thank my wife for her continuing encouragement and I extend my grateful thanks to my parents and grandparents.